



Open Access This file is licensed under a Creative Commons Attribution 4.0 International License, which permits use, sharing, adaptation, distribution and reproduction in any medium or format, as long as you give appropriate credit to the original author(s) and the source, provide a link to the Creative Commons license, and indicate if changes were made. In the cases where the authors are anonymous, such as is the case for the reports of anonymous peer reviewers, author attribution should be to 'Anonymous Referee' followed by a clear attribution to the source work. The images or other third party material in this file are included in the article's Creative Commons license, unless indicated otherwise in a credit line to the material. If material is not included in the article's Creative Commons license and your intended use is not permitted by statutory regulation or exceeds the permitted use, you will need to obtain permission directly from the copyright holder. To view a copy of this license, visit <http://creativecommons.org/licenses/by/4.0/>.

REVIEWER COMMENTS

Reviewer #1 (Remarks to the Author):

In this manuscript, Zhao and colleagues show that the pulmonary vasculature plays a key role in blood platelet release. They developed a technologically challenging approach using an ex vivo mouse heart-lung model. They perfused pre-stained mouse MKs obtained from in vitro culture and found that multiple passages through the lungs were required to maximally fragment MKs. In parallel, they recovered particles in the perfusate that they characterized as young platelets, capable of being activated and incorporated into a thrombus in vitro. They also developed an in vitro chamber mimicking the microvasculature of the lungs that effectively releases platelets, but nevertheless to a lesser extent than the lungs. They demonstrated that ventilation and oxygenation of the lungs were essential for maximal MK fragmentation. Finally, they found that tropomyosin 4 was essential for the final stages of platelet formation in the lungs.

The manuscript is really interesting and very well written. This is the first study to show that a platelet count equivalent to the theoretical calculation can be obtained in vitro from MK grown in culture. The novelty clearly lies in the use of the heart-lung model, allowing for optimal platelet release from cultured MKs and the study of a new platelet release pathway. Nevertheless, I have a few points that I would like the authors to clarify.

Major points.

1. What is the size range of the perfused MKs?
2. Figure 1e is not clear to me. The histogram on the left shows the P1 gate, and there is a large proportion of CD41-negative cells while the "generated platelets" are only a small fraction. Since the lungs are washed prior to infusion of labeled MKs, what is this CD41-negative population with the size of platelets? Please explain.
3. Figure 1h and 1j: the authors should show the statistics.
4. The idea that lung ECs contribute to platelet release is really interesting. The authors should detail in Materials and Methods how they isolate lung ECs. To take this a step further, what happens if MKs are perfused into the heart-lung model that has been previously fixed with PFA and flushed? Can platelets be generated by a passive endothelium?
5. Also, if the microfluidic chamber is kept under N₂ during perfusion, does this change the final platelet release ratio?
6. Figure 4a: Please show the non-activated control platelets to see the baseline for Jon/A-PE and CD62P labeling. If the mean \pm SEM, as indicated in the legend, is reported here, then the experiment is very heterogeneous, especially with the generated platelets. The authors should also show the individual points and discuss why some batches of generated platelets are less able to be activated. In Fig. 3b,

there appear to be 2 populations of generated platelets with different sizes rather than a continuum, while still being different from native platelets. Do these 2 populations respond differently to agonist stimulation?

7. Figure 4d. It would be useful to also have the bright field to visualize platelet thrombi. In the text, the authors mention that the generated platelets are "white", whereas in the fluorescent image, the blue is visible but not the white. Please make it clearer.

8. Figure 5a: The authors mention the presence of a naked nucleus. It could be very interesting to verify whether this is really a naked nucleus or a nucleus surrounded by a plasma membrane. In erythrocytes, for example, the nucleus is lost when it is extruded as a pyrenocyte, a nucleus surrounded by a plasma membrane that exposes phosphatidylserine on its surface to attract macrophages. This can be assessed by non-specifically labeling the plasma membrane or by performing TEM.

9. Throughout the discussion, the authors suggest that under normal conditions, whole MKs enter the lungs to release platelets, and that lung defects prevent MKs from being fragmented into platelets, resulting in higher numbers of MKs in patients with lung disease. What is the evidence for significant transmigration of whole MKs under homeostatic conditions? Have the authors quantified the fraction of MK nuclei in the mouse lungs versus MKs in the marrow? The authors should consider that the passage of whole MKs into the circulation might rather be a rare event under physiological conditions, which is greatly increased during inflammatory reactions, especially as reported during a viral infection such as Covid19, explaining the higher amount of MKs in the lungs (and other organs). This does not question the fact that the lungs are key to the release of platelets from MK fragments that enter the marrow vasculature.

Minor points.

Page1 line 65, from the recent literature it seems that contrary to what is written, platelets produced in vitro are now able to satisfactorily respond to agonists.

The scale of the bar in Supplemental Figure 1 is lacking

The schema of the microfluidic chamber (right panel) is not so clear. Could you indicate the flow direction and provide also a photomicrograph?

Figure 6C: Please use the same scale for the graph as the one in Fig. 5b to help compare the bar size.

Statistics: why use paired t-test? some data clearly do not present a normal distribution, hence the tests should be adjusted accordingly.

Reviewer #2 (Remarks to the Author):

The focus of this manuscript by Zhao and colleagues is on mechanisms by which megakaryocytes release platelets in the lung vasculature. There is ample indirect and direct in vivo evidence that the lung plays a major role in thrombopoiesis, but the mechanisms involved have not been fully elucidated. The authors use an ex vivo lung-heart block to repeatedly infuse megakaryocytes through the lung vasculature and they observed that megakaryocytes can repeatedly passage through the lung with increasing platelet production and progressive enucleation. The final component of this process is dependent on the actin regulator, TPM4.

Major criticisms:

1. Some references are missing on the role of the lung in platelet production, such as those by the Poncz group where they injected megakaryocytes intravenously and showed that the lung is capable of functional platelet production (PMID: 20972336; PMID: 25852052).
2. More detail is needed on the lung-heart block set-up. For example, with the ventilation, was end-expiratory pressure applied, like is conventionally done in the mechanical ventilation of mouse or human lungs? If not, this could promote end-expiratory lung collapse and shunting. Megakaryocytes were “pumped into the right ventricle” per the Methods section. Was this just a push of the syringe or were they placed into the perfusion pump and infused at 0.35 ml/min per the Methods? How was this infusion rate selected and is it physiologic? This is relevant regarding perfusion pressures and sheer stress in the lung microvasculature.
3. Where is the evidence for the statement that “MKs substantially, rapidly and reversibly, deform their shape to passage through the capillary network of the lung.” Direct imaging evidence is needed to support this statement as it does stretch credulity that MKs of up to 100 um in size could squeeze through a lung capillary segment that is on average 5 um in diameter and sometimes smaller.
4. Overall, the study has merit for advancing methodology for the in vitro production of platelets but in terms of advancing concepts of homeostatic, in vivo platelet production in the lung, the limitations of the ex vivo heart-lung perfusion setup with the lack of a systemic circulation are problematic.

Reviewer #3 (Remarks to the Author):

There has been a debate over the last 130 years as to where the tiny (3 μ diameter) anucleate platelets are released from very large (100 μ diameter) multinucleated megakaryocytes, a process called thrombopoiesis. The majority camp says that this occurs in the bone marrow venous sinuses, but a persistent minority says it is also (or mostly) the lungs. This argument is of importance for reasons including strategies applicable to providing non-donor-derived platelet transfusions.

This manuscript by Xiaojuan Zhao, et al., "Highly efficient platelet generation in lung vasculature reproduced by microfluidics" focuses on a technical tour-de-force mouse model of repeatedly reinfused murine megakaryocytes into a heart-lung controlled model, resulting in the release of a large number of platelets. The model provides further support to the in situ pulmonary observations made by E Lefrançois in Nature that bone marrow-derived megakaryocytes migrate to the lung to release platelets. Moreover, if correct, it also provides two new important insights into this process: 1) thrombopoiesis is not a one-and-done process, but requires multiple recycling of the processed megakaryocytes to release all of the platelets. 2) That the pulmonary bed may be unique in this process because of air exchange and the endothelial lining and the process of ventilation.

There are significant issues with this paper though:

1. The model is under-detailed for a full critical review.

Critical details as to what is left circulating after the mouse is prepped and their blood is washed out is missing and should be included in a Supplement.

What are the blood counts in the animals under study as part of the observed outcome may be due to severe anemia and hypoxic injury within and without the lung-heart model. Is there DIC for example. Was it measured?

Is the heart still functional and beating or is blood flow through the lungs all regulated by an artificial pump? One would expect a nonfunctioning heart to develop intramural thrombi.

How long is each experiment if you recycle the blood 18 times? What are the details of each recycle? Is the reperfused sample hypoxic during this process or reoxygenated.

In some experiment an anti-platelet antibody was given, presumably in addition to the blood washout to decrease native platelet levels? Why this added step and what were the final platelet counts with and without this treatment? Wouldn't the antibody also bind to the infused megakaryocytes and the generated platelets?

2. There are other biological questions about the data and its interpretation. The anti-CD41 antibody should label the alpha granules as well as the megakaryocyte surface but that was not apparent in the images. No granules were noted. Furthermore, if this is an intact anti-CD41 antibody, it may also activate the megakaryocytes and generated platelets and often a F(ab)₂ fragment needs to be used instead in in vivo mouse models.

It is also concerning that under N₂ that the pulmonary endothelium was uninjured and still functional. Markers of apoptosis should have been investigated compared to controls in the various stages and should have shown injury at least under the marked hypoxic condition of N₂ ventilation for a significant time window. The data saying that the endothelium was healthy is thus a concern and also goes against the video of the lungs in the N₂ mouse, which clearly shows a large thrombus.

3. The videos are technically problematic. There are a number of mislabeled videos, especially internal within the videos. Most of these videos are highly pixelated, making data interpretation difficult and the two-photon microscopy do not contribute to better-quality prior videos by Junt and Massberg.

4. Platelet-generating device in Fig. 3C platelet is noncontributory to the bottomline message nor is it well-developed to explain how it is informed by the heart-lung model or tests distinct aspects of the pulmonary bed (especially oxygenation and ventilation. At a minimum it should be in the supplement and a photograph of the device and a high-quality video of thrombopoiesis are needed. Finally having shown that one can infuse MKs into recipients and have functional platelets released, the authors then punt to a device for clinical platelet transfusion instead of completing the circle of their thought and suggest that infused MKs may be an alternative therapy.

5. The presentation is repetitive at points and often imprecise. The discussion is too long and cumbersome.

An annotated PDF will hopefully be returned with additional smaller issues noted.

Morty POncz

REVIEWER COMMENTS

Reviewer #1 (Remarks to the Author):

In this manuscript, Zhao and colleagues show that the pulmonary vasculature plays a key role in blood platelet release. They developed a technologically challenging approach using an ex vivo mouse heart-lung model. They perfused pre-stained mouse MKs obtained from in vitro culture and found that multiple passages through the lungs were required to maximally fragment MKs. In parallel, they recovered particles in the perfusate that they characterized as young platelets, capable of being activated and incorporated into a thrombus in vitro. They also developed an in vitro chamber mimicking the microvasculature of the lungs that effectively releases platelets, but nevertheless to a lesser extent than the lungs. They demonstrated that ventilation and oxygenation of the lungs were essential for maximal MK fragmentation. Finally, they found that tropomyosin 4 was essential for the final stages of platelet formation in the lungs. The manuscript is really interesting and very well written. This is the first study to show that a platelet count equivalent to the theoretical calculation can be obtained in vitro from MK grown in culture. The novelty clearly lies in the use of the heart-lung model, allowing for optimal platelet release from cultured MKs and the study of a new platelet release pathway. Nevertheless, I have a few points that I would like the authors to clarify.

Major points.

1. What is the size range of the perfused MKs?

We have now included this size range of the perfused MKs in Supplementary Fig. 1c, with a range of 12.7 - 79.2 μm .

2. Figure 1e is not clear to me. The histogram on the left shows the P1 gate, and there is a large proportion of CD41-negative cells while the "generated platelets" are only a small fraction. Since the lungs are washed prior to infusion of labeled MKs, what is this CD41-negative population with the size of platelets?

Thank you for raising this. These additional cells are likely to be stem cells, which are also small in size and often run within the same gate as platelets. We have now expanded Fig. 1d to include data from 0 passages, i.e, just prior to running cells through the lung-heart preparation for the first time. In Fig. 1e legend, we also now clarify that the CD41-negative populations are ones that include stem cells and host-derived platelets.

3. Figure 1h and 1j: the authors should show the statistics.

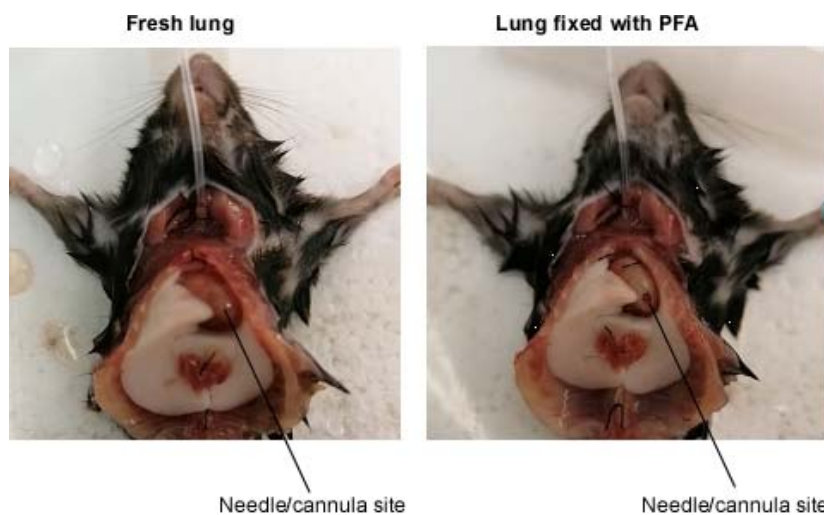
In Fig. 2a (original Fig. 1h) and its legend, we have now shown the statistics, which was performed using two-way ANOVA with Tukey's multiple comparisons. In Fig. 2c (original Fig. 1j) however, the data are not actually to be compared, because we were not looking to assess the relative contribution of platelets in the perfusate versus those retained in the lung vasculature. These are absolute numbers that, when added together, provide the total number of platelets generated per megakaryocyte, and so it is not appropriate to conduct any comparison for the data in Fig. 2c (original Fig. 1j).

4. The idea that lung ECs contribute to platelet release is really interesting. The authors should detail in Materials and Methods how they isolate lung ECs.

The method of how to isolate lung ECs is now described in the “Flow cytometry” part of the Methods section.

To take this a step further, what happens if MKs are perfused into the heart-lung model that has been previously fixed with PFA and flushed? Can platelets be generated by a passive endothelium?

We thank the reviewer for this suggested experiment, which is certainly of interest. We have tried to perform it several times, but experimentally it is difficult. The reason is that after perfusion of the tissue with PFA for 10 mins, its compliance and elasticity is markedly reduced. This meant that when we tried cannulating the right ventricle/pulmonary artery, the seal around the influx cannula was poor. In non-fixed tissue, we get a good seal because the tissue effectively closes up around the needle/cannula site (see comparison figures below), forming an effective seal. In the PFA-fixed tissue this was not the case, and there was substantial leakage of medium when fluid was perfused in. We could not therefore effectively generate enough pressure to allow perfusion of the vasculature for the experiment.



5. Also, if the microfluidic chamber is kept under N₂ during perfusion, does this change the final platelet release ratio?

Thank you for this question, which is an interesting one. We have gone back to conduct the generation experiment in the chamber under N₂, as suggested, and the new data are now shown in Fig. 3e. Importantly, the generation was reduced to almost zero, as in the lung system, indicating more clearly the critical role of oxygenation of megakaryocytes, specifically, in platelet generation. We have therefore included additional text in Results section.

6. Figure 4a: Please show the non-activated control platelets to see the baseline for Jon/A-PE and CD62P labeling.

We now show the levels of integrin activation and P-selectin expression on resting platelets in Fig 5a.

If the mean \pm SEM, as indicated in the legend, is reported here, then the experiment is very heterogeneous, especially with the generated platelets. The authors should also show the individual points and discuss why some batches of generated platelets are less able to be activated.

In the original submission we had shown S.D. rather than S.E.M. We have now changed the graph to show S.E.M. and have included individual datapoints as requested.

In Fig. 3b, there appear to be 2 populations of generated platelets with different sizes rather than a continuum, while still being different from native platelets. Do these 2 populations respond differently to agonist stimulation?

We agree with the reviewer that there are two apparent subpopulations of generated platelets, according to their size, and we have now explained this in the legend of Fig. 4b.

The subpopulation with the larger size were more responsive, by comparison with the smaller subpopulation, to thrombin and CRP in both integrin α IIb β 3 activation and P-selectin expression. These data are now shown in a modified Fig. 5a.

7. Figure 4d. It would be useful to also have the bright field to visualize platelet thrombi.

We agree and have now included a brightfield image from a middle plane of the thrombus, in the righthand panel of Fig. 5c.

In the text, the authors mention that the generated platelets are "white", whereas in the fluorescent image, the blue is visible but not the white. Please make it clearer.

We agree and have now corrected it by changing "white" to "blue".

8. Figure 5a: The authors mention the presence of a naked nucleus. It could be very interesting to verify whether this is really a naked nucleus or a nucleus surrounded by a plasma membrane. In erythrocytes, for example, the nucleus is lost when it is extruded as a pyrenocyte, a nucleus surrounded by a plasma membrane that exposes phosphatidylserine on its surface to attract macrophages. This can be assessed by non-specifically labeling the plasma membrane or by performing TEM.

We agree with the analysis of the reviewer. We find both situations and have expanded Fig. 6a (original Fig. 5a) and Supplementary Movie 9 where we had already shown images of nuclei that are genuinely naked, but now include a representative image of ones that are surrounded by thin/patchy CD41-stained membrane. In fact, the nucleus shown in lefthand panel also shows a thin staining of CD41 around the nucleus.

9. Throughout the discussion, the authors suggest that under normal conditions, whole MKs enter the lungs to release platelets, and that lung defects prevent MKs from being fragmented into platelets, resulting in higher numbers of MKs in patients with lung disease.

The literature to which we referred (Ref.30-33) showed variable platelet counts in individuals with lung pathologies or individuals living at high altitude. In other words that there is no consistent effect on platelet number by these conditions, and that the explanation for this is likely to be the complexity of the platelet generation process, in lung and marrow. In lung vasculature, we had described 4 factors which may influence the ability of MKs to generate platelets: oxygenation, ventilation, endothelial cells and structure of the lung microvasculature. Changes in one of these factors may therefore be compensated for by changes in other factors.

What is the evidence for significant transmigration of whole MKs under homeostatic conditions? We agree that it will be important to address this question in a future study, because clearly we would like to know the relative significance of platelet generation in the lung versus the bone marrow, in physiological conditions, in humans *in vivo*. For this question in mouse, this is more clearly defined, for example in Junt et al. (Ref.29) and Fig. 8, where it has been easier to identify whole MKs in the circulation.

Have the authors quantified the fraction of MK nuclei in the mouse lungs versus MKs in the marrow? The authors should consider that the passage of whole MKs into the circulation might rather be a rare event under physiological conditions, which is greatly increased during inflammatory reactions, especially as reported during a viral infection such as Covid19, explaining the higher amount of MKs in the lungs (and other organs). This does not question the fact that the lungs are key to the release of platelets from MK fragments that enter the marrow vasculature.

We have not determined the fraction of MK nuclei in the mouse lung versus the marrow, mainly because our study addresses an *ex vivo* and *in vitro* approach to generate platelets, but also because in the *in vivo* setting these MK nuclei are likely to be removed rapidly by tissue macrophages, making this analysis difficult to interpret.

Minor points.

Page1 line 65, from the recent literature it seems that contrary to what is written, platelets produced *in vitro* are now able to satisfactorily respond to agonists.

The problem in the field generally now is to generate large numbers of platelets per MK, that are also functional. In fact, all current publications cite numbers of platelets generated per MK as being very low, and all under 100 platelets per MK. A smaller number of these publications indicate functionality, but although these may show functionality, this is associated with a very low production efficiency (platelets per MK). So, we have rephrased this line in the Abstract and Introduction to reflect this.

The scale of the bar in Supplemental Figure 1 is lacking.

We have now added the description of the scale bar to the legend of Supplement Fig 1d.

The schema of the microfluidic chamber (right panel) is not so clear. Could you indicate the flow direction and also provide a photomicrograph?

Thank you, and these have now been provided in Fig. 3c.

Figure 5b: Please use the same scale for the graph as the one in Fig. 5b to help compare the bar size.

Thank you, and we have now amended all the scale bars throughout the manuscript to make them all comparable.

Statistics: why use paired t-test? some data clearly do not present a normal distribution; hence the tests should be adjusted accordingly.

We agree that, the data shown for platelet size in Fig. 4b for generated platelets, the distribution is not Gaussian. We have therefore ensured that we have applied normality testing to all datasets in the manuscript, and have applied appropriate tests, as described now in the revised Methods: A value of $p < 0.05$ was considered statistically significant and was determined using either unpaired t-test for normally distributed data (comparison of two groups) or Mann-Whitney U test for non-normally distributed data (comparison of two groups) or two-way ANOVA with Tukey's multiple comparisons test, as indicated in figure legends. Choice of test was determined by assessment of normality of data (Kolmogorov-Smirnov analysis), and whether single or multiple comparison was required. We have included details of the test used in the individual figure legends.

Reviewer #2 (Remarks to the Author):

The focus of this manuscript by Zhao and colleagues is on mechanisms by which megakaryocytes release platelets in the lung vasculature. There is ample indirect and direct *in vivo* evidence that the lung plays a major role in thrombopoiesis, but the mechanisms involved have not been fully elucidated. The authors use an *ex vivo* lung-heart block to repeatedly infuse megakaryocytes through the lung vasculature and they observed that megakaryocytes can repeatedly passage through the lung with increasing platelet production and progressive enucleation. The final component of this process is dependent on the actin regulator, TPM4.

Major criticisms:

1. Some references are missing on the role of the lung in platelet production, such as those by the Poncz group where they injected megakaryocytes intravenously and showed that the lung is capable of functional platelet production (PMID: 20972336; PMID: 25852052).

We now have included these two references (Ref 14 -15) in Introduction section.

2. More detail is needed on the lung-heart block set-up. For example, with the ventilation, was end-expiratory pressure applied, like is conventionally done in the mechanical ventilation of mouse or human lungs? If not, this could promote end-expiratory lung collapse and shunting.

We have now added this additional detail to the Methods section on mouse *ex vivo* lung-heart preparation. To avoid end-expiratory lung collapse, as indicated in Fig 1a, the connector for expiration air was connected to a Gottlieb valve (tube immersed in water; immersion 2-3 cm depth to induce a positive end-expiratory pressure).

Megakaryocytes were “pumped into the right ventricle” per the Methods section. Was this just a push of the syringe or were they placed into the perfusion pump and infused at 0.35 ml/min per the Methods?

This has been correctly described now in the Methods section also, on mouse *ex vivo* lung-heart preparation.

How was this infusion rate selected and is it physiologic? This is relevant regarding perfusion pressures and shear stress in the lung microvasculature.

The flow rate we used in our experiments achieves a pressure of 2.1–3.5 mmHg, as measured by a pressure transducer as shown in Fig. 1a. This is substantially lower than physiological pressures in the mouse pulmonary artery, which has been estimated to be 25 mmHg. We have added this to the text of the Methods section in the manuscript.

3. Where is the evidence for the statement that “MKs substantially, rapidly and reversibly, deform their shape to passage through the capillary network of the lung.” Direct imaging evidence is needed to support this statement as it does stretch credulity that MKs of up to 100 μm in size could squeeze through a lung capillary segment that is on average 5 μm in diameter and sometimes smaller.

Our Fig. 1b and 1c data show that we can recover intact MKs in perfusates of lung vasculature *ex vivo* and *in vivo*. We have interpreted this as meaning that these large cells deform their shape to progress through the microvasculature, and indeed *in vivo* imaging of MKs in bone marrow sinusoids, for example, indicates that they are capable of substantial change in shape and appear in the vasculature (reference to Brown et al⁶, and Junt et al²⁹ and to intravital imaging in bone marrow in Fig. 8 and Supplementary 13-14). However, although we cannot think of alternative explanations for interpretation of these data, we agree that we lack direct imaging data here, which would form a major new piece of work. For this reason, we have removed this statement from the manuscript.

4. Overall, the study has merit for advancing methodology for the *in vitro* production of platelets but in terms of advancing concepts of homeostatic, *in vivo* platelet production in the lung, the limitations of the *ex vivo* heart-lung perfusion setup with the lack of a systemic circulation are problematic.

We agree that this work advances our understanding and development of systems to generate platelets *in vitro*, and also agree that it will be important now to determine the relative role of pulmonary intravascular platelet generation in the *in vivo* setting, both in the mouse model system but also importantly in the human. However, the merits of the *ex vivo* system we have developed here, and the *in vitro* microfluidic model, have allowed us to understand details of platelet generation that had previously not been known, and also will serve as a platform for further discovery science into the molecular and cellular processes, as well as potentially for development of larger scale platelet generation systems with human cells. These are all future developments that can springboard from the work presented in this manuscript.

Reviewer #3 (Remarks to the Author):

There has been a debate over the last 130 years as to where the tiny (3 μ diameter) anucleate platelets are released from very large (100 μ diameter) multinucleated megakaryocytes, a process called thrombopoiesis. The majority camp says that this occurs in the bone marrow venous sinuses, but a persistent minority says it is also (or mostly) the lungs. This argument is of importance for reasons including strategies applicable to providing non-donor-derived platelet transfusions.

This manuscript by Xiaojuan Zhao, et al., “Highly efficient platelet generation in lung vasculature reproduced by microfluidics” focuses on a technical tour-de-force mouse model of repeatedly reinfused murine megakaryocytes into a heart-lung controlled model, resulting in the release of a large number of platelets. The model provides further support to the *in situ* pulmonary observations made by E Lefrançois in Nature that bone marrow-derived megakaryocytes migrate to the lung to release platelets. Moreover, if correct, it also provides two new important insights into this process: 1) thrombopoiesis is not a one-and-done process, but requires multiple recycling of the processed megakaryocytes to release all of the platelets. 2) That the pulmonary bed may be unique in this process because of air exchange and the endothelial lining and the process of ventilation. There are significant issues with this paper though:

1. The model is under-detailed for a full critical review.

Critical details as to what is left circulating after the mouse is prepped and their blood is washed out is missing and should be included in a Supplement.

What are the blood counts in the animals under study as part of the observed outcome may be due to severe anemia and hypoxic injury within and without the lung-heart model. Is there DIC for example. Was it measured?

Is the heart still functional and beating or is blood flow through the lungs all regulated by an artificial pump? One would expect a nonfunctioning heart to develop intramural thrombi.

We thank the reviewer for these comments. All the experiments in the manuscript are based on an *ex vivo* model, not an *in vivo* one, where the animal is first sacrificed before the heart-lung vasculature is isolated *in situ* and perfused.

So, the experimental details are described for this *ex vivo* model, and for this reason there is no remaining circulation because the heart is no longer pumping. Because of this, there are also no associated blood counts for these preparations, and there are no intramural thrombi in the heart as well. This is because the fluid we perfuse through the system is not blood but rather megakaryocytes in suspension in cell culture medium. Also, prior to the perfusion we flush the vasculature with heparinized Krebs-HEPES buffer (detailed in the Methods section), therefore the chances of any clotting in the system are minimized.

We have provided additional details of our experimental approach, in Fig. 1a and in the Methods section. These details include how we ensure that the lung does not collapse by including end-expiratory positive pressure. We have also included measurement of perfusion pressures to ensure that this is not so high that it would damage pulmonary vasculature or structure.

How long is each experiment if you recycle the blood 18 times? What are the details of each recycle? Is the reperfused sample hypoxic during this process or reoxygenated.

For these experiments we suspend megakaryocytes in 2mLs medium, and perfuse these cells through the lung vasculature at 0.35 mL/min. Each passage through the lung-heart model therefore takes approximately 5-6 mins. The full time for 18 passages therefore takes approximately 2 hours. This point has been highlighted in the Results section of the text. During all this time, as samples perfuse, the lung is artificially ventilated with air (or in some experiments not ventilated, or ventilated with pure N₂, as described).

In some experiment an anti-platelet antibody was given, presumably in addition to the blood washout to decrease native platelet levels? Why this added step and what were the final platelet

counts with and without this treatment? Wouldn't the antibody also bind to the infused megakaryocytes and the generated platelets?

Here we use antibodies to label infused megakaryocytes, prior to perfusion through the lung vasculature, in our *ex vivo* lung-heart preparation. So, the antibodies are not used to decrease any native platelet levels, but simply to mark the megakaryocytes, and platelets generated from them, so that we may be able to recognize them subsequently by FACS or imaging approaches.

2. There are other biological questions about the data and its interpretation. The anti-CD41 antibody should label the alpha granules as well as the megakaryocyte surface but that was not apparent in the images. No granules were noted.

We labelled the megakaryocytes (MKs) with anti-CD41 antibodies, so as to mark the membrane of the MKs. We found that incubation of MKs with labelled anti-CD41 for 3 hours marks both the surface plasma membrane, but also allows time for the antibody to penetrate through surface-connected canalicular system to the internal membrane of the demarcation membrane system (DMS), which acts the reservoir for membranes for the generated platelets. So, since there is no permeabilization of the MKs, it is not possible for the labelled antibody to reach the alpha-granules, and this is why we do not see granule staining, using this protocol.

Furthermore, if this is an intact anti-CD41 antibody, it may also activate the megakaryocytes and generated platelets and often a F(ab)₂ fragment needs to be used instead in *in vivo* mouse models. In this study we have only used mouse MKs, which lack expression of Fc receptor FcγRIIA, unlike their human counterpart. So, for the mouse system in *ex vivo*, we are able to use intact antibodies without the possibility of activation of the MKs or their derived platelets.

It is also concerning that under N2 that the pulmonary endothelium was uninjured and still functional. Markers of apoptosis should have been investigated compared to controls in the various stages and should have shown injury at least under the marked hypoxic condition of N2 ventilation for a significant time window. The data saying that the endothelium was healthy is thus a concern and also goes against the video of the lungs in the N2 mouse, which clearly shows a large thrombus. We thank the reviewer for these comments. All the experiments in the manuscript are based on an *ex vivo* model, not an *in vivo* one.

In Fig. 3a and b, we address the health status of the endothelial cells in the system upon exposure to N2. We showed that their viability, as determined by retention of the vital dye Calcein Deep Red, was normal. However, the cells are clearly under some degree of stress, because the mitochondrial membrane potential, as measured by the fluorescence dye tetramethyl rhodamine methyl ester (TMRM), was decreased by comparison with air-ventilated lung-derived endothelial cells.

TMRM (and related molecules, such as Tetramethylrhodamine, ethyl ester (TMRE)) is used as a dye to distinguish dead and apoptotic cells from live and non-apoptotic cells (e.g. Barteneva et al. 2014, J Histochem Cytochem. 62(4): 265–275), and so the majority of cells in our analysis have been shown to be viable and non-apoptotic.

The large fluorescent objects that can be seen in lung structure in N2-ventilated lungs are not thrombi, but rather are clusters of MKs.

3. The videos are technically problematic. There are a number of mislabeled videos, especially internal within the videos. Most of these videos are highly pixelated, making data interpretation

difficult and the two-photon microscopy does not contribute to better-quality prior videos by Junt and Massberg.

We have now addressed the issues with the videos, which are now saved in a different file format so as not to lose resolution or pixel density. The labelling is now correct for all videos.

The paper by Junt et al, 2007, shows imaging of MKs in mouse marrow in living tissue. This differs from the model we have established, which is *ex vivo* (not *in vivo*) in mouse pulmonary vasculature. We have used two-photon microscopy to image lung after perfusion of MKs into the pulmonary vasculature, to determine numbers of MKs lodged in that vasculature and generated platelets retained there. This imaging is of fixed lung tissue, not live cell imaging.

4. Platelet-generating device in Fig. 3C platelet is noncontributory to the bottom line message nor is it well-developed to explain how it is informed by the heart-lung model or tests distinct aspects of the pulmonary bed (especially oxygenation and ventilation. At a minimum it should be in the supplement and a photograph of the device and a high-quality video of thrombopoiesis are needed. Finally having shown that one can infuse MKs into recipients and have functional platelets released, the authors then punt to a device for clinical platelet transfusion instead of completing the circle of their thought and suggest that infused MKs may be an alternative therapy.

This microfluidic chamber was used to mimic the flow of MKs in the capillary bed of the pulmonary vasculature. In this way, particularly because there is no mechanical ventilation or endothelium in this system, was helpful to determine the relative contribution of these elements in platelet generation. The chambers are made from PDMS, which is a gas-permeable structure, and has also enabled us to address the role of oxygenation, in isolation from other factors, as now shown in the new Fig. 3e where N₂ replacement of air ablates platelet generation. We have also provided a further diagram of the details of the microfluidic device, plus a photomicrograph (Fig. 3c).

5. The presentation is repetitive at points and often imprecise. The discussion is too long and cumbersome.

The work presented has been complexed to perform and therefore details were needed in the descriptions. The data show several novel findings, including demonstration of passage of MKs through pulmonary vasculature, enucleation of MKs as part of the platelet generation process, a critical role for oxygenation shown in both the *ex vivo* lung preparation and the microfluidic chamber and the generation of very large numbers of platelets from MKs *in vitro*. These novel findings needed detailed presentation and discussion, and the text falls within the word limit for the journal.

REVIEWER COMMENTS

Reviewer #1 (Remarks to the Author):

I thank the authors who responded satisfactorily to all my comments and the manuscript is acceptable for publication

Reviewer #2 (Remarks to the Author):

Thank you for the responses. The details of the heart-lung prep are now much clearer. I have one remaining question. Did the application of the end-expiration device (Gottlieb valve) affect any of the results such as those in Figure 1b or Figure 2a? If possible, data should be shown with and without the device.

Reviewer #3 (Remarks to the Author):

This revised manuscript by Zhao, X, et al “Highly efficient platelet generation in lung vasculature reproduced by microfluidics” is an innovative examination of the process by which the lungs release platelets from megakaryocytes that should be impactful to readers interested in hematopoiesis and platelet biology and may also have impact on clinical platelet transfusions. The manuscript focuses on two complementary systems, a mouse heart-lung model where efflux containing megakaryocytes are reinfused up to 18 times and a microfluidic device to try to simulate the lungs.

Overall, the demonstration that megakaryocytes require multiple passage through the lungs to release platelets is convincing as are the studies on the subsequent processing of the cytoplasmic fragments to functional platelet-like particles.

There were a few concerns that need to be addressed in these studies:

1) In Fig 1d, why is that P1 window more “plt-like” at 0 passages and the P2 larger after 18 passages. Seems the reverse of what to expect.

2) In Fig 1f, annexin v or p-selectin or Jon A binding would have been useful and more commonly done to show that you were generating “happy” platelets.

3) While EC injury/death by inhalation of nitrogen or no ventilation is mentioned, it needs to be given more equal time as a possible explanation in the Results and Discussion for why platelet formation was not seen. Staining for surface markers compatible with endothelial injury like loss of surface thrombomodulin or extrusion of VWF would have been important.

The microfluidic studies are complementary but not as well developed.

1) The similarity between the microfluidic design and lung vasculature is not demonstrated and the discussion should be altered to reflect that especially as no other design was studied.

2) The device has no endothelial lining and that limitation and its implications discussed.

3) Fig 3 was shown with no mouse platelet control and that would have been an important comparative. Again, markers of activated platelets should have been measured.

The manuscript with additional comments is hopefully also returned.

1 **Highly efficient platelet generation in lung vasculature**
2 **reproduced by microfluidics**

3 Xiaojuan Zhao^{1*}, Dominic Alibhai², Tony G. Walsh¹, Nathalie Tarassova¹, Maximilian
4 Englert³, Semra Z. Birol¹, Yong Li¹, Christopher M. Williams¹, Chris R. Neal², Philipp
5 Burkard³, **Stephen J. Cross²**, Elizabeth W. Aitken¹, Amie K. Waller⁴, Jose Ballester-Beltran⁴,
6 Peter W. Gunning⁵, Edna C. Hardeman⁵, Ejaiife O. Agbani⁶, Bernhard Nieswandt³, Ingeborg
7 Hers¹, Cedric Ghevaert⁴ & Alastair W. Poole^{1*}

8
9 ¹School of Physiology, Pharmacology and Neuroscience, Biomedical Sciences Building,
10 University of Bristol, Bristol, BS8 1TD, UK.

11 ²Wolfson Bioimaging Facility, Biomedical Sciences Building, University of Bristol, Bristol,
12 BS8 1TD, UK.

13 ³Institute of Experimental Biomedicine, University Hospital Würzburg, and Rudolf Virchow
14 Center for Integrative and Translational Bioimaging, University of Würzburg, Würzburg,
15 97070, Germany.

16 ⁴University of Cambridge / NHS Blood and Transplant, Wellcome-MRC Cambridge Stem Cell
17 Institute, Jeffrey Cheah Biomedical Centre, Cambridge Biomedical Campus, University of
18 Cambridge, Cambridge, CB2 0AW, UK.

19 ⁵School of Medical Sciences, University of New South Wales, Sydney, NSW 2052, Australia.

20 ⁶Cumming School of Medicine, University of Calgary, Calgary, AB, T2N 1N4, Canada.

21
22 *** Correspondence and requests for materials should be addressed to X. Z. (email:**
23 **xz14926@bristol.ac.uk) or to A.W. P. (email: A.Poole@bristol.ac.uk).**

26 **Abstract**

27 Platelets, small hemostatic blood cells, are derived from megakaryocytes. Both bone marrow
28 and lung are principal sites of thrombopoiesis although underlying mechanisms remain unclear.

29 **Outside the body, however, our ability to generate large number of functional platelets is poor.**

30 Here we show that perfusion of megakaryocytes *ex vivo* through the mouse lung vasculature
31 generates substantial platelet numbers, up to 3,000 per megakaryocyte. Despite their large size,
32 megakaryocytes were able repeatedly to passage through the lung vasculature, leading to
33 enucleation and subsequent platelet generation intravascularly. Using *ex vivo* lung and an *in*
34 *vitro* microfluidic chamber we determined how oxygenation, ventilation, healthy pulmonary
35 endothelium and the microvascular structure support thrombopoiesis. We also show a critical
36 role for the actin regulator Tropomyosin 4 in the final steps of platelet formation in lung
37 vasculature. This work reveals the mechanisms of thrombopoiesis in lung vasculature and
38 informs new approaches to large-scale generation of platelets.

39

40

41

42

43

44

45

46

47

48

49

50

51

52 **Introduction**

53 Platelets are small anucleate blood cells^{1,2}, with critical roles in hemostasis, thrombosis,
54 inflammation, vascularization, innate immunity and tissue regeneration^{3,4}. Platelets are formed
55 from mature polyploid megakaryocytes (MKs), their precursor cells⁵, although the process of
56 their generation remains incompletely understood^{6,7}. *In vitro* studies suggest that dynamic
57 changes⁸ and regulation⁹ in the actin cytoskeleton play important roles in platelet production
58 from MKs.

59 Bone marrow is proposed to be the main site of MK maturation and platelet production,
60 however much of the evidence since the original observations in 1893 are indirect. MKs have
61 been observed within lung tissue or vasculature¹⁰, and more platelets and fewer MKs have been
62 shown to be in the blood exiting the lungs compared to blood entering the lungs^{11,12}, supporting
63 the concept that platelet generation may take place from circulating MKs in the lung
64 vasculature. Recently, direct evidence presented by Lefrancais et al. has shown that the lung
65 is a primary site of platelet biogenesis¹³. **Data from the Poncz group also show that**
66 **intravenously infused murine¹⁴ or human MKs¹⁵ release functional platelets within the lungs**
67 **of recipient mice.** However, the mechanisms underlying platelet biogenesis in the lung
68 vasculature have not been explored.

69 *In vitro*-derived platelets, as an alternative to native platelets, are attractive for fundamental
70 research because of their rapid genetic tractability, as vectors for drug and genetic component
71 delivery¹⁶ and in clinical platelet transfusion. **At present, however, the inability to generate**
72 **large number of functional platelets efficiently *in vitro* is a major obstacle.**

73 **In this work,** we established an *ex vivo* mouse heart-lung model (Fig.1a) through which we
74 were able to perfuse murine MKs. Remarkably, we could show for the first time that MKs,
75 despite their large size (50-100 μm)⁵, can pass multiple times through the lung vasculature, and
76 that this leads to the generation of very large number of fully functional platelets (up to 3,000
77 per MK^{6,17}). Using this system and a novel *in vitro* microfluidic chamber we show roles for

78 oxygenation, physical ventilation, healthy pulmonary endothelium and the microvascular
79 structure in platelet generation, demonstrating how the lung may be uniquely suited to
80 thrombopoiesis. Our data show that MKs undergo enucleation upon repeated passage through
81 the pulmonary vasculature prior to platelet generation, with the final steps dependent on the
82 actin regulator Tropomyosin 4 (TPM4). This contrasts with our observations of MK behaviour
83 in the bone marrow, which looks similar to WT controls, suggesting distinct mechanisms of
84 thrombopoiesis in the lung vasculature versus the bone marrow. Altogether, our study advances
85 our understanding of platelet formation and establishes a novel approach to generate large
86 number of them outside the body.

87

88 **Results**

89 **Efficient platelet generation in lung vasculature *ex vivo***

90 The lung has been proposed as a site of platelet generation by several groups periodically, there
91 is now a need to understand the mechanism underlying this platelet generation. For this reason,
92 we established an *ex vivo* mouse heart-lung model (Fig.1a) through which we were able to
93 perfuse murine MKs. The *ex vivo* mouse heart-lung model is based upon isolating the heart and
94 lungs as a single unit, ligating the venae cavae and the aortic arch and perfusing prestained
95 mature MKs (Supplementary Fig.1b shows DNA ploidy analysis for cultured mature MKs,
96 Supplementary Fig.1c shows the diameters of perfused MKs, Supplementary Fig.1d shows
97 staining of demarcation membrane system (DMS) with PE- or FITC- conjugated CD41 and
98 nuclei with Hoechst 33342, respectively) through the pulmonary circulation from the right
99 ventricle, collecting the perfusate from the left ventricle. This allows quantitation and imaging
100 of cells passaged through the pulmonary vasculature. In the first instance, lungs were
101 artificially ventilated with air. We were expecting that the vast majority of MKs would be
102 trapped within the lung vasculature due to their large size (around 50-100 μm diameter)⁵, but
103 unexpectedly more than 50% of the intact MKs (showing a circular shape and central nucleus)

WHERE'S SUPPL. FIG. 1A IN TEXT?

104 emerged in the perfusate after the first passage (Fig.1b). The perfusate could be re-injected
 105 through the lungs and upon multiple passages the numbers of intact MKs in the perfusate
 106 continued to decrease (Supplementary Fig.1a shows the experimental flowchart). We also
 107 demonstrated that intact mouse MKs could pass through the pulmonary vasculature *in vivo*, as
 108 intact mouse MKs prestained with CellTracker™ Red CMTPX dye and Hoescht 33342 could
 109 appear in the blood of the left common carotid artery of an anaesthetized recipient C57BL/6
 110 after being infused into the right external jugular vein (Fig.1c). It was also apparent that CD41-
 111 labelled particles also appeared in the perfusate that were similar in size and granularity to
 112 mouse platelets. We term these “generated” platelets (CD41-positive events in gate P1 in
 113 Fig.1d). The generated platelets were *bona fide* live platelets rather than cellular fragments,
 114 using the vital dye calcein-AM (Fig.1e) and showing mitochondrial membrane potential
 115 comparable to normal mouse platelets using tetramethyl rhodamine methyl ester (TMRM, an
 116 indicator of healthy cells, determined by accumulation of TMRM in active mitochondria)
 117 (Fig.1f-g). Generated platelets were anuclear, showing no staining with the DNA dye Draq5
 118 (Fig.1e). The numbers of generated platelets per MK gradually increased with increasing
 119 passages, up to around 932.6 ± 138.4 platelets/MK after 18 passages (Fig.2a and c). Two-
 120 photon microscopy of **fixed lung** sections after 18 passages showed that **many generated**
 121 **platelets could be seen** in the lung microvasculature (Fig. 2b and Supplementary Movies 1-3).
 122 These were quantified in a defined lung volume and the total lung volume measured using a
 123 fluid displacement method (Supplementary Fig.1e) to estimate numbers of retained platelets.
 124 We calculated this to be 2066.0 ± 274.7 per MK injected (Fig. 2c). Adding this to the number
 125 contained in the perfusate (Fig. 2a and c), we estimate that after 18 passages through the lung
 126 approximately 2998.3 ± 270.2 platelets were generated per MK (Fig.2c), in keeping with
 127 previous estimates that each MK *in vivo* produces approximately 1000-4000 platelets^{6,17}.
 128 Platelets were not generated simply as a consequence of passage through small-bore needles,
 129 since we showed that repeated passage of MKs through 21G needles 18 times is not sufficient

WHAT IS P2 THAT
 APPEARS TO BE
 THE DOMINANT
 SPECIES
 AFTER 18 PASSAGES?

SHOULD'VE
 MEASURED
 ANNEXIN V OR
 P-SELECTIN
 SURFACE
 LEVELS OR
 JON-A TO SHOW
 THAT THESE AREN'T
 ACTIVATED
 CYTOPLASMIC
 FRAGMENTS

130 to generate platelets (Fig. 2c). Altogether, we could generate physiological numbers of platelets
131 after multiple recirculation of MKs through the lung microvasculature.

132 **Mechanisms of platelet generation in mouse vasculature**

133 The *ex vivo* mouse heart-lung model (Fig. 1a) can be a useful tool to allow artificial ventilation
134 with either ambient air or with pure nitrogen, or no ventilation, to assess the roles of physical
135 ventilation and gaseous oxygen in regulating MK biology and thrombogenesis. We first
136 explored whether air ventilation is essential for platelet generation in our model. In the absence
137 of ventilation, the numbers of platelets generated per MK in the perfusate still gradually
138 increased with increasing passages (498.4 ± 117.9 platelets/MK, Fig. 2a), but the numbers
139 generated were substantially lower than in the air-ventilated condition. Two-photon
140 microscopy of fixed lung sections after 18 passages showed that fewer **generated platelets could**
141 **be seen** in the lung microvasculature (Fig. 2b and Supplementary Movie 4), compared to the
142 air-ventilated lung. Therefore this indicates that air ventilation is important in platelet
143 generation in the lung, but may result either from an effect directly on MKs and/or through an
144 effect on endothelial viability. Pulmonary endothelial cells (ECs), which play key roles in gas
145 exchange in the lung¹⁸, interact closely with MKs as they passage through the vasculature. We
146 therefore compared their viabilities (determined by the Calcein Deep Red retention assay) and
147 mitochondrial membrane potential in the lungs under air ventilation or unventilated conditions
148 **for approximately 2 hours**. Surprisingly, ECs from preparations of unventilated lungs were
149 fully viable, and comparable with those ventilated under air (Fig. 3a). However, the mean
150 intensity of TMRM of ECs from unventilated lungs was approximately half that of air-
151 ventilated lung or fresh lung (Fig. 3b).

152 Strikingly, when lungs are ventilated with pure nitrogen to completely de-oxygenate the heart-
153 lung preparation, the number of generated platelets in the perfusate was almost ablated, reduced
154 to just 43.1 ± 16.7 platelets/MK after 18 passages (Fig. 2a). Two-photon imaging of nitrogen-
155 ventilated lungs showed mature MKs were trapped in the lung vasculature (Fig. 2b and

156 Supplementary Movie 5), a feature not observed under air ventilation or unventilated lung.
157 Importantly, the mean intensity of endothelial cell TMRM was approximately halved by
158 nitrogen-ventilation relative to air-ventilated controls, and equivalent to the unventilated lung
159 (Fig.3b).

NEED TO BE CAREFUL HERE. SHOW FSC COMPARE TO DONOR PLTS AND NEED TO MEASURE
MARKER OF ACTIVATION (EG, ANNEXIN V) TO MAKE YOUR STATEMENT OR NEED TO MODIFY STATEMENT.
ALSO IS THIS A SIZE SELECTED STUDY. NO BIG MKS DRAQ5 POSITIVE COME THROUGH?

160 To further verify whether the structural arrangement of the lung capillary bed could mediate
161 platelet generation, we designed a polydimethylsiloxane (PDMS)-based (gas permeable)
162 microfluidic chamber with channel arrangement mimicking tissue microcirculation. The
163 channels were of uniform depth of 10 μm throughout, where the entry and exit channels had a
164 width of 100 μm and where branches emerged halving the channel width each time, to a
165 minimal width of 12.5 μm , as per the diagram shown in Fig.3c. This channel arrangement
166 allowed us to flow through cells and determine platelet generation in the perfusate after
167 repeated passage. Fig.3e shows that the numbers of generated platelets per MK, when MKs are

168 flowed through the microfluidic chamber conditioned in normal air, gradually increased with
169 increasing passages, similar to the numbers generated in the unventilated lung, with $492.3 \pm$
170 47.6 platelets/MK after 18 passages. The generated platelets were live anuclear platelets (Fig.

WHAT DOES THIS
MEAN HERE?
SHOW DONOR PLTS
FOR COMPARIOSN

171 3d). We also conditioned microfluidic chambers with pure nitrogen to completely de-
172 oxygenate them, causing the generation of platelets to be almost ablated, reducing them to 56.4
173 ± 1.4 platelets/MK after 18 passages, similar to those generated in lungs ventilated with pure
174 nitrogen (Fig. 2b). Altogether, these data suggested that (1) air-ventilation and healthy ECs are

175 required for MKs to generate physiological levels of platelets in the heart-lung preparation; (2)
176 the structural arrangement of the pulmonary microcirculation plays a role in platelet generation;

177 (3) lack of ventilation or nitrogen-ventilation for 2 hours caused partial loss of the
178 mitochondrial membrane potential in pulmonary ECs; (4) exclusion of oxygen from either the
179 lung-heart system or the microfluidic system ablates platelet generation.

YOU DIDN'T TEST
THIS HERE, SO
MODIFY YOUR
STATEMENT.

180 **Generated platelets are morphologically and functionally normal**

AGAIN NOT TESTED.
PLEASE MODERATE SENTENCE

DID THE MKS NOW CLOG THE
CHANNELS?

NEED TO MAKE CLEAR THIS IS NOT MICROFLUIDIC "PLTS".

IF THE DATA IS AVAILABLE, WHAT IS THE CHANGE IN THE TWO POPULATIONS WITH RECYCLING NUMBER

181 We next determined whether generated platelets display classical morphology and function.
182 Platelets display an almost uniquely characteristic sub-plasma membrane microtubular ring,
183 running circumferentially in resting platelets^{19,20}. Our generated platelets, immunolabelled for
184 α -tubulin, display this characteristic ring structure (Fig. 4a), and the mean size of the cells is
185 larger than controls ($3.6 \pm 0.2 \mu\text{m}$ vs $1.9 \pm 0.1 \mu\text{m}$, Fig. 4b). However, it is also clear that there
186 appear to be two subpopulations of generated platelets, based on their diameter ranges as shown
187 in Fig. 4b: approx. 33% of generated platelets (diameter range: 1.7-2.4 μm) have sizes similar
188 to control platelets (diameter range: 1.2-2.4 μm) and 67% of generated platelets (diameter
189 ranges: 3.7-5.6 μm) are significantly larger than control platelets. We next visualized the
190 ultrastructure of generated platelets by transmission electron microscopy (TEM, Fig. 4c), after
191 depletion of host platelets using anti-GPIb α antibodies. Generated platelets displayed a discoid
192 shape with classical characteristics including α -granules, dense granules, mitochondria, open
193 canalicular system, and microtubule coils.

194 We then determined the functionality of generated platelets from mouse heart-lung model by
195 comparing against control mouse platelets. Both generated and control platelets showed
196 equivalent responses to agonists (CRP and thrombin) in terms of integrin $\alpha\text{IIb}\beta\text{3}$ activation and
197 degranulation (P-selectin expression, Fig.5a). Given that generated platelets appeared to
198 segregate into two size subpopulations, we then compared the responses in these two
199 subpopulations. The subpopulation with the larger size (diameter ranges: 3.7-5.6 μm) were
200 more responsive, by comparison with the subpopulation with the smaller size, to thrombin and
201 CRP in both integrin $\alpha\text{IIb}\beta\text{3}$ activation and P-selectin expression. It has been shown that larger
202 platelets are more responsive^{21,22}, and our data are therefore consistent with this observation.

203 We next compared the key glycoprotein expression on the surface of generated platelets. The
204 proportion of cells expressing CD61 and CD42b (Supplementary Fig.1g), and the mean
205 fluorescence intensity (MFI) of those markers (Fig.5b), were comparable between generated
206 and control platelets. The MFI of three collagen receptors CD42d²³, CD49b and GPVI²⁴ was

WHERE IS THESE DATA AND WHAT DO "MORE RESPONSIVE" MEAN? IDEALLY, USED AN AGONIST DOSE RESPONSIVENESS

207 higher in generated platelets than controls (Fig.5b), while the proportion of cells expressing
208 these receptors was lower (Supplementary Fig. 1g). **It has been reported that surface expression**
209 **of CD61, CD42b, CD49b and GPVI were higher in larger platelets, commensurate with their**
210 **larger surface area²⁵. The subpopulation of generated platelets with the larger size has higher**
211 **surface expression of CD61,CD42b CD42d, CD49b and GPVI by comparison with the**
212 **subpopulation with the smaller size (Supplementary Fig.1f).**

213 Thrombus formation *in vitro* was also assessed, determining how generated platelets mixed
214 into whole blood interact with a collagen-coated surface under flow. Generated platelets
215 (stained with both DiOC6 and CellTracker™ Red CMTPX dye, **blue**) occupied all levels of the
216 thrombus whilst control platelets (stained with CellTracker™ Red CMTPX dye alone,
217 magenta) were mainly situated on top of the thrombus, suggesting generated platelets showed
218 a higher responsiveness to collagen, or were primary reactors to it (Fig.5c-e and Supplementary
219 Movie 6). This may suggest that generated platelets are early interactors with collagen,
220 displaying the greater adhesive functionality of younger platelets^{21,22}, possibly due to higher
221 levels of collagen adhesive receptors (GPVI and CD49b²⁴, and CD42d²³) (Fig. 5b).

222 **Megakaryocytes undergo enucleation and platelet release intravascularly**

223 We wanted to explore the details of the release of platelets from MKs upon repeated passage
224 through the pulmonary vasculature. The cells in the perfusate were imaged after collected over
225 a defined numbers of passages (0, 1, 2, 3, 6 and 9) (Supplementary Fig.1a), and strikingly, upon
226 repeated passages, MKs gradually move their nuclei to the periphery and subsequently
227 enucleate, generating both naked nuclei and enucleated MKs. Although small numbers of
228 enucleated round MKs were found, we saw the gradual accumulation of larger anuclear objects
229 (>10 µm). Fig. 1b, Fig. 6 and Supplementary Movies 7-10 show the steps involved in the
230 process, with images shown in Fig. 6a, quantified in Fig. 1b and Fig. 6b. As shown in Fig. 1b,
231 the percentage of intact MKs decreased from 53.7% after 1 passage (P1) to 6.7% after 9
232 passages (P9), while in Fig. 6b the percentage of large naked nuclei (>20 µm diameter)

233 increased from 5.0% after P1 to 22.0% after P9. At the same time, large anuclear objects (>10
234 μm) also increased, as a proportion of total MKs and derivatives, from 16.7% after P1 to 45.5%
235 after P9. These data suggested that the large polyploid nucleus moves from a central position
236 to the periphery of the cell, in a process of polarization. The nucleus is then extruded from the
237 cell upon further passages through the lung vasculature, until by approximately 9 passages
238 there are very few nucleated MKs left. After 12 passages, large naked nuclei (>20 μm) also
239 became rare, being replaced by irregular small sub-nuclei. These sub-nuclei appeared
240 connected to each other, probably by membranous structures or thin DNA bridges²⁶ that have
241 been described previously between segregated chromosomes which were too fine for
242 visualization by light microscopy (Fig. 6c and Supplementary Movie 11). **Sub-nuclei were**
243 **characterized by depth (Fig. 6d) , aspect ratio (width: height, Fig. 6e), major axis (Fig. 6f) and**
244 **minor axis (Fig. 6g) all of which decreased substantially with increasing passages (from P3 to**
245 **P18, parameters: depth 8.9 μm to 5.5 μm , aspect ratio 1.8 to 1.1, major axis 14.1 μm to 6.5 μm ,**
246 **minor axis 8.1 μm to 5.7 μm).** The extruded naked nuclei therefore undergo a process of
247 division into multiple component sub-nuclei, which proceed to condense into compact sub-
248 nuclear units with a greater circularity. The anucleate MK proceeds to fragment into platelets
249 after multiple passages, to reach plateau numbers by 15-18 passages (see Fig. 2a). This is the
250 first time these enucleating behaviors have been observed for MKs when releasing platelets.

251 **Tropomyosin 4 is required for platelet generation in lung vasculature**

252 The release of platelets is understood to require cytoskeletal reorganization involving the actin
253 cytoskeleton. Tropomyosins form co-polymers with actin filaments and regulate filament
254 function in an isoform-specific manner²⁷. TPM4 has been shown to have a role in platelet
255 formation. In the *Tpm4*^{-/-} mouse *in vivo*, platelet counts drop by approximately 35% compared
256 to wild-type and with a slightly larger mean platelet volume²⁸. Strikingly however, in our *ex*
257 *vivo* lung system, *Tpm4*^{-/-} MKs generate no platelets in the perfusates (Fig. 7a-b). We therefore
258 wanted to explore the steps in platelet generation requiring TPM4. Compared to wild-type

259 MKs, during the first 3 passages, fewer *Tpm4*^{-/-} MKs underwent transformation to large
 260 anuclear objects (Fig. 7c). However, this represented only a delay in these events, since by 6-
 261 9 passages the numbers of large anuclear objects were comparable with wild-type (Fig. 6b).
 262 Two-photon microscopy of fixed lung sections, after 18 passages, showed abundant anuclear
 263 fluorescent objects, sized ~10 μm (Fig. 7d and Supplementary Movie 12). These data therefore
 264 suggest a small and non-essential role for TPM4 in regulating enucleation, but a critical role in
 265 regulating the final steps of platelet formation and their release into the circulation (summarized
 266 in Fig. 9). This unexpected and striking observation of the critical role for TPM4 in platelet
 267 generation in our heart-lung model, together with the observation that *Tpm4*^{-/-} mice still have
 268 65% of normal platelet numbers, caused us to investigate whether *Tpm4*^{-/-} MKs behave
 269 similarly to WT in the bone marrow. We observed the 4 different MK morphologies described
 270 by Junt et al.²⁹ in the progression of MKs from marrow space to sinusoid equally in WT or
 271 *Tpm4*^{-/-} mice: (i) the majority of *Tpm4*^{-/-} MKs were seen as isolated cells within the bone
 272 marrow space, in close contact with sinusoidal walls; (ii) some MKs within the marrow space
 273 produced extensions into sinusoids; (iii) some MKs were clearly visible wholly within the
 274 sinusoid vessels themselves and had cellular extensions; (iv) some appeared as large fragments
 275 in the sinusoid, releasing heterogeneous structures in the direction of blood flow (Fig. 8 and
 276 Supplementary Movies 13-14). These observations suggested that TPM4 in MKs does not play
 277 an essential role in platelet release in the bone marrow, in contrast to its role in these cells in
 278 the lung vasculature.

I'D SUGGEST MODIFYING THIS. ITS EITHER THAT MK OR LARGE CYTOPLASMIC FRAGMENT RELEASE IS NORMAL IN THE MARROW. PLT FORMATION MAY BE TPM4-DEPENDENT BUT NOT THESE EARLIER PROCESSES THAT CAN GO ON IN BOTH THE MARROW AND LUNGS BUT FINAL PLT FORMATION MAY BE IMPAIRED.

280 Discussion

281 In this study, we established an *ex vivo* pulmonary vascular model, which we show generates
 282 platelets from cultured MKs outside the body with an output similar to estimated *in vivo* MK
 283 capabilities. These generated platelets display classical morphology such as α-tubulin ring, α-
 284 granules, dense granules, mitochondria, and microtubule coils and show comparable

285 functionality to native platelets. The *ex vivo* model therefore provides a useful tool to efficiently
286 generate platelets and explore the mechanisms of platelet generation, and also demonstrates the
287 capability of the lung as a site of platelet generation.

NEITHER WAS TESTED IN THIS PAPER.
THE ONE MICROFLUIDIC DEVICE
DOESN'T TEST VASCULAR STRUCTURE

288 The study presented makes several advances in our understanding of the mechanisms of platelet
289 generation in lung vasculature. First, our data show that ~~there are~~ four factors ^{may} which affect

290 platelet generation from MKs in lung vasculature: oxygenation, physical ventilation, healthy
291 pulmonary endothelium and the microvascular structure. These factors suggest the lung is a

292 ~~primary and unique~~ site for platelet biogenesis. This may partially explain the range of platelet
293 counts reported in patients with lung disease^{30,31} or in people living at altitude^{32,33}. The wide
294 range of platelet counts may be because the process of platelet generation in the lung is
295 complex, with inputs from the four factors we describe and possible redundancy or partial
296 redundancy between these four factors. For example, there may be compensation for low
297 oxygenation by an increase in respiratory rate.

298 Second, in this study, we found that MKs have a substantial ability to reversibly deform to
299 passage through the lung microvasculature, despite the mismatch in size of giant MKs (50-100
300 μm)⁵ and the narrow internal diameter of pulmonary capillaries (mean 5-8 μm)³⁴ which further
301 decrease upon lung ~~inflation~~ ^{deflation?}³⁵. We and others have shown that intact mature MKs can egress
302 from the bone and enter the circulation^{6,36,37} whereupon they find their way to the first
303 microvascular bed in the lung^{38,39}. It has been observed that they will lodge in the pulmonary
304 vasculature where they release platelets, and consistent with this substantial numbers of MKs
305 with reduced cytoplasmic content or no visible cytoplasm (denuded MKs) have been found in
306 aortic circulation^{37,39}. However, whether intact mature MKs can squeeze through the
307 pulmonary circulation and enter the left side of the heart and then the arterial circulation
308 remains unclear. Our data show approximately 50% of infused intact mature MKs (with
309 circular shape and central nuclei) are able to pass through the lung microvasculature after the
310 first passage through the lung in the *ex vivo* model (Fig. 1b). We also demonstrated that intact

311 mouse MKs could pass through the pulmonary vasculature *in vivo* and appear in the blood of
312 the left common carotid artery of an anaesthetized recipient C57BL/6 after being infused into
313 the right external jugular vein (Fig.1c). Interestingly, mature MKs with abundant, finely
314 granular cytoplasm and compact lobulated nucleus have been observed in peripheral blood
315 smears⁴⁰⁻⁴², consistent with our findings. These large cells were usually found at the feathered
316 edge of the peripheral blood smear. Although it is possible that some intact MKs pass through
317 the lung circulation via physiological shunts, these only account for approximately 2% of blood
318 flow through the lung, and therefore the majority of MKs are likely to passage through the
319 capillary bed of the lung. NEED TO BE FAIR & BALANCED AND THE OXYGEN RELATIONSHIP MAY BE
PHYSIOLOGIC AND MK AND/OR EC- DEPENDENT OR ARETIFICIAL DUE TO
ENDOTHELIAL INJURY DUE TO HYPOXIA AND MK ADHERENCE TO THE
INJURED EC AND FURTHER STUDIES ARE NEEDED TO DISTINGUISH THESE.
320 The ability of MKs to pass through the lung microvasculature is oxygen-dependent in our *ex*
321 *vivo* system, as longer term exposure of the lung to pure nitrogen, to completely de-oxygenate
322 the lung over 2 hours, effectively caused MKs to be retained in the lung vasculature. Oxygen-
323 dependent MK motility might partially explain why pulmonary MK levels observed at autopsy
324 are increased in COVID-19 patients who had died with acute lung damage⁴³.
325 Third, we found that giant nuclei extrude from MKs over the process of multiple passages, as
326 part of the process leading to platelet generation, and then divide into multiple component sub-
327 nuclei, and further condense into compact sub-nuclear units. This observation is consistent with
328 the phenomenon that denuded MKs have been found in both the bone marrow and peripheral
329 circulation^{37,44}. The extruded naked giant nuclei are rapidly removed by the mononuclear
330 phagocyte system³⁷ in healthy individuals, but become apparent in people with impaired
331 immunity such as in patients with human immunodeficiency virus (HIV)⁴⁵ and in the lungs of
332 severe Covid-19 patients⁴⁴. Few cells are known to enucleate, but importantly these include
333 erythrocytes. This may be important because MKs and erythrocytes are developmentally
334 closely related, sharing a common precursor, the MK/erythroid progenitor (MEP)^{46,47}, and may
335 therefore indicate a common mechanism.

336 The prevalent model for thrombogenesis, extension of proplatelets and their detachment under
337 flow, proposes that MKs extend long (>100 μm) branched processes that appear “beaded” by
338 virtue of intermediate swellings⁴⁸, and then undergo reorganization into platelets. However, in
339 our intravascular model the data show that after extruding their nuclei, MKs generate smaller
340 and smaller fragments, eventually forming platelets. Mature MKs first fragmenting into large
341 anuclear structures in our heart-lung model is consistent with Junt’s study in bone marrow *in* AS WELL AS
342 *vivo* which showed MKs shedding large cytoplasmic fragments at the vascular niche in the INTACT MK!
343 bone marrow and almost all MK fragments releasing into the vasculature were 10 to 100 times
344 as large as circulating platelets²⁹. Some of these elements may well be proplatelets, which form
345 an intermediate structure on the path from large anuclear MKs finally to generate platelets.

346 Fourth, multiple passage of MKs through the pulmonary vasculature in the *ex vivo* lung model
347 is crucial to induce a reproducible sequence of events (Fig. 9). These include enucleation,
348 enucleation may precede pit formation, but these events need not and can be parallel events
nuclear fragmentation and condensation, prior to efficient platelet generation. This might
349 suggest an essential and dynamic conversation between the pulmonary microvasculature and
350 MKs, a process effectively of ‘education’. This education is required to induce reversible
351 deformation of MKs, stimulate their motility through the microvasculature and drive platelets
352 release. However, since some MKs pass through the pulmonary vasculature, it is possible that
353 some platelet generation may take place in other organs of the body, such as spleen⁴⁹. This is
354 supported by the observation that we can generate substantial numbers of platelets by passage
355 NO PROOF PROVIDED THAT THE MICROFLUIDIC SYSTEM USED MIMICS THE LUNG VASCULATURE. ONLY 1
MODEL TESTED. PLEASE REWORD TO BE LESS DOGMATIC.
of MKs through the microfluidic chamber that mimics the microvasculature. This *in vitro*
356 system lacks endothelium and physical ventilation but retains an architecture that approximates
357 ~~to~~ the microvasculature. Production of platelets in the microfluidic chamber is about one sixth
358 of that produced in the *ex vivo* lung model (492.3 platelets per MK by microfluidic chamber vs
359 2998.3 per MK generated in pulmonary vascular model) (Fig.2c and Fig.3e). This suggests that
360 there is synergy between the features of the lung vasculature that makes this organ likely to be

361 an important site of vascular production of platelets, but also suggests that platelet production
362 can still take place, less efficiently, if not all features are present.

363 The lung is an important site of platelet generation, with reports of production ranging from 7-
364 17% of total body platelets¹⁷ to 50%¹³. Mice lacking *TPM4* in the MK lineage display
365 macrothrombocytopenia, with approximately 35% decrease in platelet number²⁸. In our *ex vivo*
366 lung system, despite undetectable platelets in the perfusate (Fig.7a-b), abundant anuclear
367 fluorescent objects, sized ~10 μm , could be seen in the lung vasculature (Fig.7d and
368 Supplementay Movie 12). This suggests that TPM4 is required for the final steps in platelet
369 generation. Importantly, our data from intravital observation of *Tpm4*^{-/-} bone marrow suggests
370 that MK protrusion/extrusion process, which may be proplatelet formation *in vivo*, is similar
371 to normal (Fig.8 and Supplementary Movies 13-14). This therefore makes it likely that the
372 lower platelet count seen in *Tpm4*^{-/-} mice is a product of defective platelet formation outside of
373 the bone marrow, in the lung vasculature.

374 Finally, the work introduces a novel system for generating platelets *in vitro*, by multiple
375 passage of MKs through a microfluidic chamber. Current systems developed to generate
376 platelets *in vitro* include 2D and 3D culture systems, 3D bioreactors and big tank bioreactors,
377 including the use of ~~the latter using~~ turbulence to generate platelets from MKs⁵⁰⁻⁵². Thon *et al.* developed a
378 microfluidic system that applies shear to emergent proplatelets from MKs⁵³. Our system differs
379 in that cells are required to pass through small channels, equivalent to capillaries, with internal
380 dimensions 12.5 \times 10 μm . The approach is therefore mechanistically different to other systems
381 and is capable of generating large numbers of platelets, approximately 500 platelets per MK.

382 In summary, this work identifies a ~~highly efficient~~ mechanism ^{for} of platelet generation, by
383 repeated passage of MKs through lung vasculature under air ventilation, involving enucleation
384 and final TPM4-dependent **steps to** generate platelets. The findings will inform new

SEE PRIOR COMMENT
THAT THIS MAY
NOT BE PROPLT
BUT LARGE
FRAGMENT FORMATION
ONLY. IT MAY BE
THAT TPM4 IS
NOT NEEDED FOR MEGS
TO MIGRATE OUT
OF THE MARROW
BUT IMPORTANT
FOR FUTURE
PROCESSING

SHOULD POINT OUT THAT YOUR SYSTEM LACKS
EC LINING. ALSO NEEDED TO SHOW THAT THE
RESULTING PLTS ARE NOT PREACTIVATED
IF THIS IS OF CLINICAL RELEVANCE, BUT
IF WORDED CORRECTLY, NEED NOT DO
FURTHER STUDIES IN THIS MANUSCRIPT

385 approaches, such as the microfluidic system reported here, to large scale generation of human
386 platelets.

387

388 **Methods**

389 **Animal experiments and Ethics statement**

390 C57BL/6 mice were purchased from Harlan UK. The study protocol of **C57BL/6 mouse** care
391 and experiments was approved by the local research ethics committee (AWERB) and licensed
392 under UK Home Office project license PPL 30/3445 and PP5643338. *Tpm4^{-/-}* mice were
393 generated as we have previously described²⁸. The study protocol of *Tpm4^{-/-}* mice was approved
394 by the district government of lower Franconia, Germany (Bezirksregierung Unterfranken). **Age**
395 **and sex matched mice were used for each experiment. Both female and male mice were used**
396 **at an age of 8-12 weeks (no selection for sex of mice).**

397 **Mouse *ex vivo* heart-lung preparation**

398 Mice were sacrificed by a Schedule 1 process, by exposure to rising CO₂. A tracheostomy was
399 then performed, and lungs ventilated with room air or pure nitrogen via a rodent ventilator
400 (Minivent type 845, Harvard Apparatus, USA). **To avoid end-expiratory lung collapse, as**
401 **indicated in Fig 1a, the connector for expiration air was connected to a Gottlieb valve (tube**
402 **immersed in water; immersion 2-3 cm depth to induce a positive end-expiratory pressure).**
403 Respiratory rate was maintained at around 150-200 breaths/min and tidal volume was 10 mL/kg
404 (~250 µL). The inferior vena cava was then exposed by laparoscopy, and the chest opened by
405 median sternotomy and fat tissue carefully removed. A 21-gauge catheter was passed into the
406 right ventricle and approx. About 100 mL warm (36-38 °C) perfusion buffer (Krebs-Hepes
407 buffer (KHB): 140 mM NaCl, 3.6 mM KCl, 0.5 mM NaH₂PO₄, 0.2 mM MgSO₄, 1.5 mM CaCl₂,
408 10 mM Hepes (pH 7.4), 2 mM NaHCO₃) containing 10 U/mL heparin was perfused at 3-4

409 mL/min into the lung vasculature. Once the colour of mouse lung turned pale, suggesting most
410 of blood in the lung circulation was flushed, the catheter was disconnected.

411 The left and right superior venae cavae, ascending aorta, inferior vena cava and descending
412 aorta were ligated using 6-0 silk, and a small incision was made in the left ventricle for
413 collection of the perfusate. A suspension of mouse MKs (usually labelled with a fluorescently
414 tagged anti-CD41 antibody) was placed into a perfusion pump and infused into the right
415 ventricle, whilst the lungs were either ventilated with air or pure nitrogen or without ventilation,
416 and the flow rate was maintained at 0.35 mL/min by a SyringeOne Programmable Syringe
417 Pump (Product SKU: NE-1000-ES). This flow rate achieves a pressure (2.1–3.5 mmHg,
418 measured by pressure transducer as shown in Fig.1a) substantially lower than physiological
419 levels of mouse pulmonary artery, which has been estimated to be ~25 mmHg⁵⁴.

420 The perfusate was collected and re-pumped into the right ventricle after samples were collected
421 for imaging and FACS analysis. The perfusate was recirculated through the pulmonary
422 vasculature in this manner for a total of 18 passages. After the final passage, 1 mL perfusion
423 buffer was pumped into the system to remove some of the remaining cells in the lung
424 vasculature, and all perfusate collected for evaluation of platelet function. The mouse lung was
425 immediately removed and the volume of the lung was measured by fluid displacement
426 (Supplementary Fig.1e). The lung was then fixed with 4% PFA/PBS at 4°C overnight and kept
427 from the light. Experimental flowchart for generating platelets from repeated infusion of mouse
428 heart-lung preparation is shown in Supplementary Fig.1a.

429 **Microfluidic chamber design, fabrication, and experimental protocol**

430 A set of channels mimicking a physiological vascular system was constructed using standard
431 PDMS approach. The design shows a branching structure such that as branching progressing,
432 the channel diameter decreases by half. All channels are rectangular in cross-section and 10
433 µm deep, with the largest channels being 100 µm across, decreasing to the smallest channels
434 which are 12.5 µm across. From each larger channel, 16 smaller channels branch off, allowing

435 for maintenance of flow resistance due to the r^4 power relationship between resistance and
436 channel diameter. Fluid then flows from larger diameter channels to smaller diameter channels,
437 and in reverse on the way out of the system. Cells are passed through the system, repeatedly.
438 The system is scaled up, through multiplexing in parallel, to allow greater cell volumes to be
439 used, as shown in Fig. 3c.

440 The mask and SU-8 master mold were fabricated by NuNano (Bristol, UK). The microfluidic
441 channels were fabricated by soft lithography. The mixture of PDMS in a 10:1 ratio was poured
442 over the SU-8 master mold after being degassed in a vacuum desiccator. The PDMS mixture
443 was cured at 80 °C for 2 hours and incubated in the oven overnight. The PDMS mold was
444 removed from the SU-8 master. Input and output holes were punched using a 0.5 mm OD
445 biopsy puncher (Elveflow, Paris, France). Finally, the PDMS microchannels were irreversibly
446 bonded to glass slides using oxygen plasma for 3 mins in a plasma device (Diener Plasma
447 Systems, Ebhausen, Germany).

448 A suspension of mouse MKs prelabelled with CD41-PE was placed into a perfusion pump and
449 infused into the microfluidic chamber at 0.30 mL/min flow rate. Suspensions were collected
450 from the output hole and re-pumped into the microfluidic chamber, after 25 μ L samples were
451 taken for FACS analysis. Suspensions were then recirculated through the microfluidic chamber
452 in this manner for a total of 18 passages.

453 **Culture and differentiation of murine megakaryocytes**

454 Briefly, bone marrow from C57BL/6 or *Tpm4*^{-/-} mice was isolated and dispersed prior to
455 centrifugation at 200 x g for 10 minutes. Bone marrow was re-suspended in IMDM- Glutamax
456 containing 1% penicillin/streptomycin and 2% serum replacement 1. Cells were cultured for 3
457 days in the presence of 20 ng/mL recombinant murine stem cell factor (rSCF) and a further 13
458 days in the presence of 10 ng/mL recombinant murine thrombopoietin (rTPO) at 37 °C and 5%
459 CO₂. From day 8 to day 16, cells were transmitted to fresh cell culture dishes every day to

460 reduce MKs to contact with fibroblast cells. On day 16, MKs were harvested and enriched with
461 a 1.5%/3% bovine serum albumin (BSA) gradient for 1 hour in cell incubator, following
462 stained with either IgG-PE/ or FITC, or CD41-PE or -FITC for 3 hours and further with DNA
463 dye Hoechst 33342 for 20 mins. Then MKs were washed and resuspended in 2 mL medium
464 containing 10 U/mL heparin prior to use.

465 ***In vivo* passage of intact megakaryocytes through lung vasulature**

466 C57BL/6 mice were anaesthetized by intraperitoneal injection of a 100 mg/kg ketamine/10
467 mg/mL xylazine mix. Mouse MKs were stained with CellTracker™ Red CMTPX dye and
468 Hoescht33342 prior to injection into the right external jugular vein of an anaesthetized recipient
469 mouse. Blood was collected from the left common carotid artery. Cells were imaged by
470 confocal fluorescence microscopy after lysis and removal of red blood cells.

471 **Flow cytometry**

472 Platelets derived from IgG-PE or IgG-FITC stained MKs were set up as negative controls.
473 Washed mouse platelets were used to set gates for generated platelets (P1) at the FSC/SSC
474 density plot by size and granularity (shown in Fig. 1d). 25 µL of CD41-PE or CD41-FITC
475 stained MK suspension, or perfusates from lung or suspensions from microfluidic chambers
476 after 1, 2, 3, 6, 9, 12, 15 or 18 passages, were measured by FACS. DNA content, viability and
477 mitochondrial membrane potential of generated platelets were determined by Draq5, Calcein
478 AM and TMRM staining, respectively.

479 To detect the viability and mitochondrial membrane potential of pulmonary endothelial cells
480 (ECs), assays for Calcein Deep Red retention in ECs and TMRM accumulation in active
481 mitochondria were conducted by FACS. Pulmonary ECs were isolated from perfused lungs
482 under air- or pure-nitrogen-ventilation or without ventilation for approximately 2 hours. **In**
483 **brief, lung was harvested and minced using scissors. The minced lung tissues were digested by**
484 **collagenase I (3 mg/mL) in serum-free IMDM medium at 37 °C for 40 mins, followed by**
485 **filtration through a 70 µm strainer. Cells were then washed twice with serum-free IMDM**

486 medium and stained with FITC-conjugated anti-CD31/PECAM-1 or anti-CD102/ICAM-2
487 antibodies, followed by loading with Calcein Deep Red or TMRM dyes for 25 mins at room
488 temperature. Pulmonary ECs from fresh lungs served as control.

489 Platelet surface glycoproteins (generated platelets derived from CD41-PE stained MKs) were
490 measured by incubating with FITC-conjugated anti-mouse CD61, CD42b, CD42d, CD49b,
491 Glycoprotein VI (GPVI) antibodies or isotype-nonspecific IgG for 20 mins at room
492 temperature before fixation.

493 To investigate the function of generated platelets (generated platelets derived from CD41-FITC
494 stained MKs), assays for α IIb β 3 integrin activation (JON/A-binding) and P-selectin exposure
495 were performed. Washed platelets were stimulated with 2 U/mL thrombin or 5 μ g/mL CRP for
496 10 mins followed by incubation with PE-JON/A or PE-P selectin antibodies for 20 mins at
497 room temperature before fixation. Tirofiban and PE-IgG were used to exclude nonspecific
498 binding for the measurement of PE-conjugated JON/A or PE-conjugated P-selectin exposure,
499 respectively. Resting platelets served as negative controls.

500 Samples were analysed on a BD Accuri™ C6 Plus flow cytometer (BD) with 50,000 gated
501 events/sample.

502 **Two-photon imaging and platelet counting in the lung vasculature**

503 After overnight fixation at 4 °C, the lung was staged on a microslicer device (Type: DTK-
504 1000N, UK) and cut into small slices with 800 μ m thickness and flat surface. Lung slices from
505 different lobes were fixed into a 100 mm cell culture dish and immersed in PBS for two-photon
506 imaging.

507 Imaging was performed using a DeepSee multiphoton laser (Spectra Physics) attached to an
508 upright SP8 confocal microscope (Leica Microsystems). All images were collected using a
509 25 \times /0.95NA water dipping lens. For CD41-FITC or CD41-PE, excitation was provided by
510 tuning the multiphoton laser to 927nm, for Hoechst 33342, excitation was provided by tuning
511 the multiphoton laser to 750 nm. The resultant fluorescence for both scans passing off a SP500

512 dichroic beam splitter and through both a SP680 filter and either a 525/50 nm bandpass filter
513 to selected only CD41-FITC signal, a 630/75 nm bandpass filter to select only CD41-PE signal
514 or a 460/50 nm bandpass to select only Hoechst 33342 signal. CD41-FITC or CD41-PE
515 fluorescence was detected using non-descanned Hybrid detectors (Leica Microsystems) and
516 Hoechst 33342 fluorescence was detected using a non-descanned PMT. Images were acquired
517 with an additional zoom of $2.5\times$ with 1772.5×1772.5 pixels (XY), with an effective pixel size
518 of 100 nm. Z stacks were captured with a z-step spacing of 2 μm . All images were capture
519 using a scan speed of 400 Hz with a bidirectional scan.

520 To count generated platelets retained in the lung vasculature, image analysis was performed
521 using Fiji ImageJ and ten z-stacks were analyzed as a single volume in extended focus. The
522 total volume of each analysed lung two-photon extended focus sample was therefore
523 $(177.25\times 177.25\times 2)\times 10=628351.25\ \mu\text{m}^3$, and the numbers of fluorescent events ($\sim 2\text{-}6\ \mu\text{m}$
524 diameter) were counted manually. Total lung volume was determined by a fluid displacement
525 approach, as per details in Supplementary Fig. 1e.

526 **Confocal microscope imaging**

527 Confocal images were obtained on an inverted SP8 confocal microscope (Leica Microsystems)
528 attached to a DMI6000 microscope frame (Leica Microsystems). All images were acquired
529 using a $100\times/1.44$ NA oil immersion objective. Excitation was provided by either a 405 nm
530 laser (Hoechst 33342) or 488 nm laser (for CD41-FITC) or 561 nm laser (for CD41-PE) and
531 the resultant fluorescence was detected using a Hybrid detector in the range 410-470 nm for
532 Hoechst 33342, 495-570 nm for CD41-FITC or 571-650 nm for CD41-PE. A total of 50
533 randomly chosen fields of view were imaged and where z-stacks were acquired, a 2 μm z-step
534 spacing was used for Supplementary Movies 7-10, or a 0.5 μm z-step spacing for
535 Supplementary Movie 11.

536 To obtain an estimate of the dimensions of each nucleus in XY, z-stacks were loaded into Fiji
537 imageJ and subjected to a maximum intensity projection and a region of interest (ROI) was

538 manually drawn around an individual nucleus. The inbuilt measure function within Fiji imageJ
539 was used. To obtain the dimensions of the major and minor axis, the ‘fit ellipse’ option was
540 enabled. To estimate the nuclear depth, analysis was performed in Fiji ImageJ stacks were
541 loaded, and a cell nucleus was selected using the ROI tool. The average intensity profile of this
542 nucleus was plotted in z and then fitted with a gaussian profile using the built-in plot and fitting
543 tools of Fiji imageJ. From the fitted parameters the depth of the nucleus was estimated using
544 the full width at half maximum (FWHM) of the gaussian fit. The FWHM was calculated as
545 $2\sqrt{(2\ln 2)} \sigma$. This process was manually repeated for multiple cell nuclei.

546 **Transmission electron microscope imaging**

547 To visualize and compare the ultrastructures of generated and control platelets by transmission
548 electron microscopy (TEM), host platelets were first depleted by intraperitoneal administration
549 of anti-GPIIb/IIIa antibody R300 (2 µg/g bodyweight) prior to MKs infusion through the heart-
550 lung preparation. After 18 passages, the generated platelets were pelleted by centrifuging the
551 collected perfusate. The platelet pellet was then resuspended in a cacodylate-buffered
552 glutaraldehyde fixative and fixed at 4-8°C overnight and then post-fixed in osmium
553 ferrocyanide. Fixed cells were then embedded in a solidifying BSA/glutaraldehyde gel. Gel-
554 embedded platelets were stained with uranyl acetate and lead aspartate followed by dehydration
555 with ethanol and infiltrated with Epon resin in a Tissue Processor (Leica EMTP). 70 nm
556 sections were cut from blocks with a Reichert Ultracut E and imaged with a Tecnai 12 electron
557 microscope (ThermoFisher UK).

558 ***In vitro* thrombus formation**

559 In brief, ibidi µ-Slide VI 0.1 chips were coated with 50 µg/mL collagen overnight at 4 °C before
560 being flushed and blocked with 2% fatty acid-free BSA prepared in HEPES-Tyrode’s buffer.
561 Freshly drawn mouse blood was collected from the inferior vena cava using 10 U/mL heparin
562 and 20 µM PPACK (D-phenylalanyl-prolyl-arginyl chloromethyl ketone) as anticoagulant,
563 following euthanasia by rising CO₂. Mouse blood was mixed with 2 mL NaCl (150 mM) and

564 centrifuged to remove PRP. MKs stained with 2 μ M DiOC₆ were passaged through the mouse-
565 lung preparation 18 times, and approx. 0.7 mL perfusate was mixed with 1.3 mL mouse blood
566 lacking PRP and incubated with CellTracker™ Red CMTPX dye (1:1000 dilution) for 10 mins.
567 The mixed sample was then transferred to a 5 mL syringe and perfused using an Aladdin AL-
568 1000 syringe pump (World precision instruments, United Kingdom) through the ibidi slide, at
569 a shear rate of 1000/s for 20 mins. Platelets were fixed by perfusion of 4% paraformaldehyde
570 through channels for 4 mins before nonadherent cells were flushed away with HEPES Tyrode
571 buffer.

572 Thrombus formation was determined by generating confocal z-stacks (1024×1024 pixels,
573 0.787 μ m z stack distance) from 5 randomly chosen fields of view using a Leica SP8 confocal
574 microscope. Images were acquired using a 20×/0.7 NA air immersion objective. Excitation was
575 provided by either a 488 nm (DiOC₆) or 561 nm (CellTracker™ Red CMTPX) laser with the
576 resultant fluorescence being detected by Hybrid detectors in the range 498-551 nm (DiOC₆) or
577 571-623 nm (CellTracker Red CMTPX).

578 **Two-photon intravital microscopy of the bone marrow.**

579 Mice were anaesthetized by intraperitoneal injection of medetomidine 0.5 μ g/g, midazolam
580 5 μ g/g and fentanyl 0.05 μ g/g body weight. A 1 cm incision was made along the midline to
581 expose the frontoparietal skull, without damaging the bone tissue. To immobilize the head
582 while imaging, the mouse was fastened with a stereotactic holder on a heated customized stage.
583 Bone marrow vasculature was visualized by intravenous injection of anti-CD105-AlexaFluor
584 546 antibody (1 μ g/g body weight) and 100 μ L AlexaFluor 546-labeled BSA. Platelets and
585 MKs were stained intravenously with anti-GPIX-AlexaFluor 488 antibody (1.5 μ g/g body
586 weight). Images and time-lapse videos were acquired using a 20× water objective with a
587 numerical aperture of 0.95 (Leica Microsystems CMS) on a confocal TCS SP8 MP (Leica
588 Microsystems CMS) equipped with a tunable broadband laser (Coherent).

589 **Image analysis and 3D segmentation**

590 All image analysis was performed using Fiji ImageJ-win 64 software. 3D cell segmentation
591 was performed in Fiji using the ModularImageAnalysis (MIA) workflow automation
592 plugin^{55,56}.

593 **Statistical information**

594 All data were analyzed using GraphPad Prism 7 software (GraphPad Software Inc., San Diego,
595 CA, USA). Quantified data are presented as mean ± S.E.M. from at least 3 independent
596 experiments. A value of $p < 0.05$ was considered statistically significant and determined using
597 either unpaired t-test for normally distributed data (comparison of two groups) or Mann-
598 Whitney U test for non-normally distributed data (comparison of two groups) or two-way
599 ANOVA with Tukey's multiple comparisons test, as indicated in figure legends. Choice of test
600 was determined by assessment of normality of data (Kolmogorov-Smirnov analysis), and
601 whether single or multiple comparison was required.
602
603
604

605 **Data availability**

606
607 The datasets generated during and/or analysed during the current study are available from the
608 corresponding author on reasonable request.

610 **References**

- 611 1 Denis, M. M. *et al.* Escaping the nuclear confines: signal-dependent pre-mRNA
612 splicing in anucleate platelets. *Cell* **122**, 379-391, doi:10.1016/j.cell.2005.06.015
613 (2005).
- 614 2 van der Meijden, P. E. J. & Heemskerk, J. W. M. Platelet biology and functions: new
615 concepts and clinical perspectives. *Nature reviews. Cardiology* **16**, 166-179,
616 doi:10.1038/s41569-018-0110-0 (2019).
- 617 3 Gaertner, F. *et al.* Migrating Platelets Are Mechano-scavengers that Collect and
618 Bundle Bacteria. *Cell* **171**, 1368-1382.e1323, doi:10.1016/j.cell.2017.11.001 (2017).
- 619 4 Heimark, R. L., Twardzik, D. R. & Schwartz, S. M. Inhibition of endothelial
620 regeneration by type-beta transforming growth factor from platelets. *Science (New*
621 *York, N.Y.)* **233**, 1078-1080, doi:10.1126/science.3461562 (1986).

- 622 5 Machlus, K. R. & Italiano, J. E., Jr. The incredible journey: From megakaryocyte
623 development to platelet formation. *The Journal of cell biology* **201**, 785-796,
624 doi:10.1083/jcb.201304054 (2013).
- 625 6 Brown, E., Carlin, L. M., Nerlov, C., Lo Celso, C. & Poole, A. W. Multiple
626 membrane extrusion sites drive megakaryocyte migration into bone marrow blood
627 vessels. *Life science alliance* **1**, doi:10.26508/lsa.201800061 (2018).
- 628 7 Potts, K. S. *et al.* Membrane budding is a major mechanism of in vivo platelet
629 biogenesis. *The Journal of experimental medicine* **217**, doi:10.1084/jem.20191206
630 (2020).
- 631 8 Bender, M. *et al.* ADF/n-cofilin-dependent actin turnover determines platelet
632 formation and sizing. *Blood* **116**, 1767-1775, doi:10.1182/blood-2010-03-274340
633 (2010).
- 634 9 Eckly, A. *et al.* Abnormal megakaryocyte morphology and proplatelet formation in
635 mice with megakaryocyte-restricted MYH9 inactivation. *Blood* **113**, 3182-3189,
636 doi:10.1182/blood-2008-06-164061 (2009).
- 637 10 Aschoff, L. Uber capillare Embolie von riesenkemhaltigen Zellen. *Arch Pathol Anat*
638 *Phys* **134**, 11–14 (1893).
- 639 11 Howell, W. H. & Donahue, D. D. The Production of Blood Platelets in the Lungs. *The*
640 *Journal of experimental medicine* **65**, 177-203, doi:10.1084/jem.65.2.177 (1937).
- 641 12 Zucker-Franklin, D. & Philipp, C. S. Platelet production in the pulmonary capillary
642 bed: new ultrastructural evidence for an old concept. *The American journal of*
643 *pathology* **157**, 69-74, doi:10.1016/s0002-9440(10)64518-x (2000).
- 644 13 Lefrançois, E. *et al.* The lung is a site of platelet biogenesis and a reservoir for
645 haematopoietic progenitors. *Nature* **544**, 105-109, doi:10.1038/nature21706 (2017).
- 646 14 Fuentes, R. *et al.* Infusion of mature megakaryocytes into mice yields functional
647 platelets. *J Clin Invest* **120**, 3917-3922, doi:10.1172/jci43326 (2010).
- 648 15 Wang, Y. *et al.* Comparative analysis of human ex vivo-generated platelets vs
649 megakaryocyte-generated platelets in mice: a cautionary tale. *Blood* **125**, 3627-3636,
650 doi:10.1182/blood-2014-08-593053 (2015).
- 651 16 Li, Y. J. *et al.* From blood to brain: blood cell-based biomimetic drug delivery
652 systems. *Drug delivery* **28**, 1214-1225, doi:10.1080/10717544.2021.1937384 (2021).
- 653 17 R M Kaufman, R. A., S Pollack, W H Crosby. Circulating megakaryocytes and
654 platelet release in the lung. *Blood Rev* **26**, 12 (1965).
- 655 18 Huertas, A. *et al.* Pulmonary vascular endothelium: the orchestra conductor in
656 respiratory diseases: Highlights from basic research to therapy. *The European*
657 *respiratory journal* **51**, doi:10.1183/13993003.00745-2017 (2018).
- 658 19 Sadoul, K. Tubulin acetylation a valuable accessory of the platelet cytoskeleton.
659 Focus on "Histone deacetylase 6-mediated deacetylation of α -tubulin coordinates
660 cytoskeletal and signaling events during platelet activation". *American journal of*
661 *physiology. Cell physiology* **305**, C1211-1213, doi:10.1152/ajpcell.00309.2013
662 (2013).
- 663 20 Dmitrieff, S., Alsina, A., Mathur, A. & Nédélec, F. J. Balance of microtubule stiffness
664 and cortical tension determines the size of blood cells with marginal band across
665 species. *Proceedings of the National Academy of Sciences of the United States of*
666 *America* **114**, 4418-4423, doi:10.1073/pnas.1618041114 (2017).
- 667 21 Hirsh, J. Platelet age: its relationship to platelet size, function and metabolism. *British*
668 *journal of haematology* **23**, Suppl:209-214, doi:10.1111/j.1365-2141.1972.tb03520.x
669 (1972).
- 670 22 Thompson, C. B., Jakubowski, J. A., Quinn, P. G., Deykin, D. & Valeri, C. R. Platelet
671 size and age determine platelet function independently. *Blood* **63**, 1372-1375 (1984).

- 672 23 Moog, S. *et al.* Platelet glycoprotein V binds to collagen and participates in platelet
673 adhesion and aggregation. *Blood* **98**, 1038-1046, doi:10.1182/blood.v98.4.1038
674 (2001).
- 675 24 Nurden, A. T. Clinical significance of altered collagen-receptor functioning in
676 platelets with emphasis on glycoprotein VI. *Blood Rev* **38**, 100592,
677 doi:10.1016/j.blre.2019.100592 (2019).
- 678 25 Moroi, M., Farndale, R. W. & Jung, S. M. Activation-induced changes in platelet
679 surface receptor expression and the contribution of the large-platelet subpopulation to
680 activation. *Res Pract Thromb Haemost* **4**, 285-297, doi:10.1002/rth2.12303 (2020).
- 681 26 Vainchenker, W. & Raslova, H. Megakaryocyte polyploidization: role in platelet
682 production. *Platelets* **31**, 707-716, doi:10.1080/09537104.2019.1667497 (2020).
- 683 27 Gunning, P. W., Hardeman, E. C., Lappalainen, P. & Mulvihill, D. P. Tropomyosin -
684 master regulator of actin filament function in the cytoskeleton. *Journal of cell science*
685 **128**, 2965-2974, doi:10.1242/jcs.172502 (2015).
- 686 28 Pleines, I. *et al.* Mutations in tropomyosin 4 underlie a rare form of human
687 macrothrombocytopenia. *The Journal of clinical investigation* **127**, 814-829,
688 doi:10.1172/jci86154 (2017).
- 689 29 Junt, T. *et al.* Dynamic visualization of thrombopoiesis within bone marrow. *Science*
690 *(New York, N.Y.)* **317**, 1767-1770, doi:10.1126/science.1146304 (2007).
- 691 30 Zinellu, A. *et al.* Platelet Count and Platelet Indices in Patients with Stable and Acute
692 Exacerbation of Chronic Obstructive Pulmonary Disease: A Systematic Review and
693 Meta-Analysis. *Copd* **18**, 231-245, doi:10.1080/15412555.2021.1898578 (2021).
- 694 31 Skoczyński, S. *et al.* Chronic Obstructive Pulmonary Disease and Platelet Count.
695 *Advances in experimental medicine and biology* **1160**, 19-23,
696 doi:10.1007/5584_2019_379 (2019).
- 697 32 Prabhakar, A. *et al.* Venous thrombosis at altitude presents with distinct biochemical
698 profiles: a comparative study from the Himalayas to the plains. *Blood advances* **3**,
699 3713-3723, doi:10.1182/bloodadvances.2018024554 (2019).
- 700 33 Lehmann, T. *et al.* Platelet count and function at high altitude and in high-altitude
701 pulmonary edema. *Journal of applied physiology (Bethesda, Md. : 1985)* **100**, 690-
702 694, doi:10.1152/jappphysiol.00991.2005 (2006).
- 703 34 Townsley, M. I. Structure and composition of pulmonary arteries, capillaries, and
704 veins. *Comprehensive Physiology* **2**, 675-709, doi:10.1002/cphy.c100081 (2012).
- 705 35 Mazzone, R. W. Influence of vascular and transpulmonary pressures on the functional
706 morphology of the pulmonary microcirculation. *Microvascular research* **20**, 295-306,
707 doi:10.1016/0026-2862(80)90030-8 (1980).
- 708 36 Kaufman, R. M., Airo, R., Pollack, S. & Crosby, W. H. Circulating megakaryocytes
709 and platelet release in the lung. *Blood* **26**, 720-731 (1965).
- 710 37 Pedersen, N. T. Occurrence of megakaryocytes in various vessels and their retention
711 in the pulmonary capillaries in man. *Scandinavian journal of haematology* **21**, 369-
712 375, doi:10.1111/j.1600-0609.1978.tb00381.x (1978).
- 713 38 Dickinson, C. J. & Martin, J. F. Megakaryocytes and platelet clumps as the cause of
714 finger clubbing. *Lancet (London, England)* **2**, 1434-1435, doi:10.1016/s0140-
715 6736(87)91132-9 (1987).
- 716 39 Levine, R. F. *et al.* Circulating megakaryocytes: delivery of large numbers of intact,
717 mature megakaryocytes to the lungs. *European journal of haematology* **51**, 233-246,
718 doi:10.1111/j.1600-0609.1993.tb00637.x (1993).
- 719 40 Ku, N. K. & Rashidi, H. Unusual finding of a megakaryocyte in a peripheral blood
720 smear. *Blood* **130**, 2573, doi:10.1182/blood-2017-08-803635 (2017).

- 721 41 Garg, N., Gupta, R. J. & Kumar, S. Megakaryocytes in Peripheral Blood Smears.
722 *Turkish journal of haematology : official journal of Turkish Society of Haematology*
723 **36**, 212-213, doi:10.4274/tjh.galenos.2019.2019.0022 (2019).
- 724 42 Zhu, J., Guo, W. & Wang, B. Megakaryocytes in peripheral blood smears of non-
725 hematological diseases. *International journal of hematology* **112**, 128-130,
726 doi:10.1007/s12185-020-02862-5 (2020).
- 727 43 Valdivia-Mazeyra, M. F. *et al.* Increased number of pulmonary megakaryocytes in
728 COVID-19 patients with diffuse alveolar damage: an autopsy study with clinical
729 correlation and review of the literature. *Virchows Archiv : an international journal of*
730 *pathology*, 1-10, doi:10.1007/s00428-020-02926-1 (2020).
- 731 44 Roncati, L. *et al.* A proof of evidence supporting abnormal immunothrombosis in
732 severe COVID-19: naked megakaryocyte nuclei increase in the bone marrow and
733 lungs of critically ill patients. *Platelets* **31**, 1085-1089,
734 doi:10.1080/09537104.2020.1810224 (2020).
- 735 45 Bauer, S., Khan, A., Klein, A. & Starasoler, L. Naked megakaryocyte nuclei as an
736 indicator of human immunodeficiency virus infection. *Archives of pathology &*
737 *laboratory medicine* **116**, 1025-1029 (1992).
- 738 46 McDonald, T. P. & Sullivan, P. S. Megakaryocytic and erythrocytic cell lines share a
739 common precursor cell. *Experimental hematology* **21**, 1316-1320 (1993).
- 740 47 Ji, P., Murata-Hori, M. & Lodish, H. F. Formation of mammalian erythrocytes:
741 chromatin condensation and enucleation. *Trends in cell biology* **21**, 409-415,
742 doi:10.1016/j.tcb.2011.04.003 (2011).
- 743 48 Italiano, J. E., Jr., Lecine, P., Shivdasani, R. A. & Hartwig, J. H. Blood platelets are
744 assembled principally at the ends of proplatelet processes produced by differentiated
745 megakaryocytes. *The Journal of cell biology* **147**, 1299-1312,
746 doi:10.1083/jcb.147.6.1299 (1999).
- 747 49 Davis, E., Corash, L., Stenberg, P. & Levin, J. Histologic studies of splenic
748 megakaryocytes after bone marrow ablation with strontium 90. *The Journal of*
749 *laboratory and clinical medicine* **120**, 767-777 (1992).
- 750 50 Di Buduo, C. A. *et al.* Programmable 3D silk bone marrow niche for platelet
751 generation ex vivo and modeling of megakaryopoiesis pathologies. *Blood* **125**, 2254-
752 2264, doi:10.1182/blood-2014-08-595561 (2015).
- 753 51 Ito, Y. *et al.* Turbulence Activates Platelet Biogenesis to Enable Clinical Scale
754 Ex Vivo Production. *Cell* **174**, 636-648.e618, doi:10.1016/j.cell.2018.06.011 (2018).
- 755 52 Di Buduo, C. A. *et al.* Latest culture techniques: cracking the secrets of bone marrow
756 to mass-produce erythrocytes and platelets ex vivo. *Haematologica* **106**, 947-957,
757 doi:10.3324/haematol.2020.262485 (2021).
- 758 53 Thon, J. N. *et al.* Platelet bioreactor-on-a-chip. *Blood* **124**, 1857-1867,
759 doi:10.1182/blood-2014-05-574913 (2014).
- 760 54 Ciuculan, L. *et al.* A novel murine model of severe pulmonary arterial hypertension.
761 *Am J Respir Crit Care Med* **184**, 1171-1182, doi:10.1164/rccm.201103-0412OC
762 (2011).
- 763 55 Schneider, C. A., Rasband, W. S. & Eliceiri, K. W. NIH Image to ImageJ: 25 years of
764 image analysis. *Nat Methods* **9**, 671-675, doi:10.1038/nmeth.2089 (2012).
- 765 56 Schindelin, J. *et al.* Fiji: an open-source platform for biological-image analysis. *Nat*
766 *Methods* **9**, 676-682, doi:10.1038/nmeth.2019 (2012).

767 **Acknowledgments**

768
769 We gratefully acknowledge the Wolfson Bioimaging Facility for their support and assistance
770 in this work. We are also grateful to Professor Jack Mellor, University of Bristol, for the use
771 of the tissue slicer machine. This work was supported by a Wellcome Trust Investigator Award
772 to A.W.P. (219472/Z/19/Z) and C.G. (219472/A/19/Z) and grants from the British Heart
773 Foundation (RG/15/16/31758 to A.W.P., SP/F/21/150023 to A.W.P., C.G. & I.H. and
774 PG/16/102/32647 to A.W.P. and E.O.A.). B.N. was funded by Deutsche
775 Forschungsgemeinschaft (DFG, German Research Foundation) (project number 374031971 -
776 TRR 240/project A01).

777

778 **Author contributions**

779 Conceptualization: X.Z., C.G. and A.W.P.; Methodology: X.Z., D.A., T.G.W., N.T., M.E.,
780 C.R.N., S.Z.B., Y.L. and **S.J.C.**; Visualization: X.Z., D.A. and C.R.N.; Resources: D.A.,
781 E.W.A., A.K.W. and J. B-B.; Writing – original draft: X.Z., D.A., C.R.N., M.E., S.Z.B., **S.J.C.**
782 and A.W.P.; Writing – review & editing: X.Z., D.A., C.M.W., P.W.G., E.C.H., E.O.A., B.N.,
783 I.H., C.G. and A.W.P.; Supervision & Investigation: X.Z. and A.W.P.; Funding acquisition:
784 E.O.A., C.G., I.H., B.N. and A.W.P; Project administration: A.W.P.

785

786 **Competing interests**

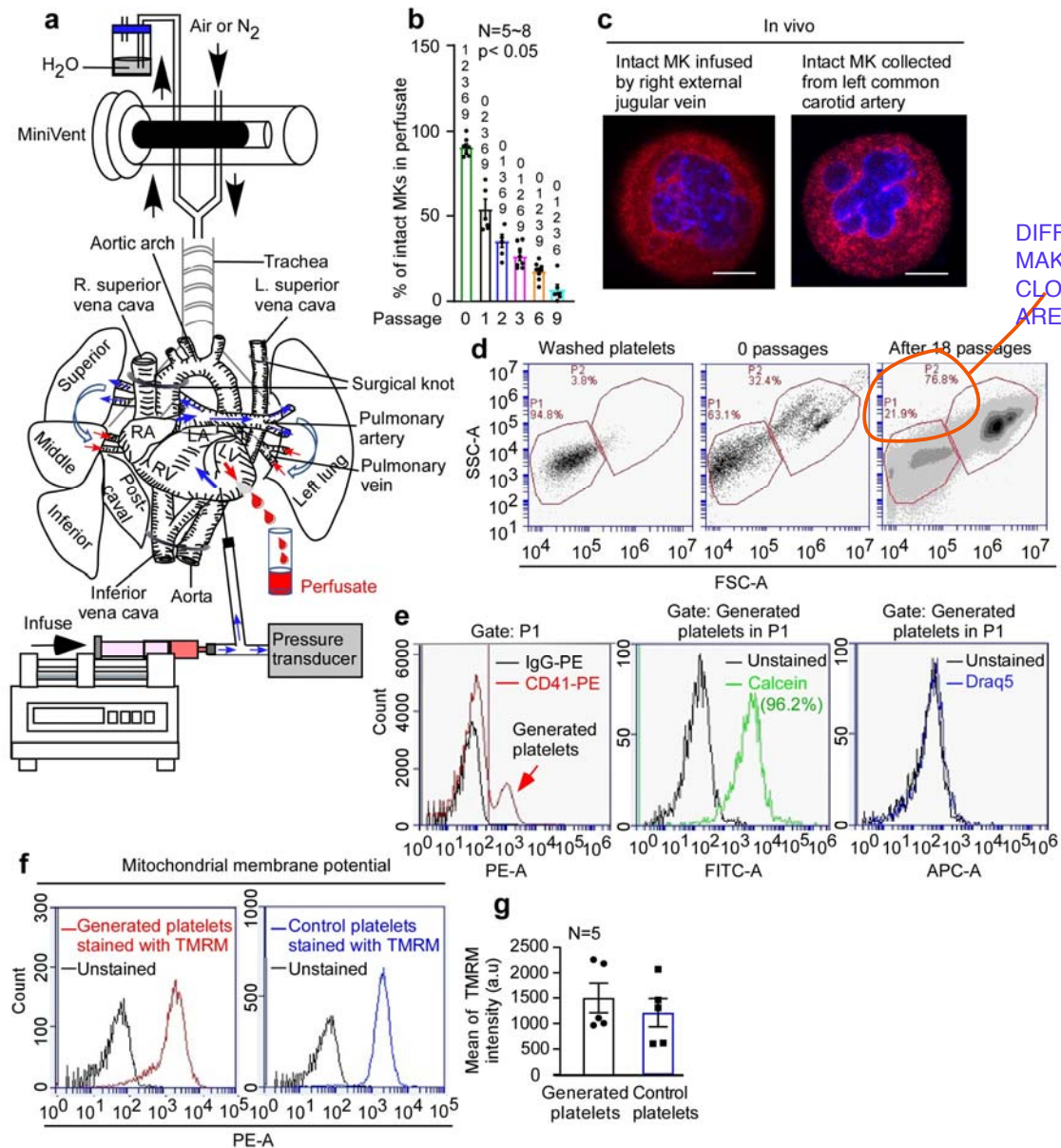
787 P.W.G. and E.C.H. receive funding from TroBio Therapeutics, a company commercialising
788 tropomyosin-targeting drugs. P.W.G. and E.C.H. are directors and shareholders of TroBio. All
789 other authors declare no competing interests.

790

791

792
793

Fig. 1



DIFFICULT TO READ.
MAKE BLACK AND MOVE
CLOSER TO CIRCLED
AREAS?

794

795 **Fig. 1: Mouse platelets are generated from megakaryocytes passed multiple times**

796 **through mouse pulmonary vasculature *ex vivo*. Mouse megakaryocytes (MKs), labelled**

797 **with CD41-PE or CD41-FITC antibodies, were passed repeatedly through the pulmonary**

798 **vasculature *ex vivo*. Lungs were ventilated with air throughout (b and d-g). a Diagram**

799 **illustrating the approach to generating mouse platelets. End-expiratory positive pressure was**

800 **applied to prevent lung collapse. b Intact MKs (showing a circular shape and central nucleus)**

801 **were imaged from samples of perfusates after passing the indicated number of times through**

802 lung vasculature. Quantification was from at least 250 fields of view, counting at least 230 cells
803 in total and displayed as a percentage of total number of cells. Numbers above each column
804 indicate significant difference to other passages. $P < 0.05$ was considered statistically
805 significant and determined using unpaired *t*-test. Data are from at least 5 independent
806 experiments. **c** *In vivo* demonstration that intact mouse MKs pass through the pulmonary
807 vasculature. Mouse MKs were stained with CellTracker™ Red CMTPX dye (red) and Hoechst
808 33342 (blue) prior to injection into the right external jugular vein of an anaesthetized recipient
809 C57/Bl6 mouse. Blood was collected from the left common carotid artery and cells were
810 imaged by confocal fluorescence microscopy. Images shown are representative of at least 4
811 independent experiments. Scale bar: 10 μ m. **d** Gating strategy for quantification of generated
812 platelets. The number of generated platelets in the perfusate collected after the 18th passage
813 was determined by the number of CD41(+) events in gate P1. **e** Events in P1 gate (from the
814 experiment shown in Fig. 1d) are defined as generated platelets (indicated by the red arrow),
815 with higher mean fluorescence compared to those derived from control IgG-PE- treated MKs.
816 Gate P1 also captures CD41-negative cells, which include stem cells (despite concentration of
817 MKs on a 1.5%/3% BSA gradient) and host-derived platelets. The viability of the generated
818 platelets, and whether they contain DNA, were checked by Calcein AM and DRAQ5 dyes,
819 respectively. **f** Mitochondrial membrane potential in generated and control platelets was
820 determined by Tetramethyl rhodamine methyl ester (TMRM) accumulation in active
821 mitochondria and measured by FACS. **g** TMRM signals from **f** were quantified and displayed
822 as mean \pm S.E.M. (n=5).

823

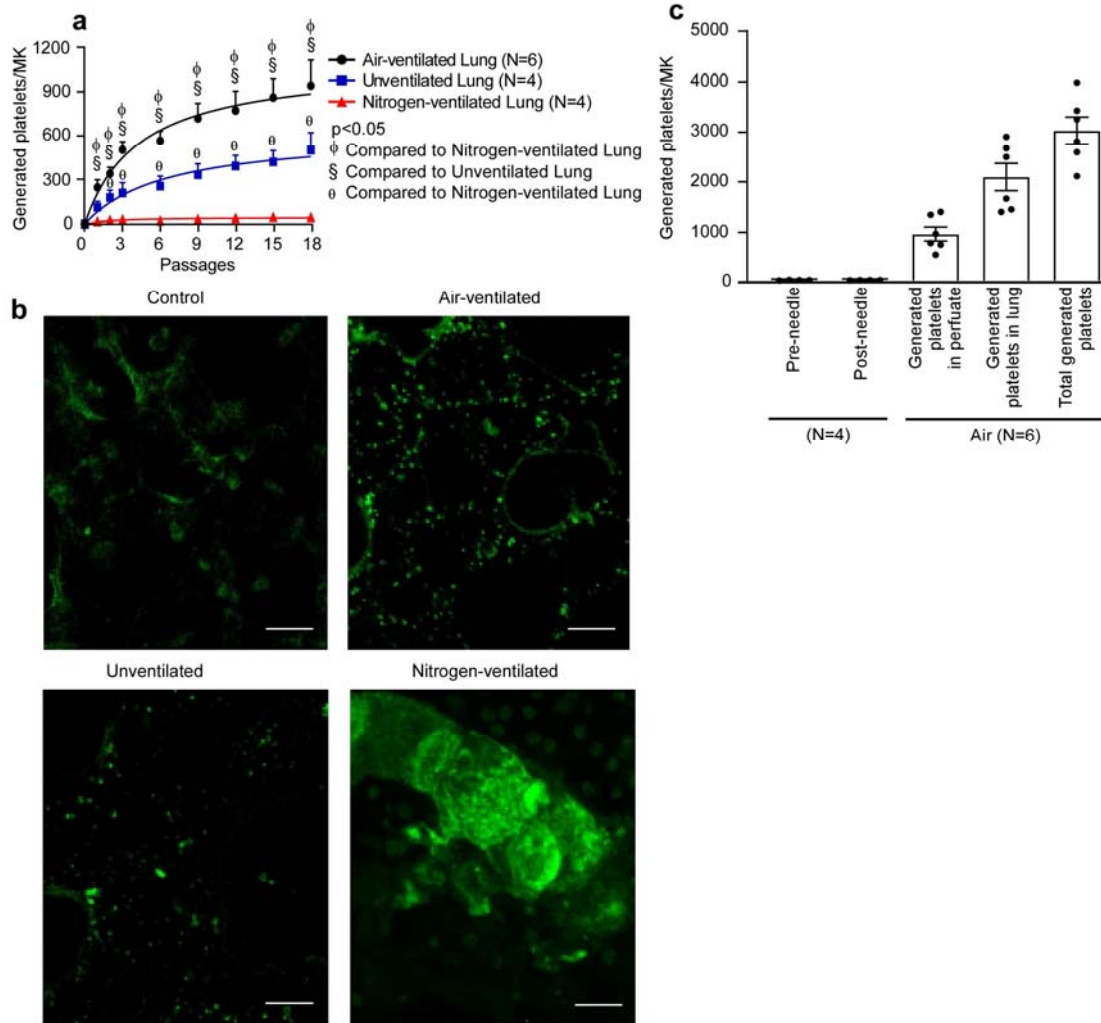
824

825

826

827

Fig. 2



829

830

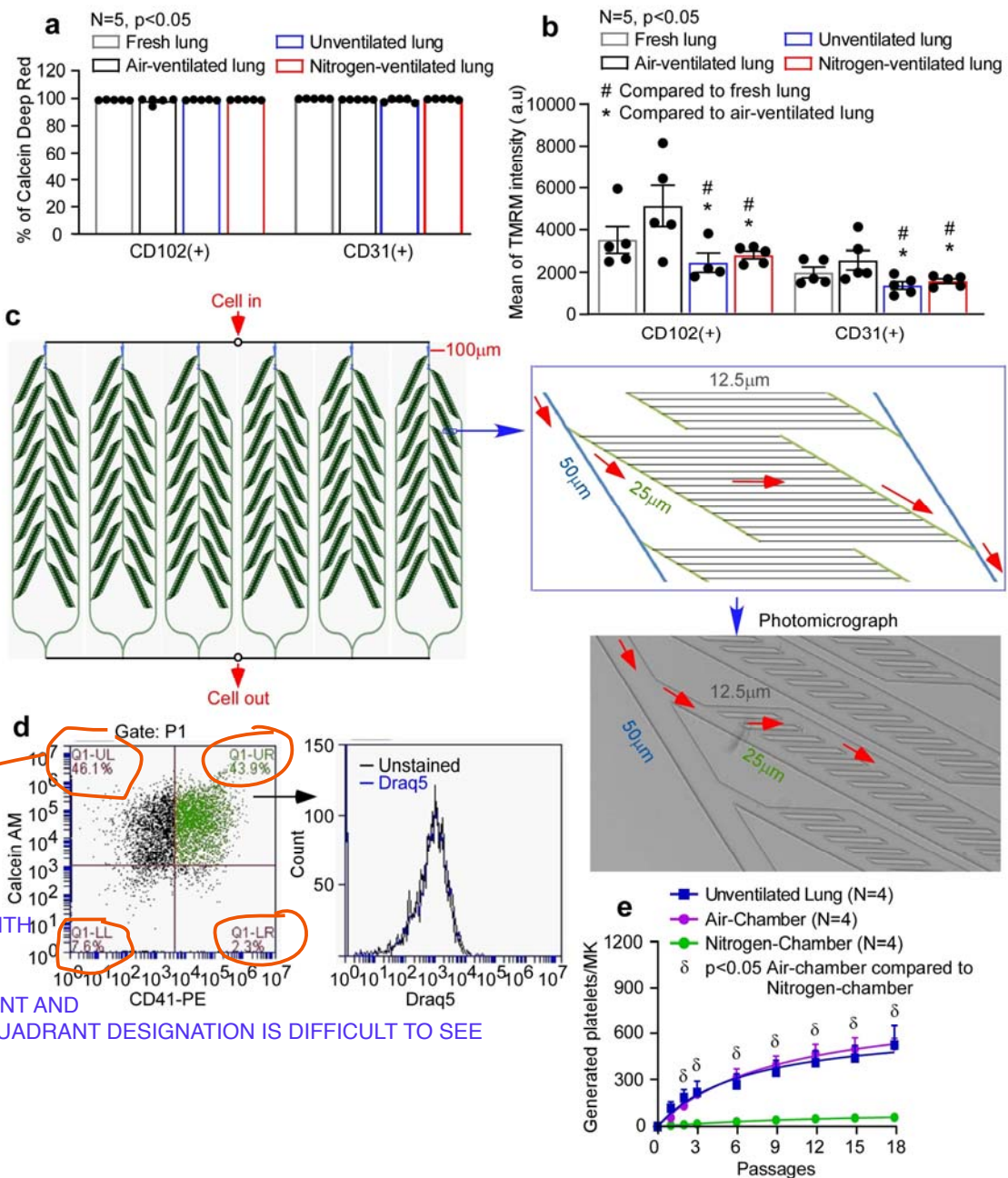
831 **Fig. 2: Quantification of platelets generated by passage of megakaryocytes through**
 832 **mouse pulmonary vasculature *ex vivo*. Mouse megakaryocytes (MKs), labelled with CD41-**
 833 **PE or CD41-FITC antibodies, were passed repeatedly through the pulmonary vasculature *ex***
 834 ***vivo*. Lungs were ventilated with air, pure nitrogen or without ventilation. a** The number of
 835 generated platelets per megakaryocytes (MKs) present in the perfusates from different passage
 836 numbers in lungs either ventilated with air (black circles), pure nitrogen (red triangles), or
 837 without ventilation (blue squares) were measured by FACS. Data are mean and S.E.M. (n as
 838 indicated). **P < 0.05 was considered statistically significant and determined using two-way**

839 ANOVA with Tukey's multiple comparisons test. **b** Stained MKs (CD41-FITC, green) were
840 passaged through pulmonary vasculature *ex vivo* 18 times, and lung tissue was fixed and sliced
841 followed by visualization of 20 stacked focal planes by two-photon microscopy. Lungs were
842 either ventilated with air or pure nitrogen, or were not ventilated, as indicated. Mouse lung
843 without MKs passed through served as control. Images shown are representative of at least 4
844 independent experiments. scale bar: 20 μ m. **c** Numbers of platelets generated per MK in
845 perfusate and retained in mouse lung under air ventilation, were calculated and displayed as
846 mean \pm S.E.M. (n as indicated). As a control, MKs passed through 21G needles 18 times
847 generated no platelets, as indicated.

848
849
850
851
852
853
854
855
856
857
858
859
860
861
862
863
864
865
866
867
868
869
870
871
872
873
874
875
876
877
878
879
880

881
882

Fig. 3



DON'T UNDERSTAND THE SIGNIFICANCE OF DIVIDING INTO 4 QUADRANTS AND USE OF GREEN AS WELL AS THE BELL SHAPE OF DRAQ5 WITH NO COMPARATIVE. FOR EITHER GRAPH. ALSO THE SMALL FONT AND COLORS FOR THE QUADRANT DESIGNATION IS DIFFICULT TO SEE

883

884 **Fig. 3: Role of pulmonary endothelial cell health and microvascular structure on platelet**

885 **generation.** a-b Pulmonary endothelial cells (ECs) were isolated from perfused lungs under

886 air- (black) or pure nitrogen-ventilation (red) or without ventilation (blue) for approximately 2

887 hours. ECs from fresh lung tissue served as control (gray). ECs were defined by staining with

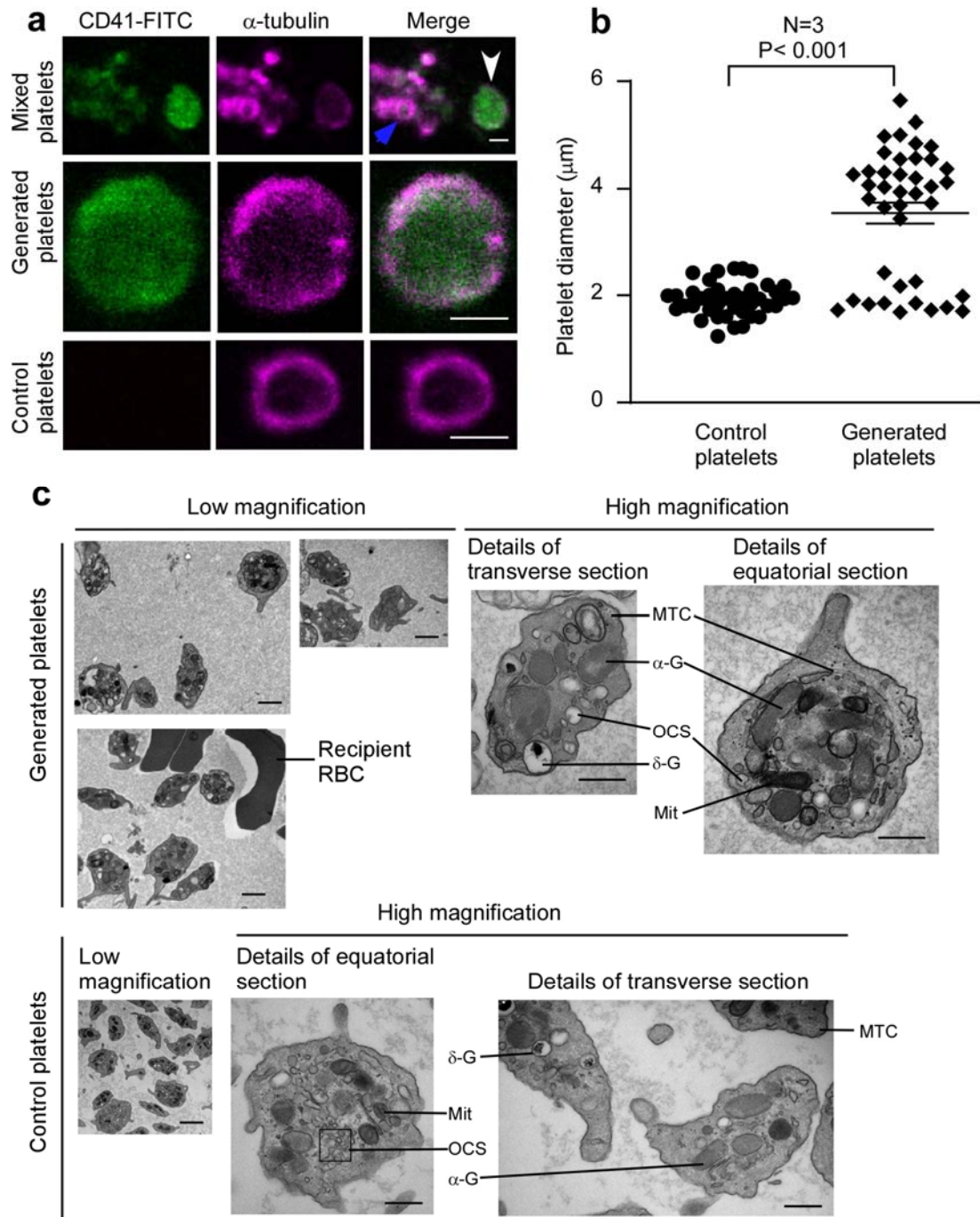
888 FITC-conjugated anti-CD31/PECAM-1 or anti-CD102/ICAM-2 antibodies. Data are from 5

889 independent experiments. $P < 0.05$ was considered statistically significant and determined
890 using unpaired *t*-test. **a** The viability of pulmonary ECs were determined by Calcein Deep Red
891 retention and displayed as mean of $\% \pm$ S.E.M. **b** The mitochondrial membrane potential was
892 determined by accumulation of Tetramethyl rhodamine methyl ester (TMRM) in active
893 mitochondria and displayed as mean fluorescence intensity \pm S.E.M. **c** Design of microfluidic
894 chamber mimicking a physiological pulmonary vascular system (details shown in Methods),
895 including a photomicrograph of the smallest channels in the system and indication of the flow
896 direction by arrows (red). Dimensions indicated on the figures are width of channels. **d-e**
897 Mouse MKs prelabelled with CD41-PE were repeatedly pumped through the microfluidic
898 chamber. **d** The viability of generated platelets from the microfluidic chamber was determined
899 by CD41 and Calcein AM staining (CD41+/Calcein AM+ in upper right quadrant, Q1-UR in
900 green). All generated platelets identified in this way showed no DNA content (DRAQ5 -ve
901 staining). **e** Quantification of generated platelets per megakaryocyte in perfusates under air
902 (purple circles) or pure nitrogen conditions (green circles), measured by FACS. For
903 comparison, numbers of platelets generated in the unventilated lung-heart system (blue
904 squares), from Fig. 2a, are shown. Data are mean and S.E.M. (n as indicated). $P < 0.05$ was
905 considered statistically significant and determined using two-way ANOVA with Tukey's
906 multiple comparisons test.

907
908
909
910
911
912
913
914
915
916
917
918
919
920

921
922

Fig. 4



923

924

925 **Fig. 4: Generated platelets demonstrate typical physical features comparable to control**

926 **platelets. a-b** Mouse megakaryocytes (MKs), prelabelled with CD41-FITC (green), were

927 **passaged repeatedly through the pulmonary vasculature *ex vivo*. Lungs were ventilated with air**

928 **throughout. a** Perfusates from ex vivo heart-lung preparation, containing both generated
929 platelets (white arrow) and host platelets (blue arrow), were stained for α -tubulin (magenta),
930 and confocal images shown as a mixed population in the top panels. More detailed images of
931 α -tubulin rings are shown in the magnified images in the middle panel (generated platelets) and
932 bottom panel (control platelets). Images are representative of 3 independent experiments. Scale
933 bars: 2 μm . **b** The diameter of platelets (40 platelets from 3 independent experiments) from **a**
934 was measured using Fiji (ImageJ-Win64), **with diameters of generated platelets: $3.6 \pm 0.2 \mu\text{m}$**
935 **vs control platelets: $1.9 \pm 0.1 \mu\text{m}$. In contrast to control platelets, there were two subpopulations**
936 **of generated platelets based on their diameter ranges: approx. 33% of generated platelets**
937 **(diameter range: 1.7-2.4 μm) have sizes similar to control platelets (diameter range: 1.2-2.4**
938 **μm) and 67% of generated platelets (diameter ranges: 3.7-5.6 μm) are significantly larger than**
939 **control platelets. Data are presented as mean \pm S.E.M. $P < 0.05$ was considered statistically**
940 **significant and determined using Mann-Whitney U test. c** Ultrastructures of generated platelets
941 and control platelets visualized by transmission electron microscopy. **Host platelets were**
942 **depleted by intraperitoneal administration of anti-GPIb α antibody R300 prior to perfusing MKs**
943 **through the heart-lung preparation under air-ventilation.** Subcellular structures are shown and
944 annotated as abbreviations, in the high magnification images: α -G, α -granules; σ -G, σ -granules
945 or dense bodies; Mit, mitochondria; OCS, open canalicular system; MTC, microtubule coils;
946 RBC, red blood cells. Scale bars: 2 μm in the images with low magnification, 500 nm in the
947 images with high magnification. Images shown are representative of 5 independent
948 experiments.

949

950

951

952

953

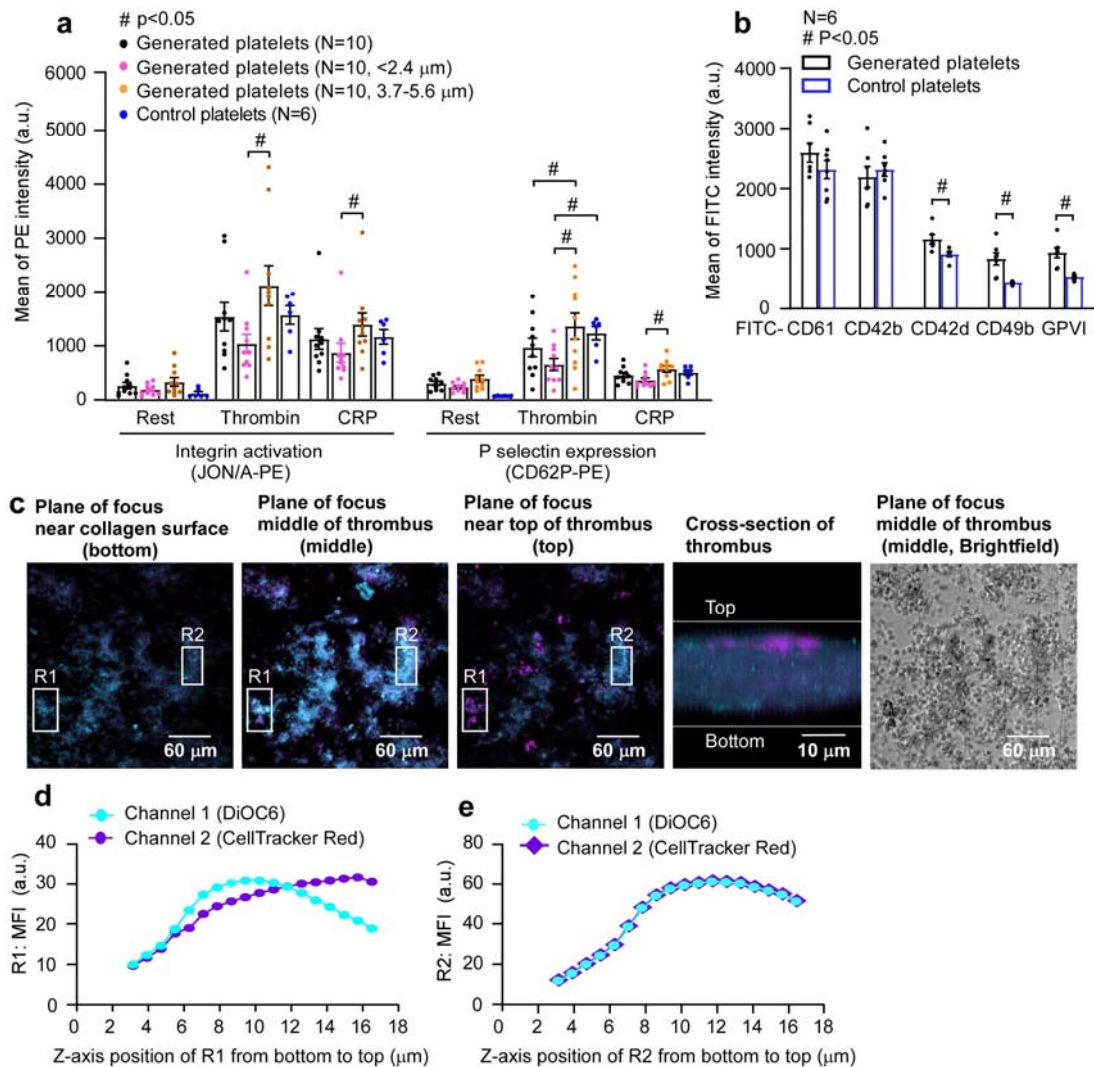
954

955

956

957
958

Fig. 5



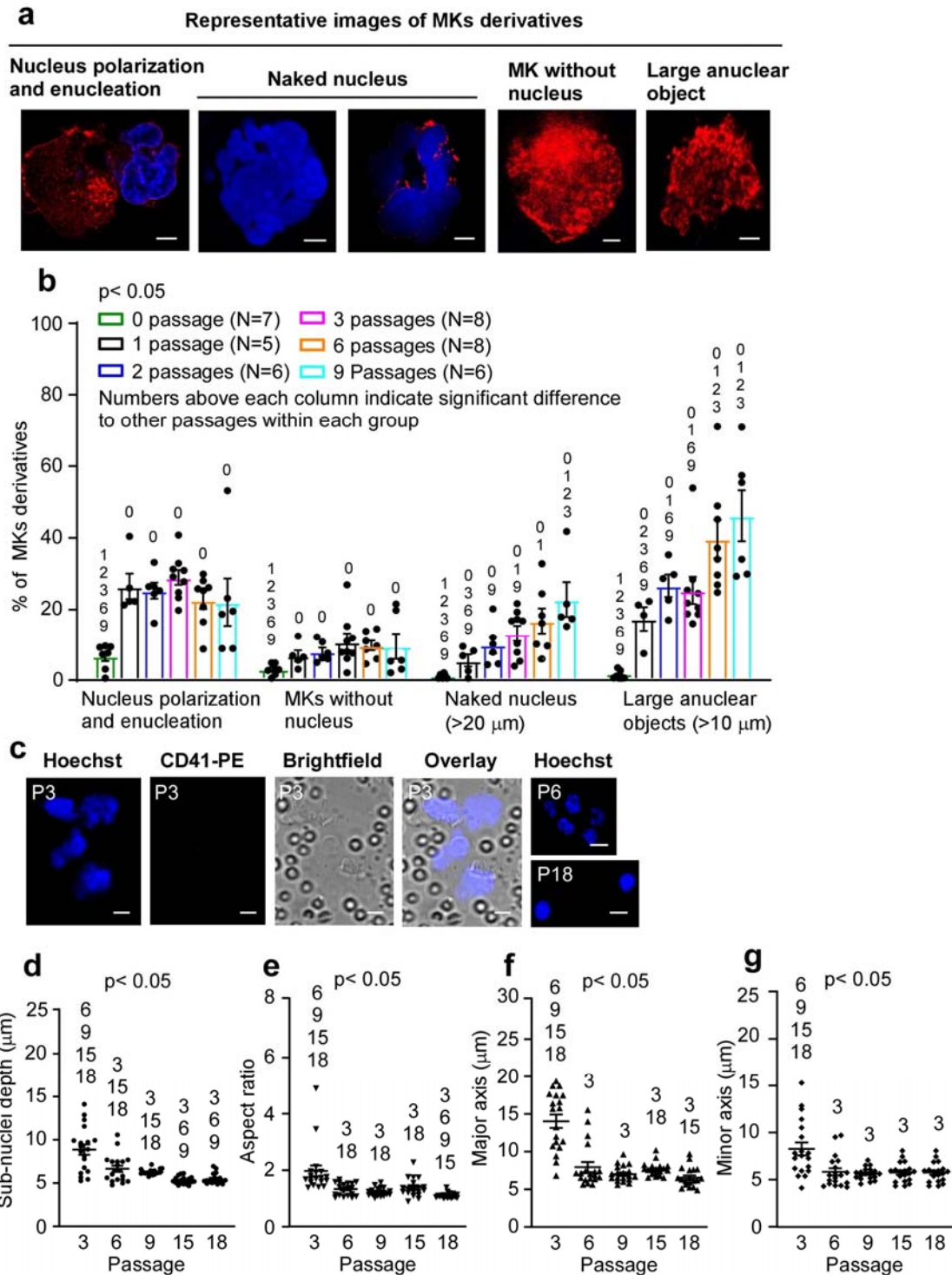
959
960
961

962 **Fig. 5: Generated platelets are functionality comparable to control platelets.** **Mouse**
963 **megakaryocytes (MKs), labelled with CD41-FITC or CD41-PE antibody or DiOC6 dye, were**
964 **passed through pulmonary vasculature *ex vivo* 18 times. Lungs were ventilated with air**
965 **throughout.** **a** Mean fluorescence intensity (MFI, a.u.), measured by FACS, of integrin α IIb β 3
966 activation (JON/A binding, PE-conjugated) and P-selectin expression (PE-conjugated) induced
967 by 2 U/mL thrombin or 5 μg/mL CRP in washed generated platelets (CD41-FITC) compared
968 to washed control platelets. **Data from generated platelets were pooled as total generated**

969 platelets (black dots), and also segregated by platelet size (diameter $<2.4 \mu\text{m}$ as pink dots,
970 diameter $3.7\text{-}5.6 \mu\text{m}$ as light brown dots), compared to control platelets (blue dots). Generated
971 platelets sizes were estimated using Flow Cytometry Polystyrene Particle Size Standard Kit
972 (Cat. PPS-6). Data were expressed as mean \pm S.E.M. (n as indicated). $P < 0.05$ was considered
973 statistically significant and determined using two-way ANOVA with Tukey's multiple
974 comparisons test. **b** Surface glycoproteins were measured by FACS. Generated platelets were
975 defined by staining with anti-CD41-PE antibody. Surface glycoproteins were stained with
976 different FITC-conjugated antibodies as indicated. Data are presented as mean \pm S.E.M. (n=6)
977 of FITC intensities. $P < 0.05$ was considered statistically significant and determined using
978 unpaired *t*-test. **c** Images of a representative platelet-rich thrombus. Generated platelets
979 (showing as blue in colour, stained with both DiOC6 (cyan) and CellTracker™ Red CMTPX
980 dye (magenta)) occupied all levels of the thrombus while host platelets (stained with
981 CellTracker™ Red CMTPX dye alone, magenta) were mainly situated on top of thrombus.
982 Images are representative of 5 independent experiments. Scale bars as indicated. **d-e** MFI
983 profiles of R1 and R2 (Region 1 and Region 2 from Fig. 5c) along the z-axis. **d** MFI profile of
984 R1 along the z-axis. In R1, generated platelets occupied the lower part of the thrombus up to
985 $\sim 12 \mu\text{m}$ (both cyan and magenta signals increased simultaneously), whilst beyond this point
986 host platelets were predominant (as magenta signals were stronger than green beyond $12 \mu\text{m}$).
987 **e** MFI profile of R2 along the z-axis. In R2, this part of thrombus was composed only of
988 generated platelets as both cyan and magenta signals changed simultaneously along z-axis.

989
990
991
992
993
994

Fig. 6



996

997

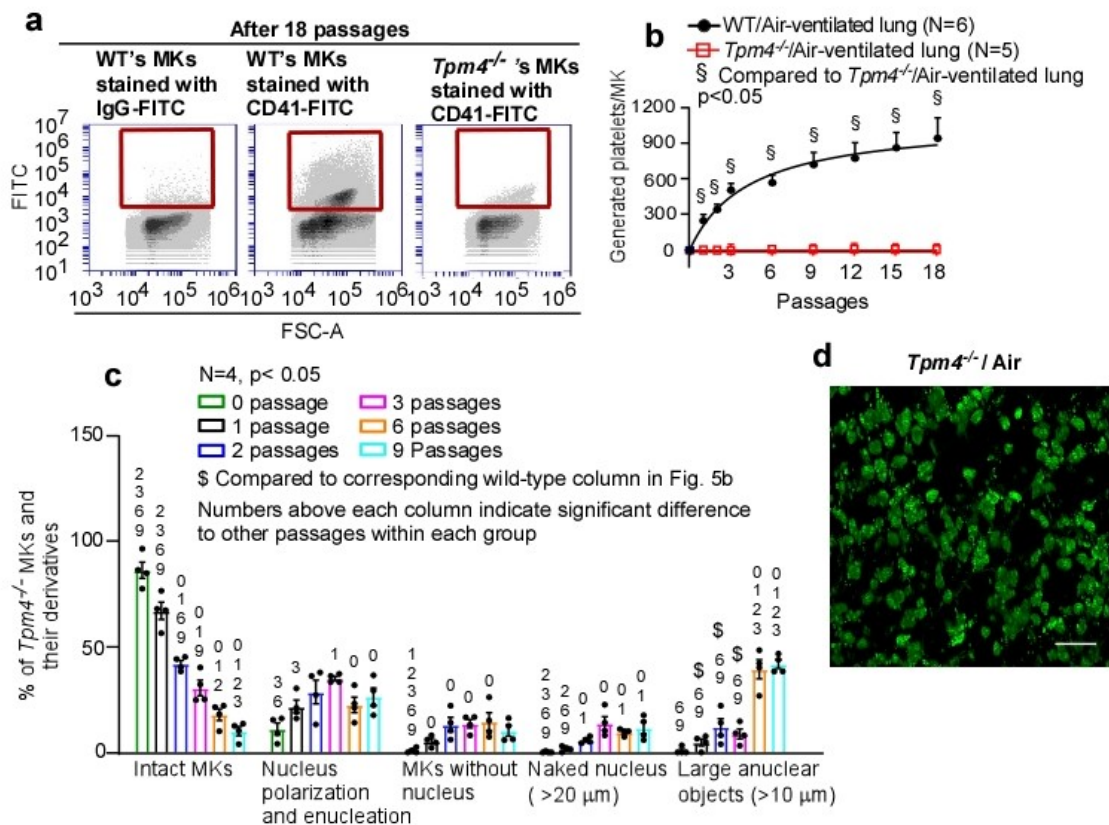
998 **Fig. 6: Megakaryocytes show nuclear marginalization and enucleation prior to**
 999 **fragmentation.** Megakaryocytes (MKs) from C57BL/6 mice, labelled with CD41-PE

1000 antibody (red) and Hoechst 33342 (blue), were passaged repeatedly through the pulmonary
1001 vasculature of a C57BL/6 mouse *ex vivo*. Lungs were ventilated with air throughout. **P < 0.05**
1002 **was considered statistically significant and determined using unpaired *t*-test.** **a** Representative
1003 images of MKs derivatives during the process of platelet generation: nuclear polarization and
1004 enucleation, where the nucleus is marginalized, of irregular shape or in the process of ejection
1005 from the cell; naked nuclei, where the ejected nucleus is larger than 20 μm in diameter and
1006 **free from the parent cell and/or partially encased in thin/patchy plasma membrane; MKs**
1007 **without nuclei**, where the MKs have an approximately circular shape but without nuclei; and
1008 **large anuclear objects**, where ghost cells are of irregular shape and larger than 10 μm in their
1009 longer axis. **b** Cells were imaged from samples of perfusates after passage numbers 1, 2, 3, 6
1010 & 9 through murine lung vasculature *ex vivo*. Five subgroups of MKs and their derivatives, as
1011 described above in **a** and in Fig. 1b, were quantified as a percentage of total number of cells.
1012 Quantification was from at least 250 fields of view, counting at least 230 cells in total for each
1013 of the subgroups. Data are from at least 5 independent experiments and presented as mean \pm
1014 S.E.M. **c-e** Nuclear lobes of MKs fragment into small condensed sub-nuclei. **c** Representative
1015 images, from n=3, of naked nuclei generated after multiple passages (as indicated) of mouse
1016 MKs through pulmonary vasculature. Scale bars: 5 μm . **d-g** **The depth **d**, aspect ratio **e**, major**
1017 **axis **f** and minor axis **g** of sub-nuclei decreased substantially with increasing passages. These**
1018 **parameters were measured from after 3 passages to after 18 passages: depth 8.9 μm to 5.5 μm ,**
1019 **aspect ratio 1.8 to 1.1, major axis 14.1 μm to 6.5 μm , minor axis 8.1 μm to 5.7 μm . Each**
1020 **symbol represents one sub-nucleus. Numbers above each column indicate significant**
1021 **difference to other passages.** Data are from 3 independent experiments displayed as mean \pm
1022 S.E.M.

1023

1024

1025



1027

1028

1029

1030

1031

1032

1033

1034

1035

1036

1037

1038

1039

Fig. 7: Tropomyosin 4 is required for the final steps in platelet generation in the pulmonary vasculature. Megakaryocytes (MKs) from Tropomyosin4^{-/-} (*Tpm4*^{-/-}) mice labelled with FITC-conjugated anti-CD41 antibody, were passaged repeatedly through the pulmonary vasculature of a C57BL/6 mouse *ex vivo*. For controls, wild-type (WT) MKs were stained either with FITC-conjugated anti-CD41 or isotype antibodies. Lungs were ventilated with air throughout. **a** Representative FACS dot plot images are shown for generated platelets (CD41-FITC positive events are within the red square). **b** Numbers of generated platelets per *Tpm4*^{-/-} MKs, or control WT MKs, in perfusates after different passage numbers through WT lung, were quantified by FACS. *Tpm4*^{-/-} platelets were consistently undetectable after up to 18 passages, in the perfusate. Data shown are platelets generated per MK from either *Tpm4*^{-/-} MKs or control WT MKs and displayed as mean ± S.E.M. (n as indicated). **P < 0.05** was

1040 considered statistically significant and determined using unpaired *t*-test. **c** Cells were imaged
1041 from samples of perfusates after passage numbers 1, 2, 3, 6 & 9 through murine lung
1042 vasculature *ex vivo*. Cells were morphologically classified as 5 subgroups: intact MKs (as per
1043 Fig. 1b) and MK derivatives (shown in Fig. 6a) and quantified as a percentage of total number
1044 of cells. Quantification was from at least 150 fields of view, counting at least 170 cells in total
1045 for each of the subgroups. Numbers above each column indicate significant difference to other
1046 passages within each group. Dollar sign (\$) above columns represents significant difference to
1047 corresponding wild-type column in Fig.6b. **P < 0.05 was considered statistically significant and**
1048 **determined using unpaired *t*-test.** Data are from 4 independent experiments and displayed as
1049 mean ± S.E.M. **d** Abundant fluorescent objects, ~10 µm diameter, were visible in sections of
1050 mouse lung after 18 passages of stained *Tpm4*^{-/-} MKs, as shown in extended focus stacks of 20
1051 continuous two-photon planes of lung. Images shown are representative of 3 independent
1052 experiments. Scale bar: 20 µm.

1053

1054

1055

1056

1057

1058

1059

1060

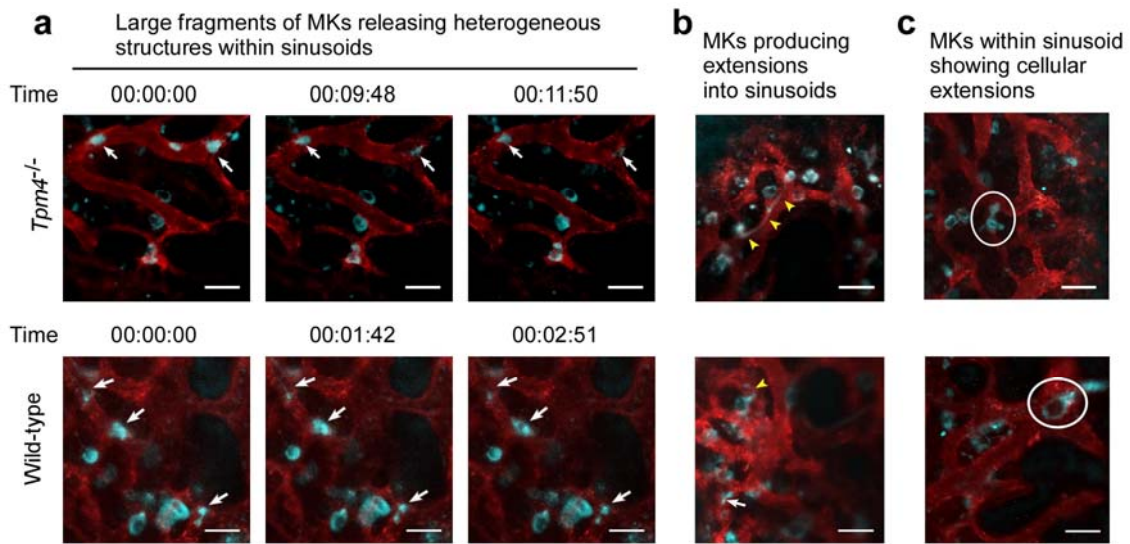
1061

1062

1063

1064

1065

Fig. 8

1067

1068

1069 **Fig. 8: Intravital two-photon microscopy of bone marrow megakaryocytes in live mouse**1070 **calvarium.** Bone marrow vasculature was visualized by intravenous injection of anti-CD105-

1071 AlexaFluor 546 antibody and AlexaFluor 546-labeled BSA (red). Megakaryocytes (MKs) and

1072 **their derivatives** were stained intravenously with anti-GPIX-AlexaFluor 488 antibody (cyan).1073 Both wild-type (WT) and *Tropomyosin 4*^{-/-} (*Tpm4*^{-/-}) MKs were generally seen in close contact1074 with the bone marrow sinusoidal walls. **a** Representative images of large fragments of WT and1075 *Tpm4*^{-/-} MKs (white arrows) within sinusoidal vessels releasing heterogeneous structures in1076 the direction of blood flow, at time points indicated. **b** Representative images of WT and *Tpm4*^{-/-}

1077 MKs, with cell bodies within the marrow space, producing extensions into sinusoids (yellow

1078 arrowheads). **c** Representative images of WT and *Tpm4*^{-/-} MKs within the sinusoid, showing1079 cellular extensions (white circles). Images were taken from 6 WT and 6 *Tpm4*^{-/-} mice. Scale

1080 bars, 50 μm.

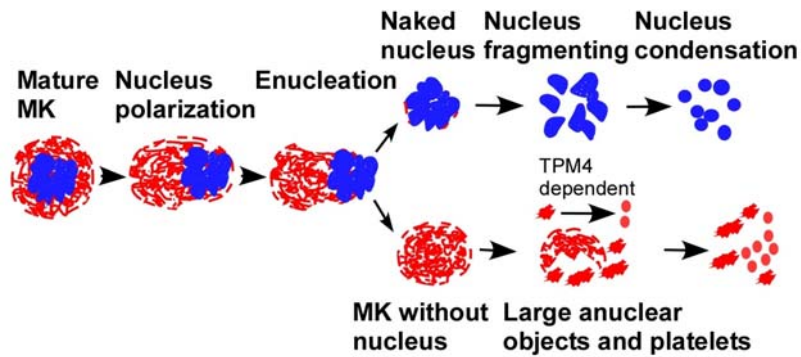
1081 .

1082

1083

1084

Fig. 9



1085

1086

1087

Fig.9: Schematic diagram of the steps in platelet generation from mature

1088

megakaryocytes. Diagram showing platelet generation pathway from intact mature

1089

megakaryocytes (MKs) to final platelet formation, by repeated passage of MKs through the

1090

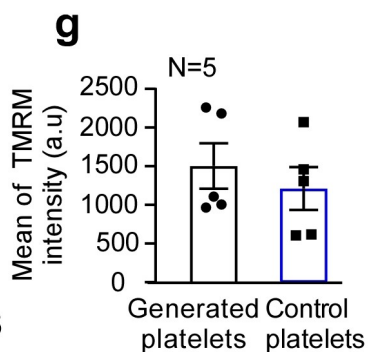
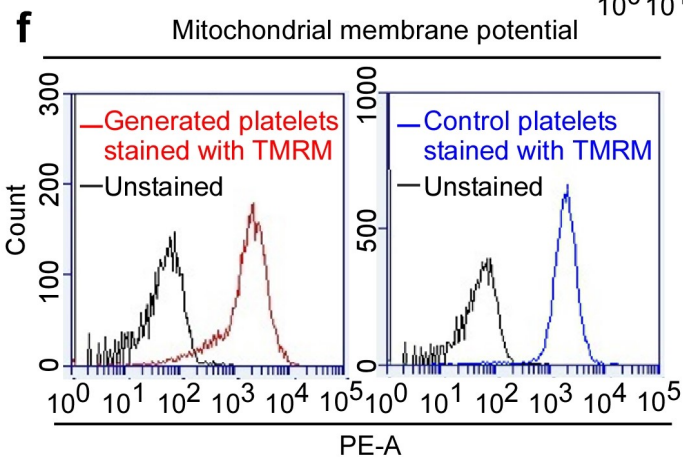
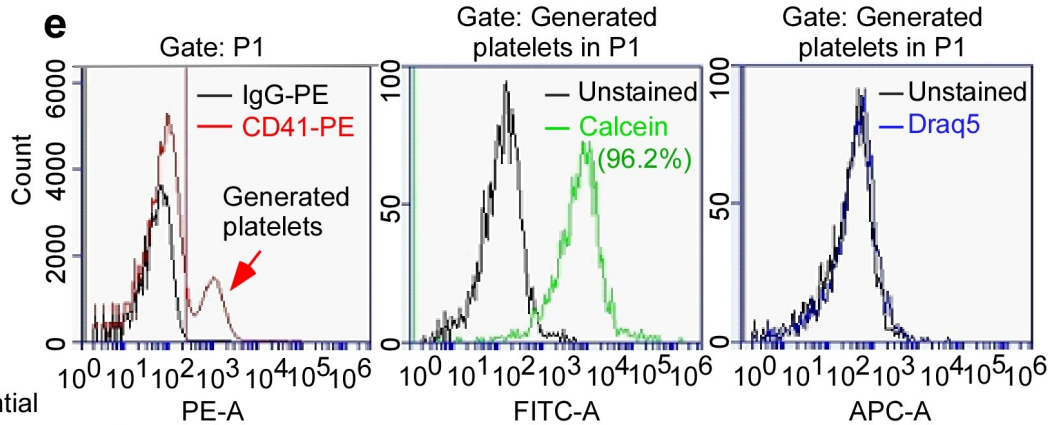
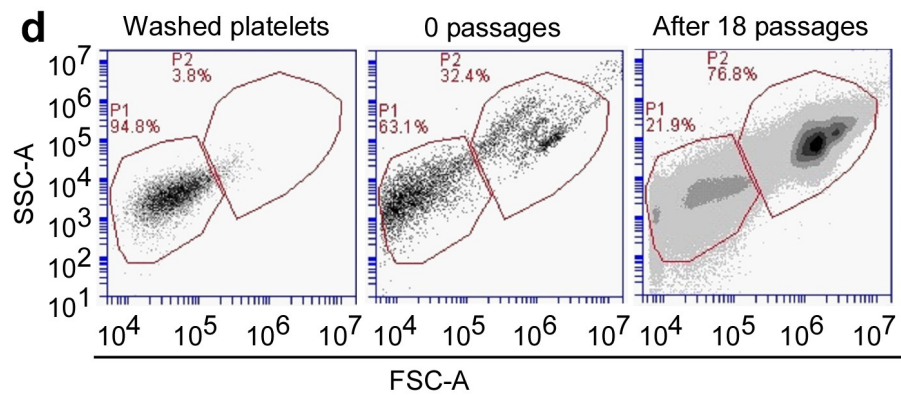
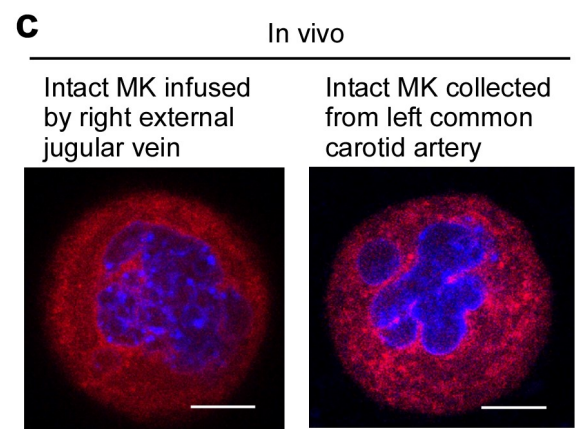
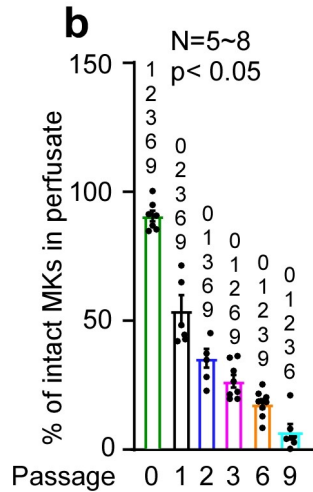
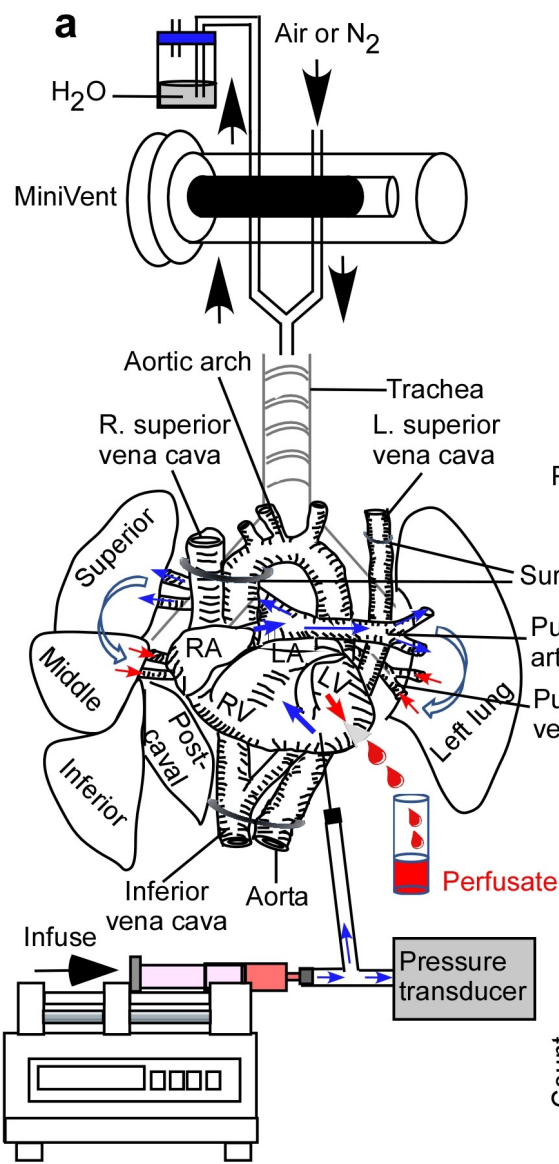
pulmonary vasculature. The process involved nuclear polarization, enucleation, gradual

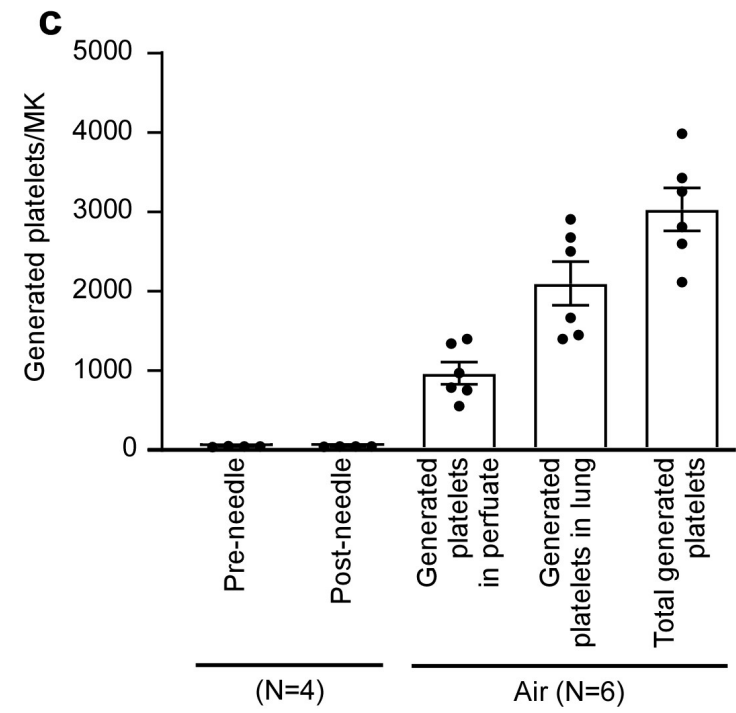
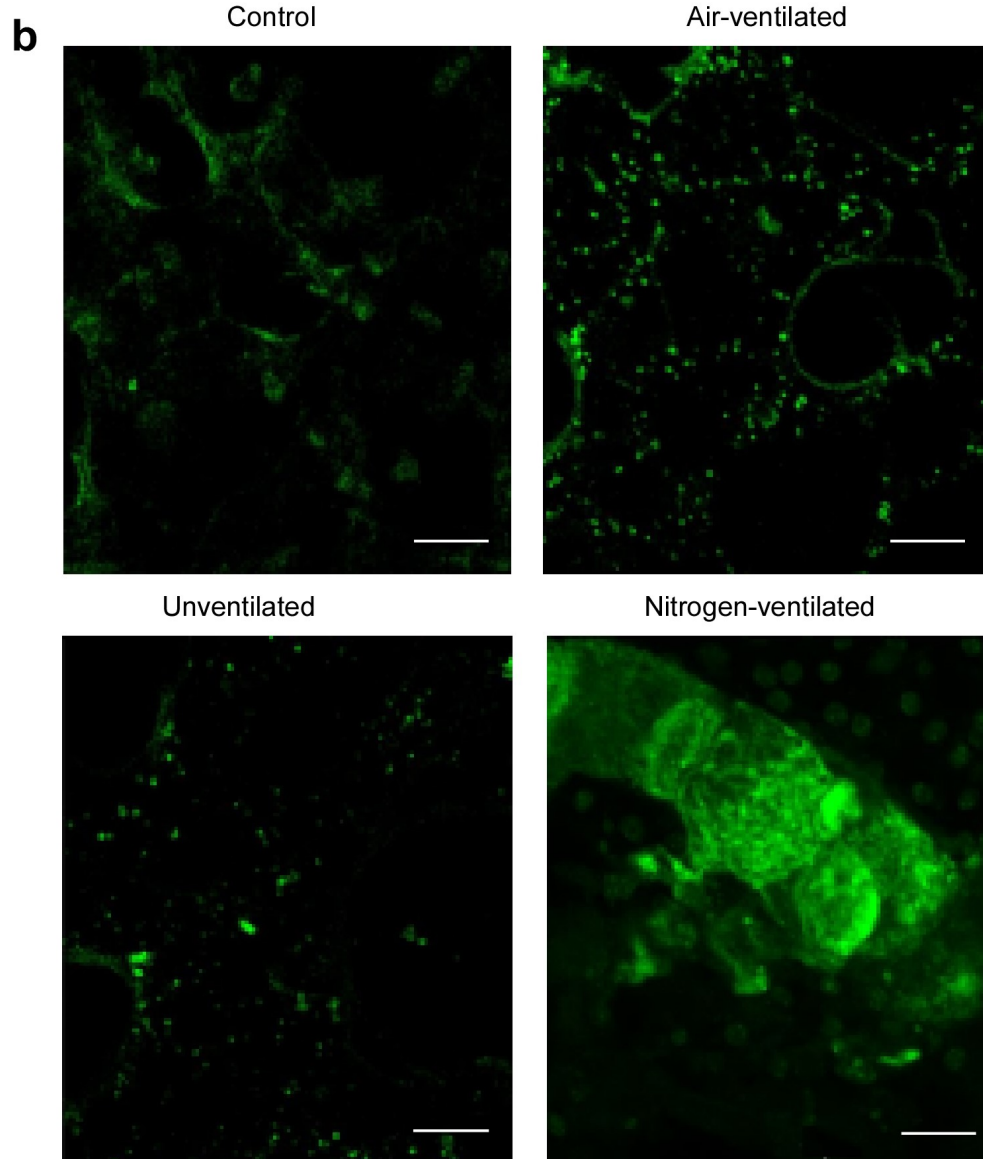
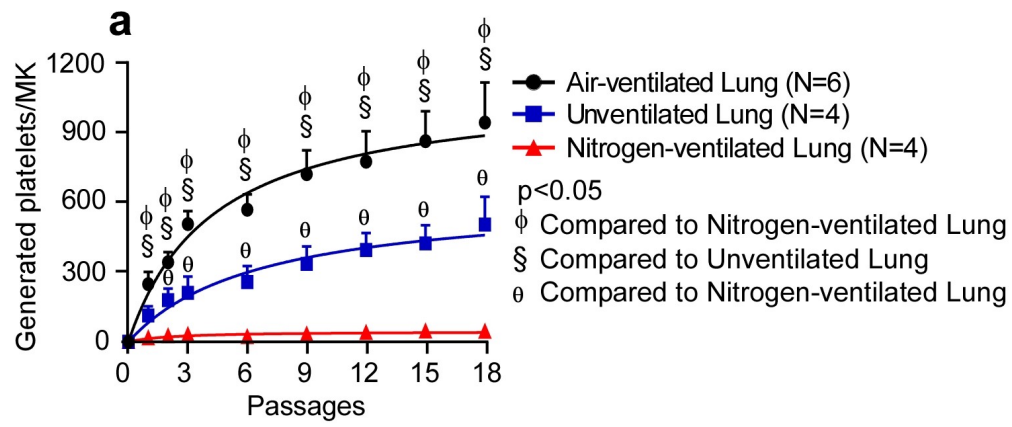
1091

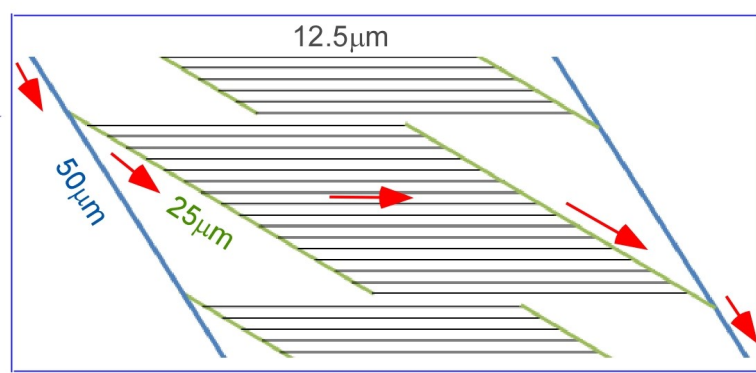
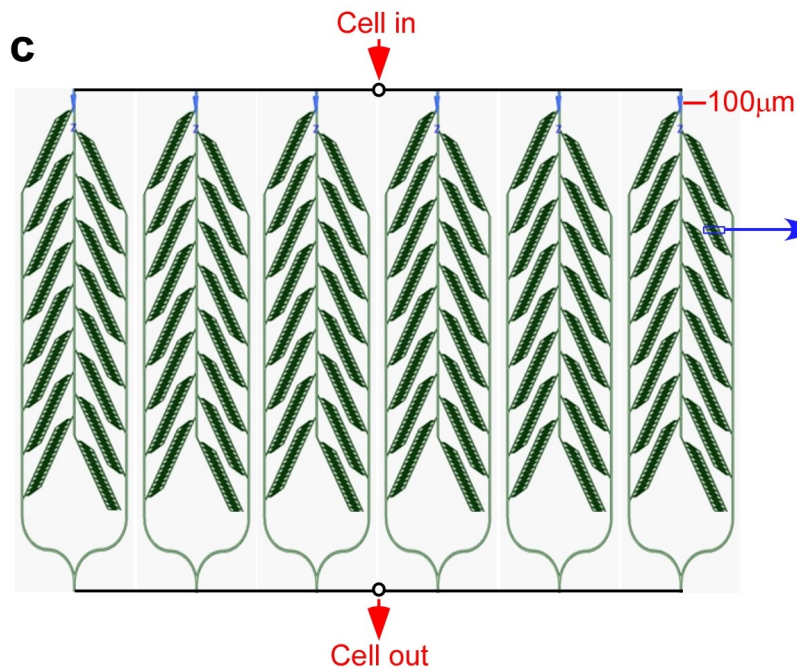
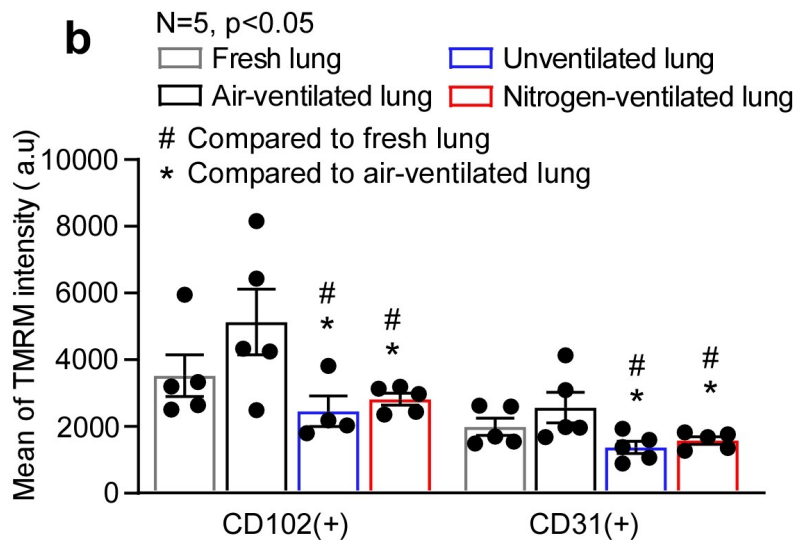
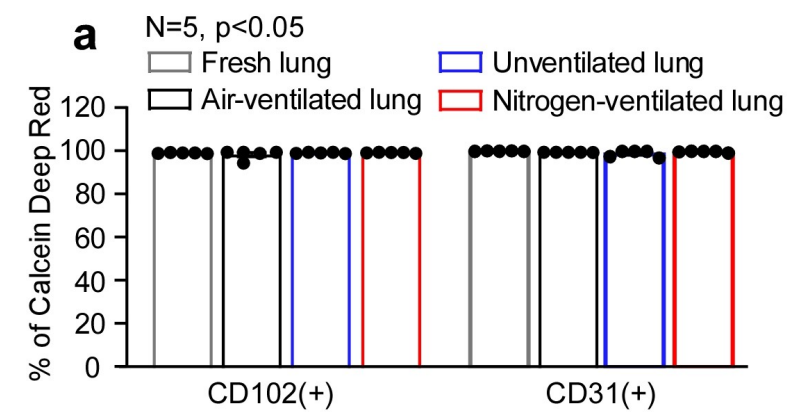
cytoplasmic fragmentation into platelets and nuclear fragmentation and condensation.

1092

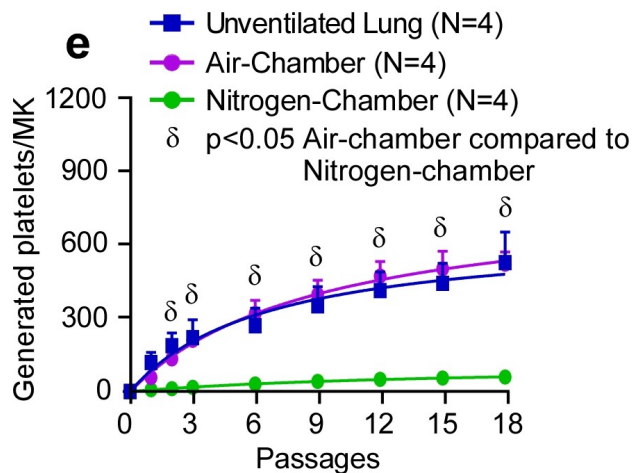
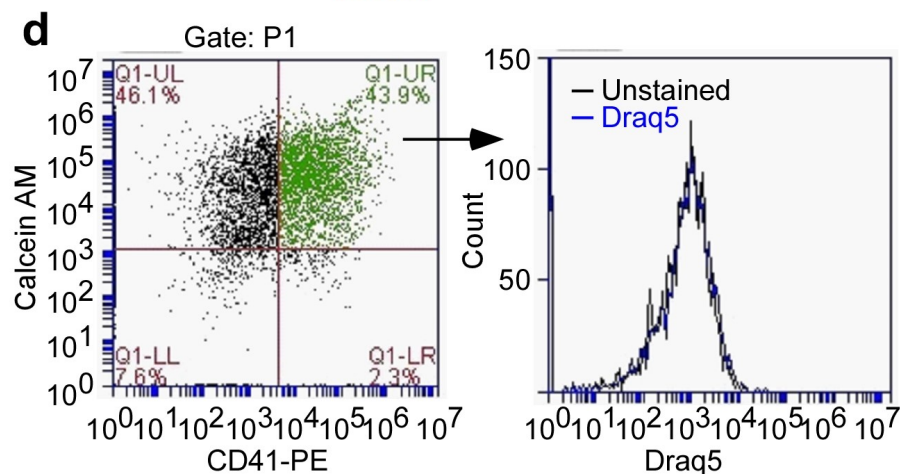
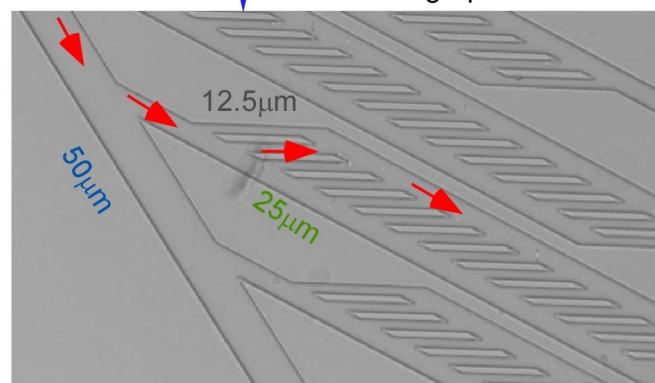
1093

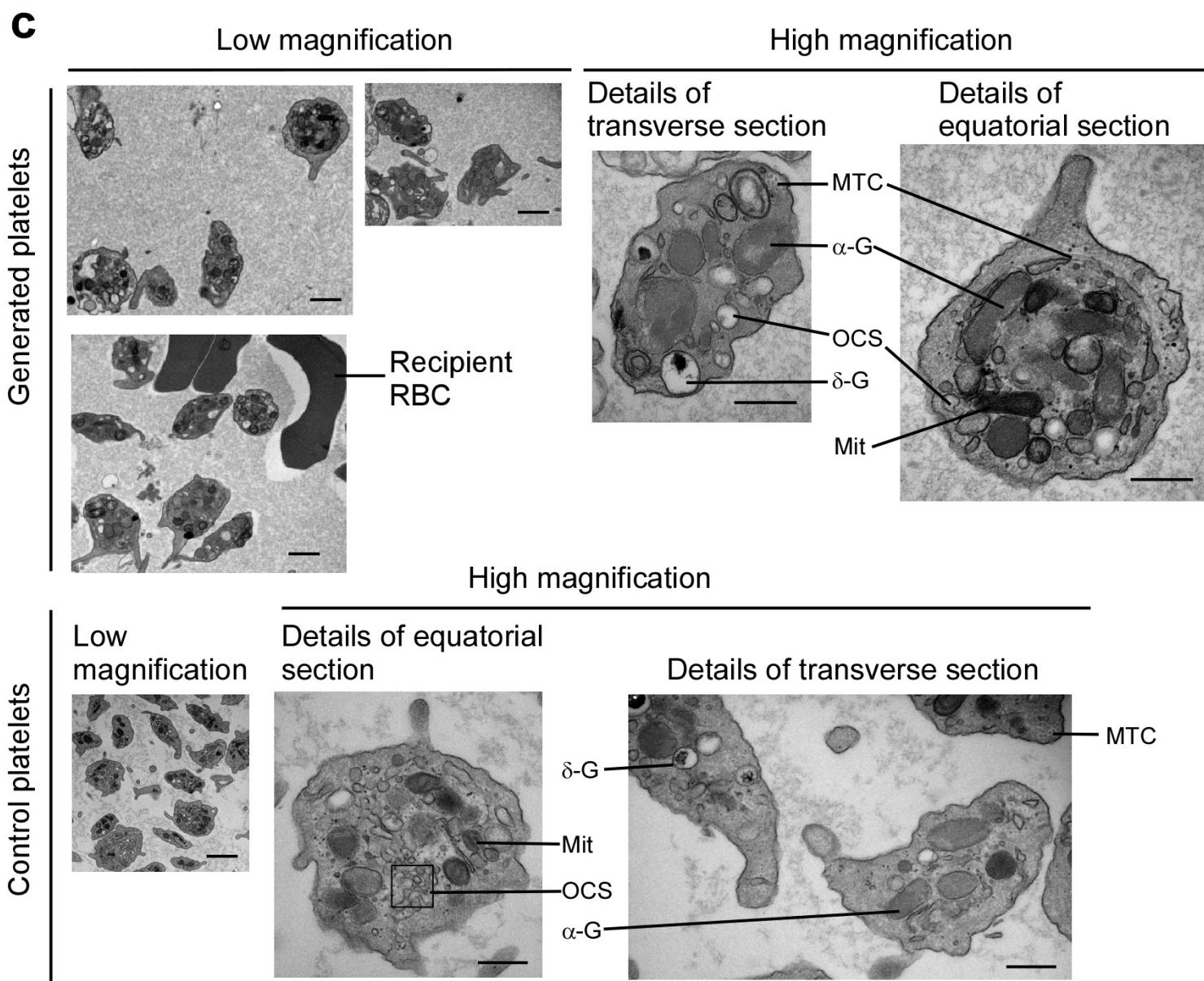
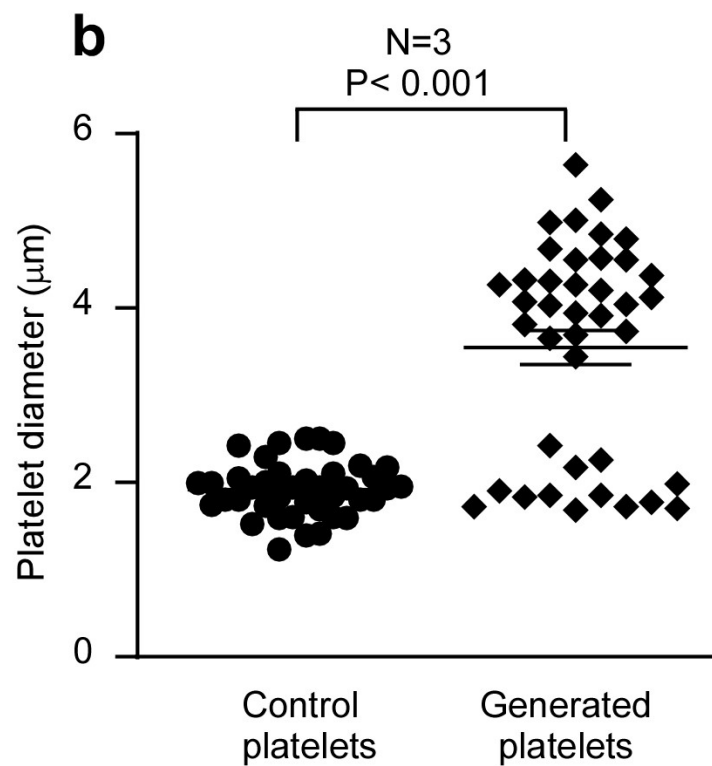
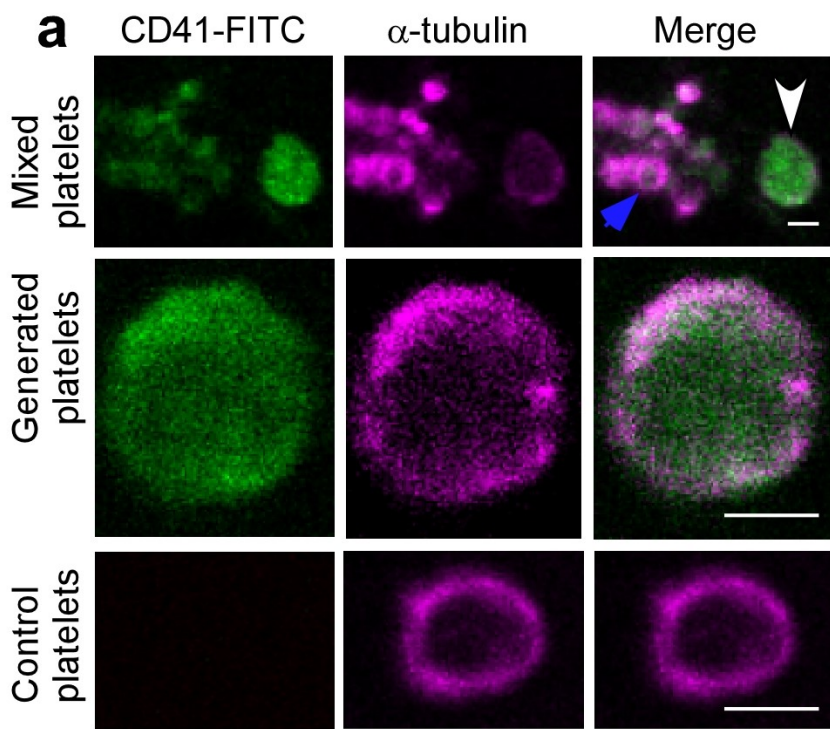


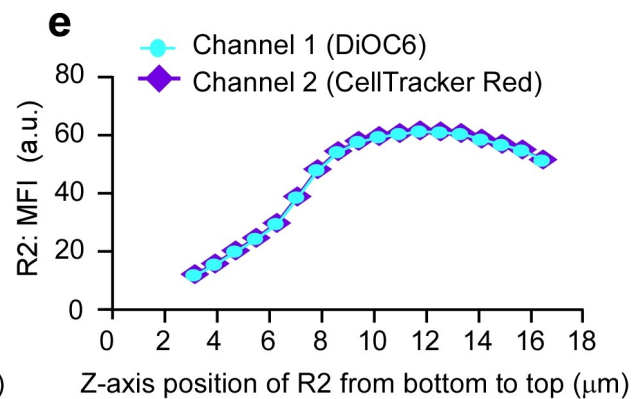
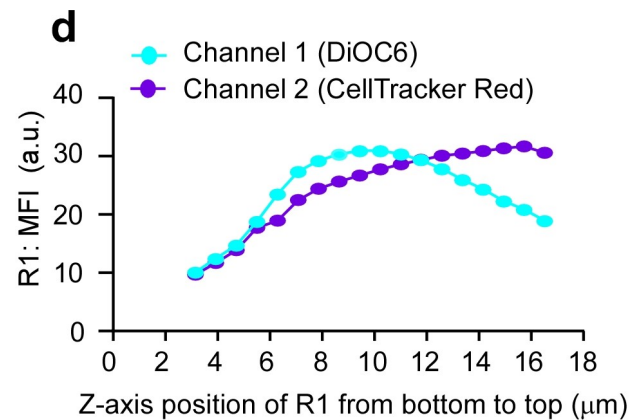
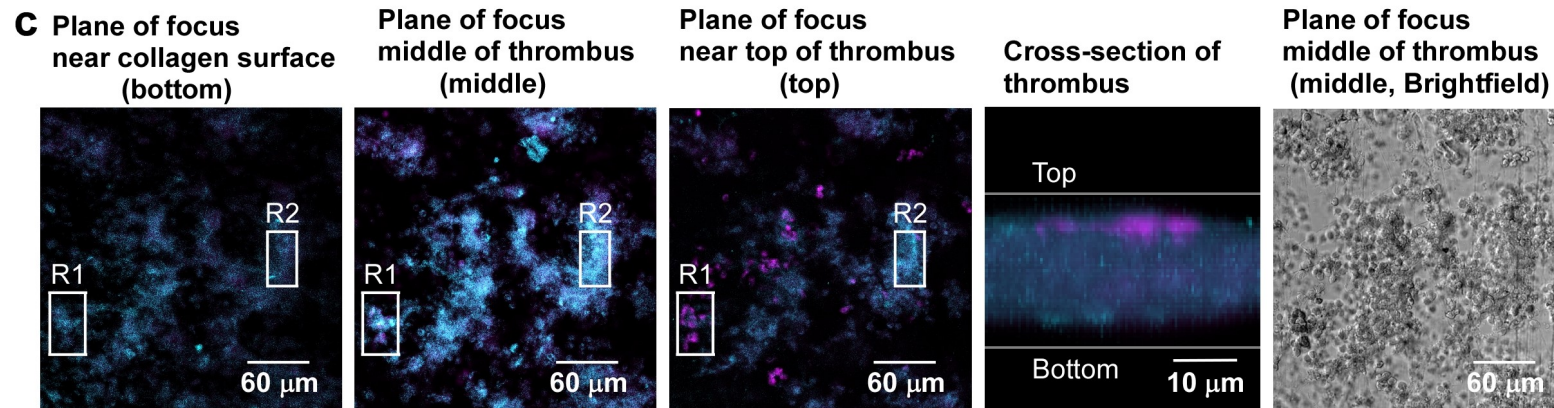
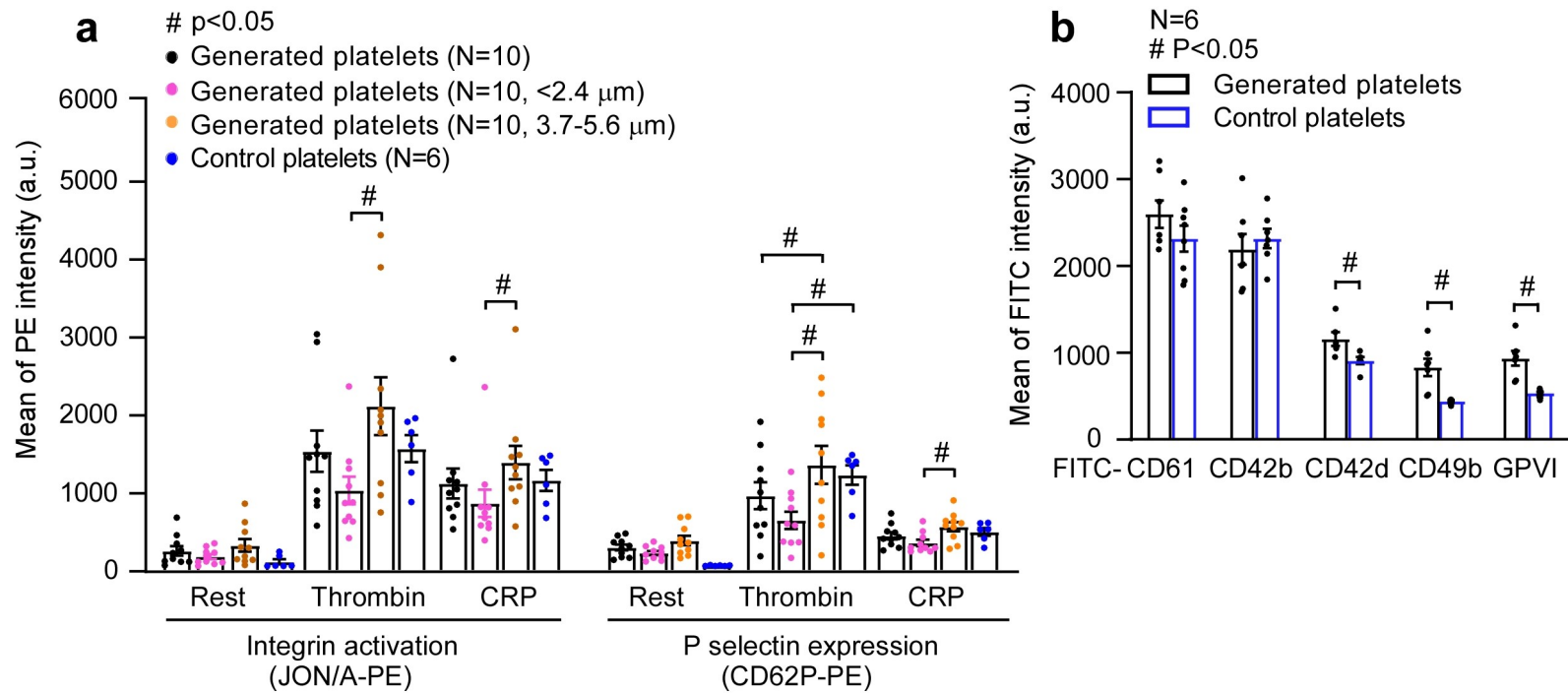




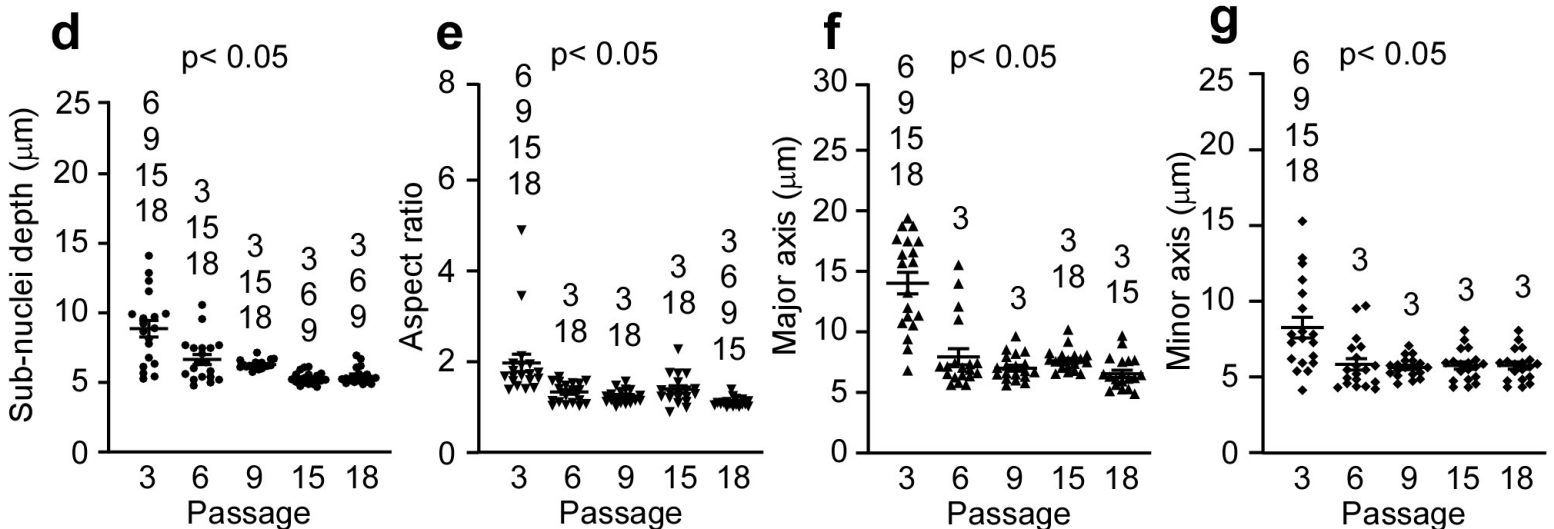
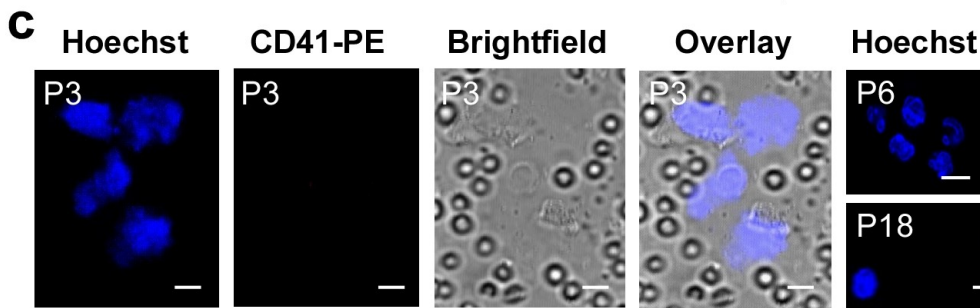
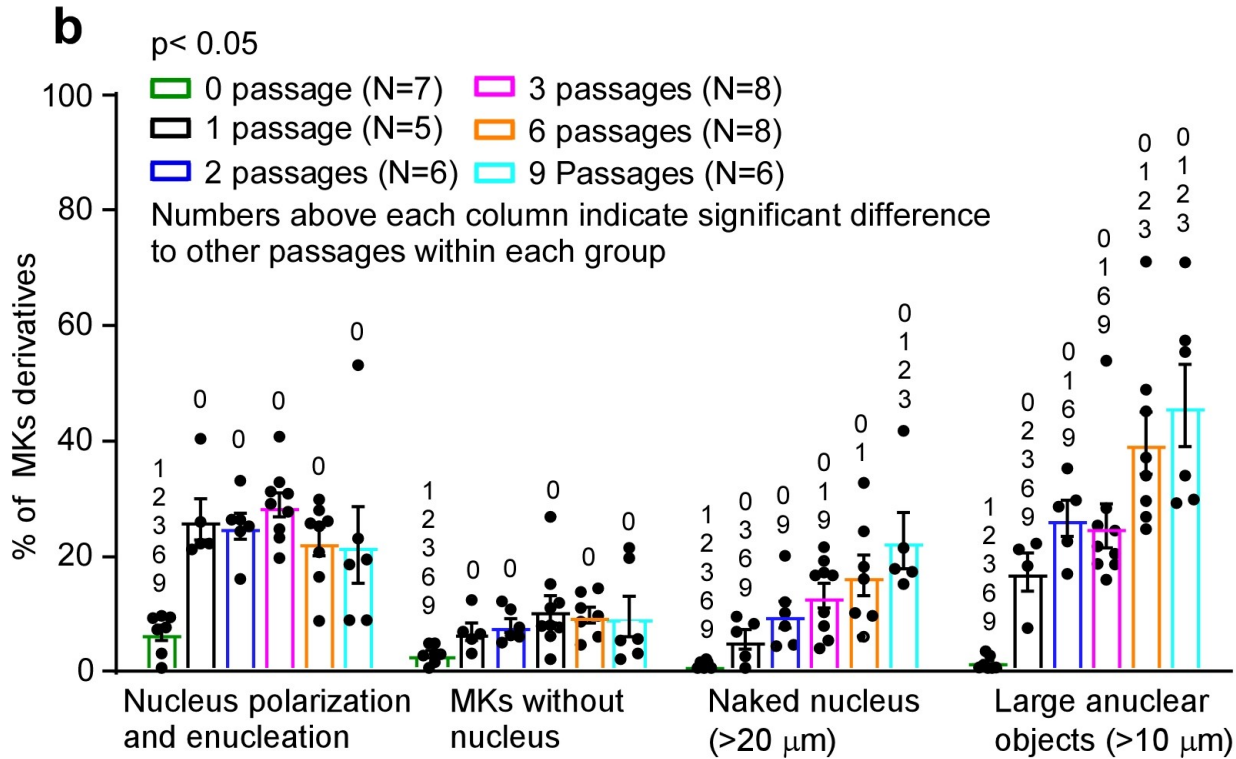
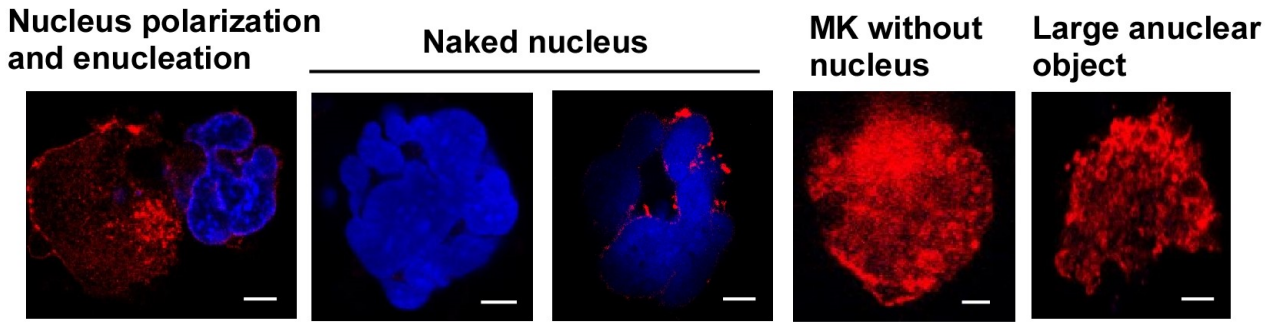
Photomicrograph

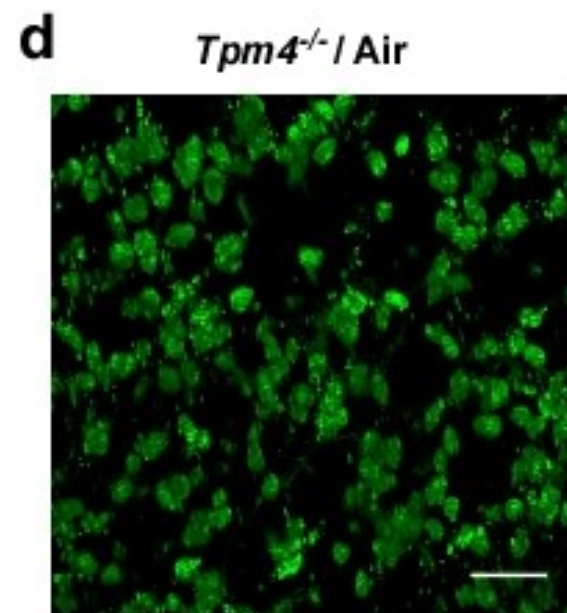
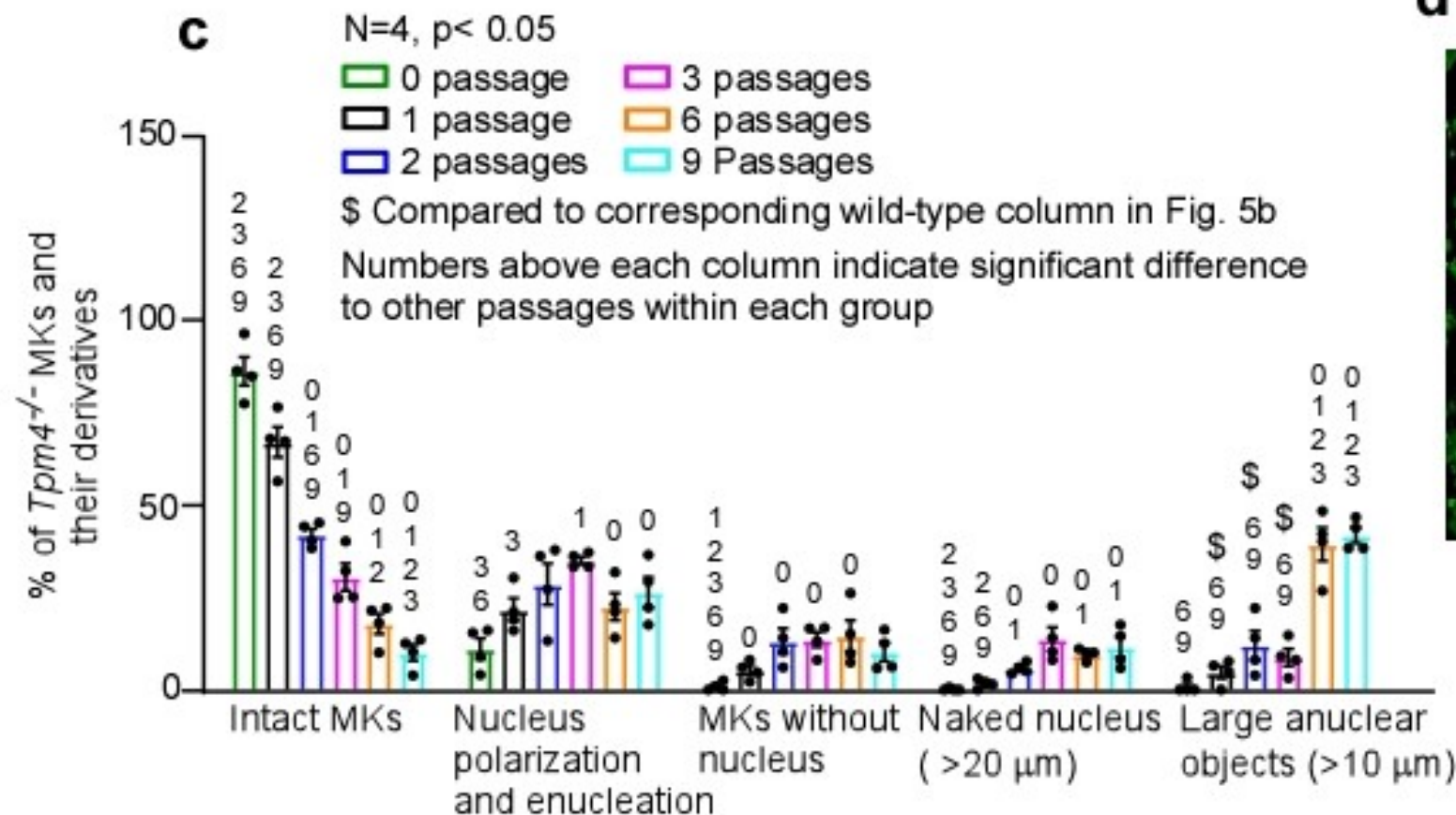
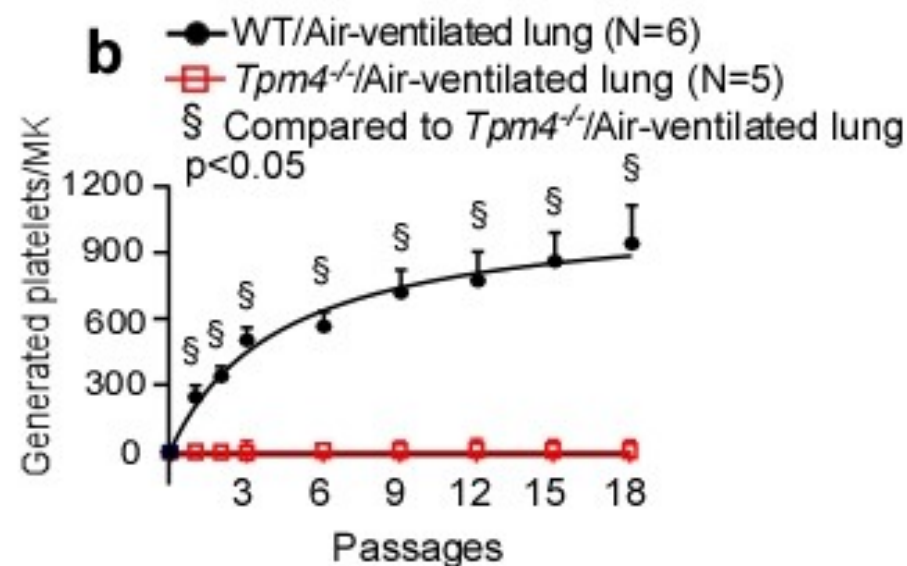
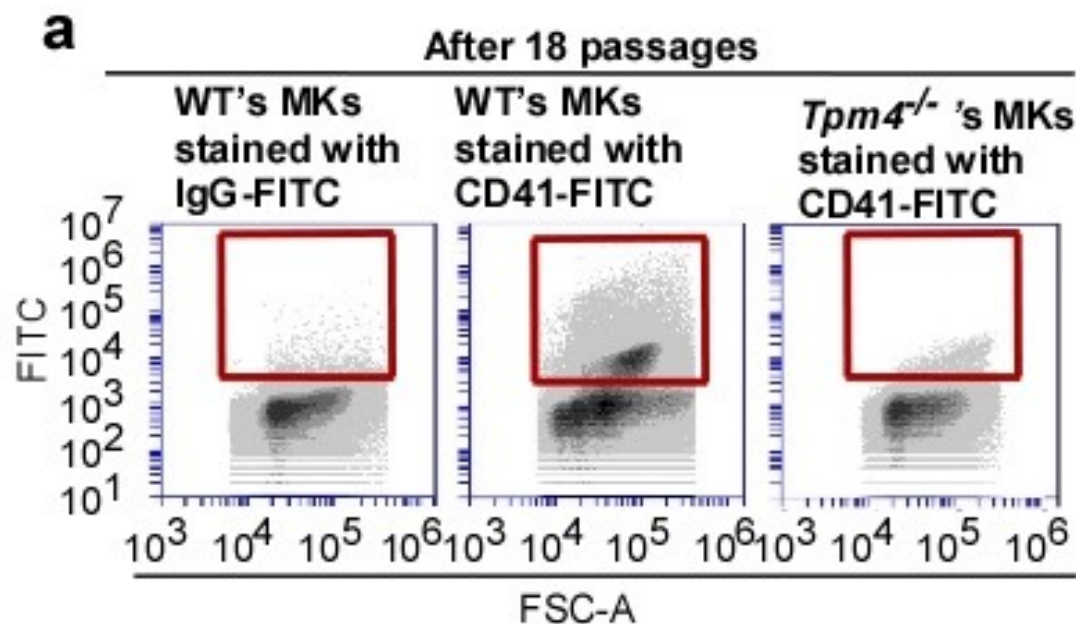




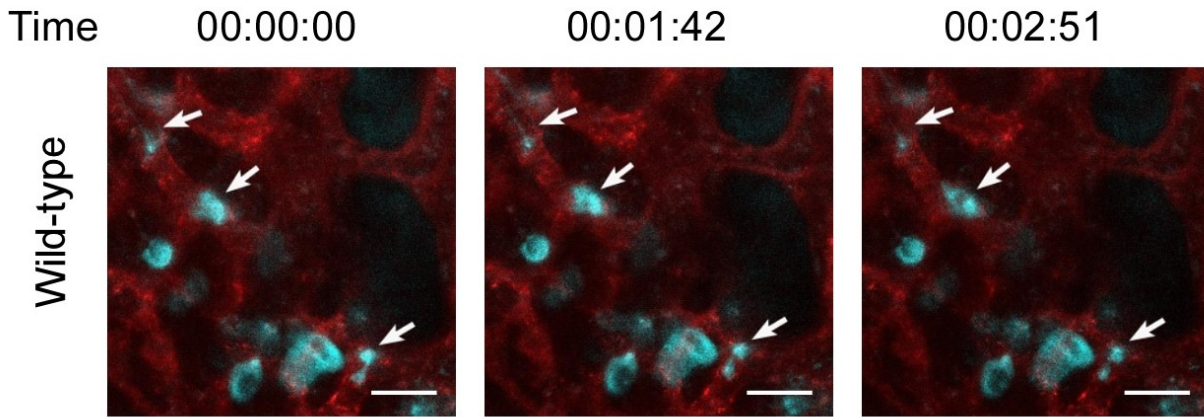
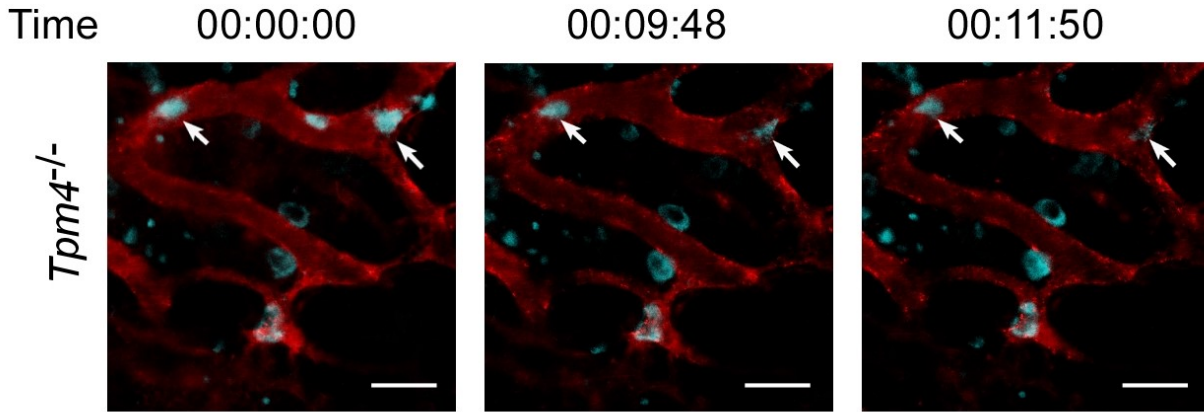


a Representative images of MKs derivatives

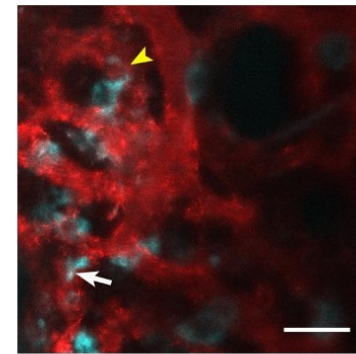
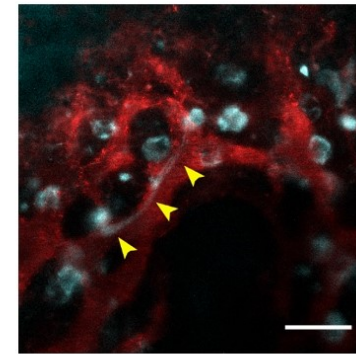




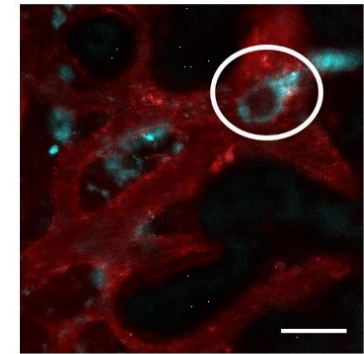
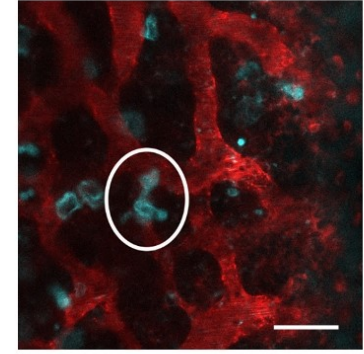
a Large fragments of MKs releasing heterogeneous structures within sinusoids

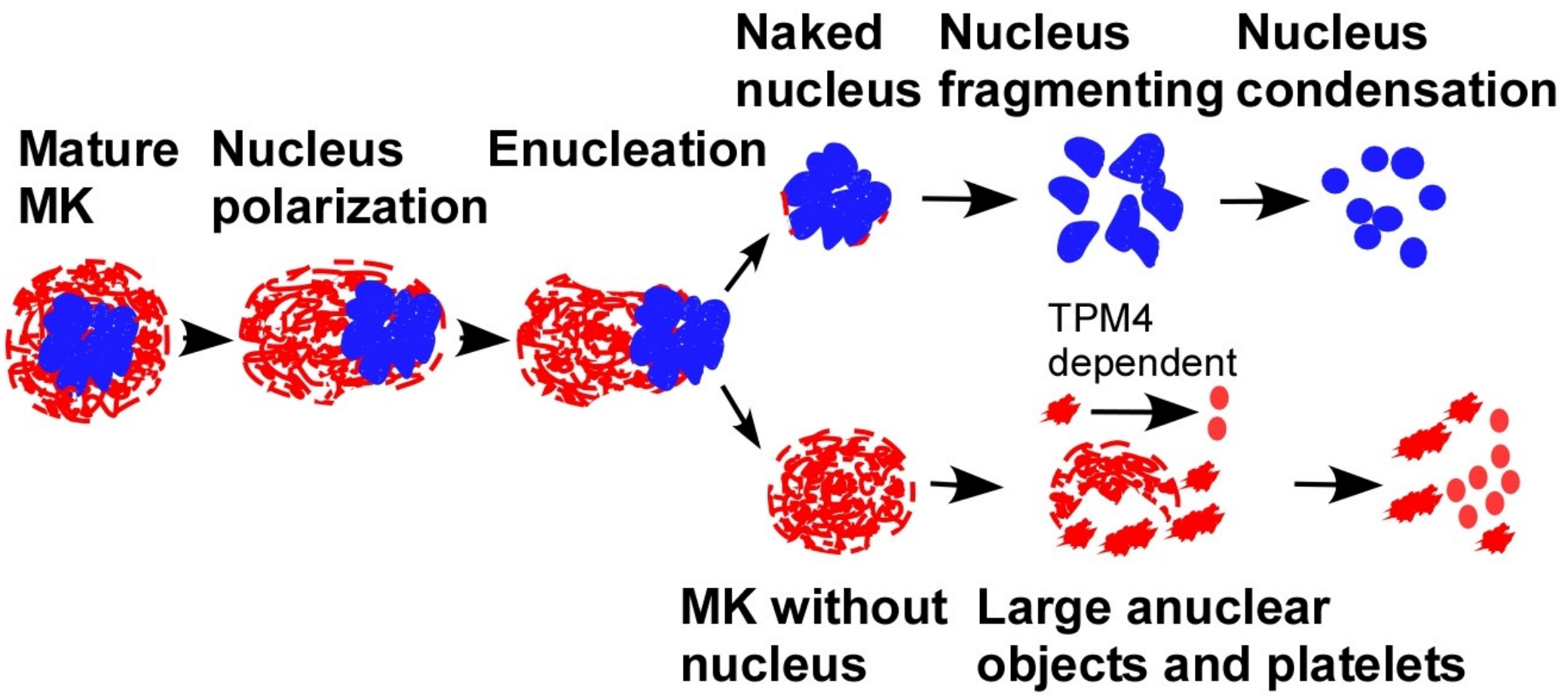


b MKs producing extensions into sinusoids



c MKs within sinusoid showing cellular extensions





REVIEWER COMMENTS

Reviewer #1 (Remarks to the Author):

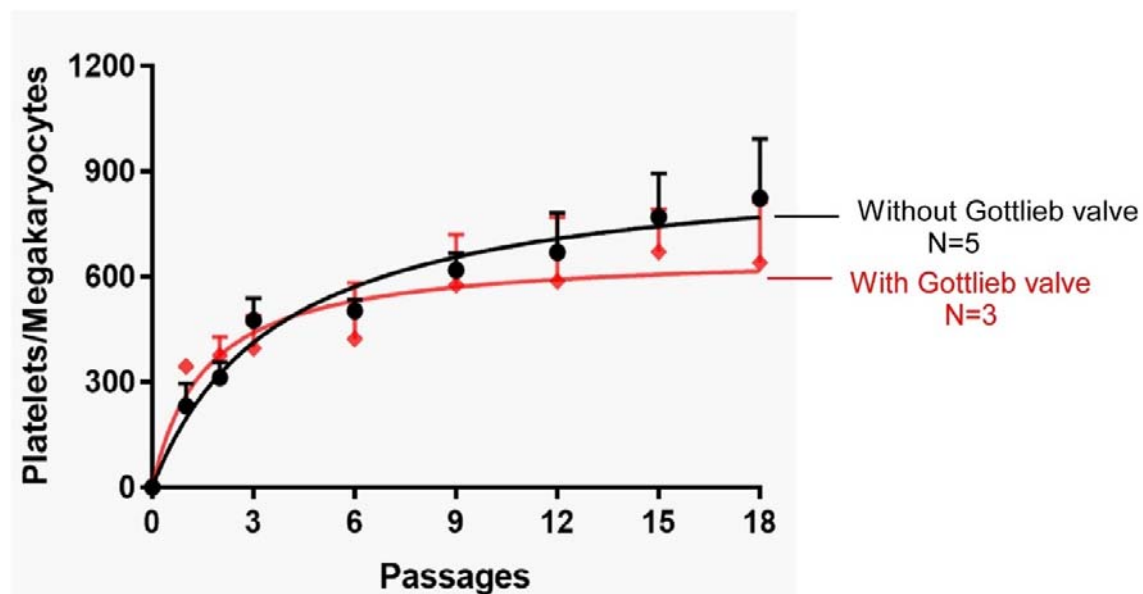
I thank the authors who responded satisfactorily to all my comments and the manuscript is acceptable for publication

Reviewer #2 (Remarks to the Author):

Thank you for the responses. The details of the heart-lung prep are now much clearer. I have one remaining question. Did the application of the end-expiration device (Gottlieb valve) affect any of the results such as those in Figure 1b or Figure 2a? If possible, data should be shown with and without the device.

Thanks for this question. Here is the comparison with or without Gottlieb valve (below). There is no significant difference between these two conditions in terms of platelet generation in the perfusates over passages.

We have not included this data in our text, because the data in that Figure showed no significant difference with or without Gottlieb valve.



Reviewer #3 (Remarks to the Author):

WHERE'S SUPPL FIG.1A IN TEXT? CHANGE ORDER IN FIG?

Thanks for the good suggestions. We now have modified these and highlighted in red colour in the text.

158 nitrogen-ventilation relative to air-ventilated controls, and equivalent to the unventilated lung
 159 (Fig.3b). NEED TO BE CAREFUL HERE. SHOW FSC COMPARE TO DONOR PLTS AND NEED TO MEASURE
 MARKER OF ACTIVATION (EG, ANNEXIN V) TO MAKE YOUR STATEMENT OR NEED TO MODIFY STATEMENT.
 ALSO IS THIS A SIZE SELECTED STUDY. NO BIG MKS DRAQ5 POSITIVE COME THROUGH?
 160 To further verify whether the structural arrangement of the lung capillary bed could mediate
 161 platelet generation, we designed a polydimethylsiloxane (PDMS)-based (gas permeable)
 162 microfluidic chamber with channel arrangement mimicking tissue microcirculation. The
 163 channels were of uniform depth of 10 μm throughout, where the entry and exit channels had a
 164 width of 100 μm and where branches emerged halving the channel width each time, to a
 165 minimal width of 12.5 μm , as per the diagram shown in Fig.3c. This channel arrangement
 166 allowed us to flow through cells and determine platelet generation in the perfusate after
 167 repeated passage. Fig.3e shows that the numbers of generated platelets per MK, when MKs are
 168 flowed through the microfluidic chamber conditioned in normal air, gradually increased with
 169 increasing passages, similar to the numbers generated in the unventilated lung, with $492.3 \pm$
 170 47.6 platelets/MK after 18 passages. The generated platelets were live anuclear platelets (Fig.
 171 3d). WHAT DOES THIS MEAN HERE?
 SHOW DONOR PLTS FOR COMPARIOSN
 We also conditioned microfluidic chambers with pure nitrogen to completely de-

In Fig. 1d, Gating strategy for quantification of generated platelets. The left panel is the donor (control) platelets.

WHAT DOES THIS MEAN HERE? SHOW DONOR PLTS FOR COMPARIOSN

In Fig. 1e, we showed the Calcein AM staining to determine the viability for generated platelets-“**live**”

We now have added donor platelets (control platelets) stained with Calcein AM and Draq5 in Fig. 1 e. Supplementary Fig 1e shows DRAQ5 staining for MKs, which provides a positive control for this stain.

1. In Fig 1d, why is that P1 window more “plt-like” at 0 passages and the P2 larger after 18 passages. Seems the reverse of what to expect.

- 1) MKs were enriched using a **1.5%/3% BSA gradient** (4 mL 1.5% BSA + 4 mL 3% BSA) for 1 hour, before infusing into the lung-heart system or microfluidic chambers. This step removes most small cells or particles.
- 2) In the P1 window, at 0 passages, in our MKs preparation, only **1.3-7.6% events** were **CD41+**. That is **8.2±2.0 CD41+ events per MK** in MKs suspension (N=4), as shown in **Fig 2c-pre-needle**. We have not identified these CD41- events.
- 3) The numbers of generated platelets in the perfusates over different passages are all given after subtraction of the number of CD41+ events at 0 passage.
- 4) We have now added new **Supplementary Fig 1e** showing the staining of events in the P2 gate after 18 passages, including Draq5 staining, which showed Draq5 staining was efficient.

WHAT IS P2 THAT APPEARS TO BE THE DOMINANT SPECIES AFTER 18 PASSAGES?

The events in P2 window after 18 passage predominantly are white blood cells, red blood cells and some CD41+ events, as shown in Supple Fig. 1e----events in P2 from Fig. 1d. 10 ul of MK suspension or perfusates were measured by FACS.

We now have added “whole blood” from host mouse, as a comparison, as gating strategies in Figure 1d.

2. In Fig 1f, annexin v or p-selectin or Jon A binding would have been useful and more commonly done to show that you were generating “happy” platelets.

SHOULD'VE MEASURED ANNEXIN V OR P-SELECTIN SURFACE LEVELS OR JON-A TO SHOW THAT THESE AREN'T ACTIVATED CYTOPLASMIC FRAGMENTS

The results of P-selectin expression and integrin activation (JON/A binding assay) for generated platelets in lung-heart system in response to agonists (thrombin and CRP) are shown in Fig. 5a and described under “**Generated platelets are morphologically and functionally normal**” section in **Result part**.

Fig. 4a shows that generated platelets display an almost uniquely characteristic sub-plasma membrane **microtubular ring**, running circumferentially in resting platelets. Fig. 4c showed the **microtubule coils**. These features **make us believe that they are platelets rather than cytoplasmic fragments**.

196 equivalent responses to agonists (CRP and thrombin) in terms of integrin α Ib β 3 activation and
197 degranulation (P-selectin expression, Fig.5a). Given that generated platelets appeared to
198 segregate into two size subpopulations, we then compared the responses in these two
199 subpopulations. The subpopulation with the larger size (diameter ranges: 3.7-5.6 μ m) were
200 more responsive, by comparison with the subpopulation with the smaller size, to thrombin and
201 CRP in both integrin α Ib β 3 activation and P-selectin expression. It has been shown that larger
202 platelets are more responsive^{21,22}, and our data are therefore consistent with this observation.
203 We next compared the key glycoprotein expression on the surface of generated platelets. The

WHERE IS THESE DATA AND WHAT DO "MORE RESPONSIVE MEAN? IDEALLY, USED AN AGONIST DOSE RESPONSIVENESS

In the thrombus formation assay, shown in **Fig. 5c-e and Supplementary Movie 6**, generated platelets occupied all levels of the thrombus whilst control platelets were mainly situated on top of the thrombus. This suggested that **generated platelets had a higher responsiveness to collagen, or were primary reactors to it**.

173 ± 1.4 platelets/MK after 18 passages, similar to those generated in lungs ventilated with pure
174 nitrogen (Fig. 2b). Altogether, these data suggested that (1) air-ventilation and healthy ECs are
175 required for MKs to generate physiological levels of platelets in the heart-lung preparation; (2)
176 the structural arrangement of the pulmonary microcirculation plays a role in platelet generation;
177 (3) lack of ventilation or nitrogen-ventilation for 2 hours caused partial loss of the
178 mitochondrial membrane potential in pulmonary ECs; (4) exclusion of oxygen from either the
179 lung-heart system or the microfluidic system ablates platelet generation.

YOU DIDN'T TEST THIS HERE, SO MODIFY YOUR STATEMENT.

In our manuscript, we have defined “healthy ECs” as “ECs with normal mitochondrial membrane potential”.

3. While EC injury/death by inhalation of nitrogen or no ventilation is mentioned, it needs to be **given more equal time** as a possible explanation in the Results and Discussion for why platelet formation was not seen.

We agree, and we did actually use similar time exposures (around 2 hours) for all conditions, including no ventilation and ventilation with nitrogen. This is described in the ‘Flow Cytometry’ section in Methods, and we have highlighted this in red in the text.

In the absence of ventilation, the numbers of platelets generated per MK in the perfusate still gradually increased with increasing passages (498.4 ± 117.9 platelets/MK, Fig.2a), but the numbers generated were substantially lower than in the air-ventilated condition.

When lungs are ventilated with pure nitrogen, the number of generated platelets in the perfusate was almost ablated, reduced to just 43.1 ± 16.7 platelets/MK after 18 passages (Fig.2a), due to mature MKs were trapped in the lung vasculature (Fig.2b and Supplementary Movie 5).

Staining for surface markers compatible with **endothelial injury** like loss of surface thrombomodulin or extrusion of VWF would have been important.

- 1) Here we investigated the **general ‘health’ state of the endothelium** by assessing the resting membrane potential across mitochondrial membranes, using a standard dye for this, TMRM. If cells are healthy and have functioning mitochondria, the signal will be bright, and we have used TMRM staining as a measure of endothelial cell health. We have therefore now modified our text, generally to indicate endothelial with normal mitochondria.
- 2) An in vitro study has shown that the increase in thrombomodulin **was closely correlated with** the loss of cell viability (2002 Nov; 107(3): 340–349). Our ECs from air-ventilated-, pure nitrogen-ventilated or unventilated lung all show normal viability, as measured by retention of Calcein Deep Red.

NEED TO MAKE CLEAR THIS IS NOT MICROFLUIDIC "PLTS".

IF THE DATA IS AVAILABLE, WHAT IS THE CHANGE IN THE TWO POPULATIONS WITH RECYCLING NUMBER

181 We next determined whether generated platelets display classical morphology and function.

182 Platelets display an almost uniquely characteristic sub-plasma membrane microtubular ring,

183 running circumferentially in resting platelets^{19,20}. Our generated platelets, immunolabelled for

184 α -tubulin, display this characteristic ring structure (Fig. 4a), and the mean size of the cells is

185 larger than controls ($3.6 \pm 0.2 \mu\text{m}$ vs $1.9 \pm 0.1 \mu\text{m}$, Fig. 4b). However, it is also clear that there

186 appear to be two subpopulations of generated platelets, based on their diameter ranges as shown

187 in Fig. 4b: approx. 33% of generated platelets (diameter range: $1.7\text{-}2.4 \mu\text{m}$) have sizes similar

188 to control platelets (diameter range: $1.2\text{-}2.4 \mu\text{m}$) and 67% of generated platelets (diameter

189 ranges: $3.7\text{-}5.6 \mu\text{m}$) are significantly larger than control platelets. We next visualized the

This is good to clarify in the text, and we now have added in the ‘heart-lung system’ or ‘microfluidic chamber’ to define the generated platelets from either approach specifically.

In regard to the question about 2 sub-populations of generated platelets, we image the cells after 18 passages, and assess using ImageJ. We have no data about the dynamic changes in these 2 sub-populations of platelets generated over different passages.

The microfluidic studies are complementary but not as well developed.

1. The similarity between the microfluidic design and lung vasculature is not demonstrated and the **discussion** should be altered to reflect that especially as no other design was studied.

Thanks for your suggestion and we now have changed the word “mimic” into “simulate” in our text.

2. The device has no endothelial lining and that limitation and its implications discussed.

In this manuscript, we have used the microfluidic design to simulate a series of parallel microvascular channels, or network of these, to demonstrate the importance of these small microchannels in platelet formation, and also to assess or exclude the role of endothelial cells in this, as these are absent from these channels.

We agree that the current microfluidic design has a lot of potential for further development, including different patterning and inclusion of endothelium as the reviewer has indicated, and this is something that we are actively pursuing particularly for generating larger scale **bioreactors** for platelet generation in vitro. We have now added a sentence to the Discussion section to include this point about endothelial cell lining in the microfluidic chamber.

3 Fig 3 was shown with no mouse platelet control and that would have been an important comparative. Again, markers of activated platelets should have been measured.

NEED TO BE CAREFUL HERE. SHOW FSC COMPARE TO DONOR PLTS AND NEED TO MEASURE MARKER OF ACTIVATION (EG, ANNEXIN V) TO MAKE YOUR STATEMENT OR NEED TO MODIFY STATEMENT. ALSO IS THIS A SIZE SELECTED STUDY. NO BIG MKS DRAQ5 POSITIVE COME THROUGH?

Thank you for your suggestion. We have now added control platelets in Fig. 1d and e. Supple Fig. 1e showed the Draq5 staining for MKs. These are the control comparators for Fig. 1, but also for Fig. 3.

Markers of activated platelets generated from microfluidic now have been shown in Fig. 3f.

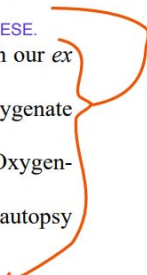
DID THE MKS NOW CLOG THE CHANNELS?

In regard to the question about our microfluidic chambers and whether MKs clog these channels when under nitrogen, we are currently establishing the approach to be able to image these dynamically in the presence of 100% nitrogen. For this reason, we have not yet been able to observe this, but can say that the channels are unlikely to be fully clogged, as suggested, since fluid does pass through the chambers in the presence of nitrogen, but that the cells have been left behind in the chamber. The fluid that exits the chamber, under 100% nitrogen, is fully clear, and devoid of cells. Therefore our understanding is that there is not fully blockade of the channels, i.e. it is not fully clogged, but clearly the cells are not able to passage through the channels.

Inflation or deflation?

This should be “inflation”, because as the transpulmonary pressure increases, narrowing of the capillaries occurs. This is described in Ref 35.

318 flow through the lung, and therefore the majority of MKs are likely to passage through the
319 capillary bed of the lung. NEED TO BE FAIR & BALANCED AND THE OXYGEN RELATIONSHIP MAY BE
PHYSIOLOGIC AND MK AND/OR EC- DEPENDENT OR ARETIFICIAL DUE TO
ENDOTHELIAL INJURY DUE TO HYPOXIA AND MK ADHERENCE TO THE
INJURED EC AND FURTHER STUDIES ARE NEEDED TO DISTINGUISH THESE.
320 The ability of MKs to pass through the lung microvasculature is oxygen-dependent in our ex
321 vivo system, as longer term exposure of the lung to pure nitrogen, to completely de-oxygenate
322 the lung over 2 hours, effectively caused MKs to be retained in the lung vasculature. Oxygen-
323 dependent MK motility might partially explain why pulmonary MK levels observed at autopsy
324 are increased in COVID-19 patients who had died with acute lung damage⁴³.



Oxygen, or lack of it, might affect both ECs and/or MKs, thereby impairing the mobility of MKs to pass through the lung microvasculature. We wanted to indicate that either or both is possible.

We suspect that lack of oxygen might predominantly affect MKs, because although the EC viability and mitochondria membrane potential are similarly affected in unventilated lungs compared to N₂-ventilated lungs, they differ in the number of platelets generated and number of MKs trapped in the lung vasculature. In particular, there are no MKs trapped in our unventilated model, whereas in the presence of 100% N₂, there are abundant MKs trapped. We are working on this, including growing ECs in the microfluidic system, and under different O₂ concentrations, to confirm whether O₂ predominantly affects the endothelial cells or the MKs, to affect the platelet generation process. We have therefore included the following sentence in the Discussion section: ‘Lack of oxygen may affect the platelet generation process through effects on the pulmonary vascular endothelium, or directly on

MKs, or some interaction between both cell types’.

346 fourth, multiple passage of MKs through the pulmonary vasculature in the *ex vivo* lung model
347 is crucial to induce a reproducible sequence of events (Fig. 9). These include enucleation,
348 nuclear fragmentation and condensation, prior to efficient platelet generation. This might
349 suggest an essential and dynamic conversation between the pulmonary microvasculature and

In our observations we found that nuclear fragmentation happened earlier than nuclear condensation, because we first saw the nuclear lobes were partially fragmenting from a naked MK nucleus after 3 passages (Fig. 6c and Supplementary Movie 3) and the sub nuclei became smaller and more condensed at later passages (6 and 18), as shown in Fig. 6c-f.

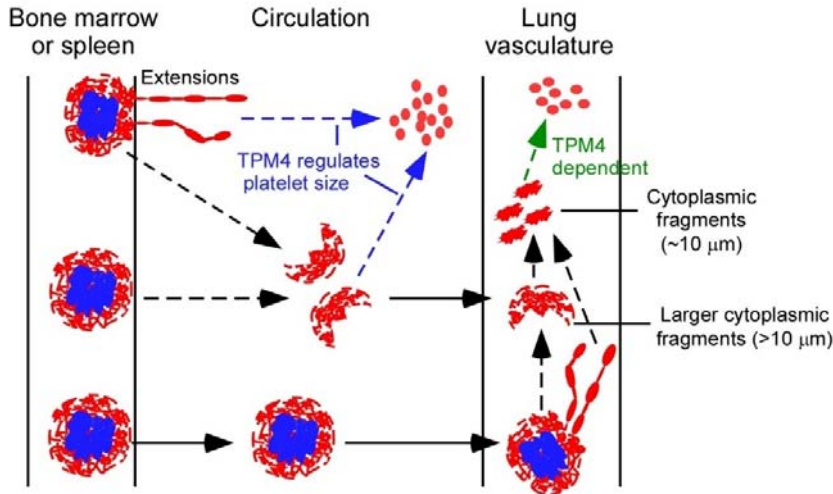
272 marrow space, in close contact with sinusoidal walls; (ii) some MKs within the marrow space
273 produced extensions into sinusoids; (iii) some MKs were clearly visible wholly within the
274 sinusoid vessels themselves and had cellular extensions; (iv) some appeared as large fragments
275 in the sinusoid, releasing heterogeneous structures in the direction of blood flow (Fig. 8 and
276 Supplementary Movies 13-14). These observations suggested that TPM4 in MKs does not play
277 an essential role in platelet release in the bone marrow, in contrast to its role in these cells in
278 the lung vasculature.

279 **Discussion**

281 In this study, we established an *ex vivo* pulmonary vascular model, which we show generates

I'D SUGGEST MODIFYING THIS. ITS EITHER THAT MK OR LARGE CYTOPLASMIC FRAGMENT RELEASE IS NORMAL IN THE MARROW. PLT FORMATION MAY BE TPM4-DEPENDENT BUT NOT THESE EARLIER PROCESSES THAT CAN GO ON IN BOTH THE MARROW AND LUNGS BUT FINAL PLT FORMATION MAY BE IMPAIRED.

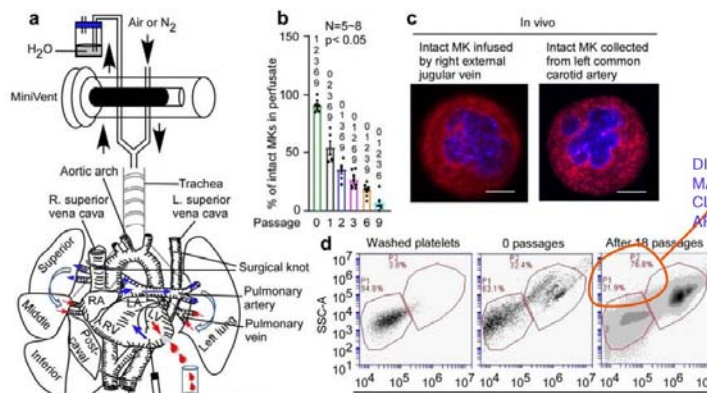
Thank you very much for this discussion. We now have modified this statement and highlighted in red colour in our text. We made a figure (below) to explain this but haven't included this in our manuscript.



366 lung system, despite undetectable platelets in the perfusate (Fig.7a-b), abundant anuclear
 367 fluorescent objects, sized $\sim 10 \mu\text{m}$, could be seen in the lung vasculature (Fig.7d and
 368 Supplementary Movie 12). This suggests that TPM4 is required for the final steps in platelet
 369 generation. Importantly, our data from intravital observation of *Tpm4*^{-/-} bone marrow suggests
 370 that MK protrusion/extrusion process, which may be proplatelet formation in vivo, is similar
 371 to normal (Fig.8 and Supplementary Movies 13-14). This therefore makes it likely that the
 372 lower platelet count seen in *Tpm4*^{-/-} mice is a product of defective platelet formation outside of
 373 the bone marrow. in the lung vasculature.

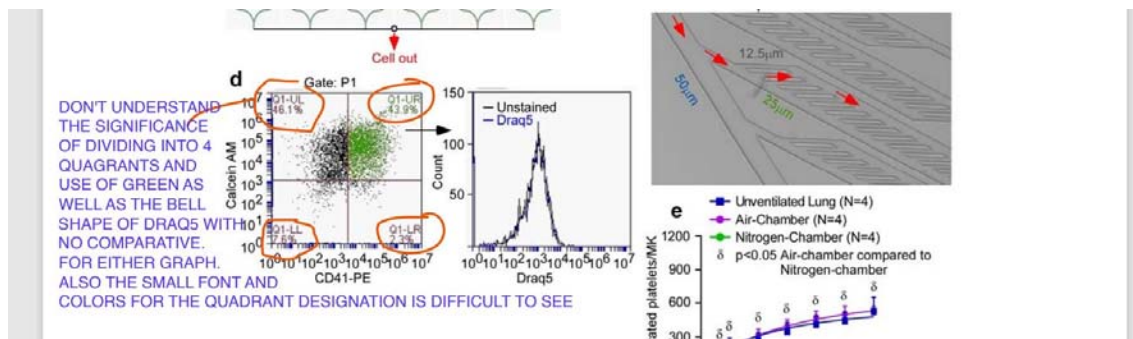
SEE PRIOR COMMENT
 THAT THIS MAY
 NOT BE PROPLT
 BUT LARGE
 FRAGMENT FORMATION
 ONLY. IT MAY BE
 THAT TPM4 IS
 NOT NEEDED FOR MEGS
 TO MIGRATE OUT
 OF THE MARROW
 BUT IMPORTANT
 FOR FUTURE
 PROCESSING

These have been addressed and highlighted in red colour in the text.



DIFFICULT TO READ.
 MAKE BLACK AND MOVE
 CLOSER TO CIRCLED
 AREAS?

Thank you for this point. This has been modified in Fig. 1d.



The quadrants define the live CD41+ events, which are generated platelets. These quadrants were defined using control platelets. We have included text in the figure legend to indicate that Q3 has been defined as generated platelets, using parameters measured using control platelets. We have coloured these events as green, just to clearly delineate them from events in the other quadrants.

Regarding DRAQ5 staining, Figure 1e had already shown equivalent data for control platelets, and Supp Fig 1e shows DRAQ5 staining for MKs, which provides a positive control for this stain.

We agree that the font for the quadrant labelling was difficult to read, and so we have replaced this with new type, and re-named the quadrants in a clearer way, as quadrants Q1-4. Appropriate reference to these quadrants in the text and legend have now been amended also.

REVIEWERS' COMMENTS

Reviewer #2 (Remarks to the Author):

Thank for the clarification.

Reviewer #3 (Remarks to the Author):

No further studies or modifications needed.